Université catholique de Louvain
École Polytechnique de Louvain

Louvain Institute of Data Analysis and Modeling in economics and statistics - Center for Operations Research and Econometrics

Mobilizing Flexible Demand in Electric Power Systems Through Service Quality Differentiation

Céline Gérard

Thesis submitted in partial fulfillment of the requirements for the degree of
Docteur en sciences de l'ingénieur et technologies

Supervisor:
Anthony Papavasiliou
(UCLouvain, Belgium)

Jury:
Philippe Chevalier (UCLouvain, Belgium)
Emmanuel De Jaeger (UCLouvain, Belgium)
Shmuel Oren (University of California, Berkeley, USA)
Leonardo Meeus (Vlerick Business School, Belgium)
Thomas Morstyn (University of Edinburgh, UK)

Chair:
Philippe Chevalier (UCLouvain, Belgium)

PhD Organization

Céline Gérard
UCLouvain
École Polytechnique de Louvain
Center of Operations Research and Econometrics

Thesis Supervisor

Anthony Papavasiliou
Associate Professor, UCLouvain
École Polytechnique de Louvain
Center of Operations Research and Econometrics

Supervisory Committee

Philippe Chevalier
Professor, UCLouvain
Louvain School of Management
Center of Operations Research and Econometrics

Damien Ernst
Professor, Université de Liège
Institut Montefiore

Abstract

Residential demand response is poised to emerge as an increasingly important aspect of power market operations due to the widespread deployment of distributed renewable supply in the form of rooftop solar panels and distributed flexibility such as batteries. A major challenge in the proliferation of residential demand response relates to the development of scalable aggregator business models that respect the requirement of consumers for privacy, simplicity, and control. This has motivated quality differentiation in the form of priority service and its generalized form, namely multilevel demand subscription. Whereas priority service relies on the differentiation of electricity service according to reliability, multilevel demand subscription further differentiates electricity service according to duration. This dissertation proposes several modeling approaches that are aimed at quantifying the impact of these two service definitions on system efficiency and costs incurred by households. The coordination achieved by these services is compared against the ideal economic benchmark, real-time pricing.

The contributions of the present dissertation are divided into four chapters. First, Chapter 2 compares priority service to real-time pricing in terms of impact on consumer comfort and billing, using a consumer-centric methodology. The role of service charges in the construction of a priority service menu is analyzed from a theoretical standpoint by extending the original theory that was developed for priority service. From an empirical perspective, service charges are shown to be crucial in alleviating the cost of priority service for households compared to real-time pricing. This observation is based on two case studies that focus on a Belgian and a Texas household. Then, in Chapter 3, we introduce a modeling approach for designing multilevel demand subscription and priority service menus that are comparable. The menus are designed as the equilibrium solution to a Stackelberg game, which is modeled as a bilevel optimization problem involving a vertically integrated utility and consumers. The problem is reformulated and solved as a mixed integer linear program. The menus and resulting household subscriptions are compared in a realistic model of the Belgian power market. Chapter 4 proposes a framework for evaluating the performances of priority service, multilevel demand subscription and real-time pricing in a system with utility-scale renewable supply, residential

renewable supply, and residential storage. The implications of each option on operational efficiency and consumer expenditures for electricity service are discussed using a realistic model of the Belgian power market. Finally, Chapter 5 describes a methodology for aggregating residential flexibility through priority service while accounting for low-voltage network physics by means of residual demand functions. Several formulations (including relaxations and approximations) of the power flow equations are used for representing the physics behind the operation of distribution systems. An analysis is conducted on an illustrative example.

Acknowledgements

The completion of these four PhD years that led to the present dissertation would not have been possible without the support of some people and organizations. I would like to take the opportunity to express my gratitude to this community in the following lines.

First and foremost, I would like to offer my special thanks to my supervisor, Professor Anthony Papavasiliou, for his continuous support, invaluable advice and precious encouragements during the course of my PhD degree. Indeed, his expertise was really appreciated and helped me to conduct my work in the right direction. I am profoundly grateful for the number of hours he passed on proofreading countless numbers of English pages.

I also acknowledge the financial and technical support without which this PhD thesis would not have been possible. The financial support for this thesis was provided by the Fonds de la Recherche Scientifique - FNRS in Belgium through a research fellowship (Aspirant). Concerning technical support, I would like to thank the Consortium des Equipements de Calcul Intensif (CECI) for granting access and computing time at the high-performance computing cluster Lemaitre3, which was used extensively (to say the least) to conduct numerical experiments throughout this work. CECI was funded by the Fonds de la Recherche Scientifique de Belgique (F.R.S.-FNRS) under Grant No. 2.5020.11 and by the Walloon Region. Thomas Keutgen as a member of this consortium at UCLouvain was of great help for parallel computing problems. I really appreciated his availability and thoughtful advice. Academic licenses for optimization solvers were provided for this work by Gurobi and Mosek.

Moreover, my thanks go to Professors Philippe Chevalier, Emmanuel De Jaeger, Shmuel Oren, Leonardo Meeus and Thomas Morstyn for agreeing to be part of my thesis jury. I would also like to thank Professors Philippe Chevalier and Damien Ernst as committee members for their encouraging words and feedback during my confirmation exam. Finally, I am very grateful for the precious comments and help of Professor Philippe Chevalier who took part in the research leading to the third and fourth chapters of this dissertation.

I would like to thank Dr. Andreas Ehrenmann (ENGIE) for his comments and thoughtful discussions during the early development of this work. I am also grateful for the feedback I received on my work as being part of the EPOC 2030-2050 project (Belgian energy transition funds).

The nice atmosphere at CORE, LIDAM, SST and UCLouvain in general made it easier to complete my goals. I particularly appreciated the help of Catherine Germain regarding administrative questions and Raphaël Tursis regarding computers.

I would like to emphasize the important role that the Energy Group (Ignacio, Yuting, Gilles, Ilyes, Quentin, Daniel, Loïc, Jacques, Jehum and Nicolas) had during the course of my studies. I am grateful to every member of the team for their feedback and comments regarding my work during seminars but also for the fun time and informal discussions we regularly had at conferences, lunches or breaks. I am especially grateful to Yuting for still taking part to discussions on my research even after going to other job horizons and to Daniel for helping me with his stochastic programming computing skills for the third and fourth chapters of this thesis.

Furthermore, I would like to thank my friends for the interesting discussions, for their interest in my work and well-being, and for the mutual aid approaching deadlines.

Last but not least, I am grateful to my family, my parents and my sisters, for providing me with their unfailing support and keeping me motivated and confident. Thank you to my partner for his patience and for enduring this long process with me. This accomplishment would not have been possible without them.

Contents

List of Figures

List of Tables

1 Introduction

1.1 Context

In our society, the use of renewable energy resources has increased remarkably for various purposes during the past few years. In order to meet the challenges of global warming, electric power systems are particularly affected by this rise of renewable supply. Indeed, in a recent United Nations report, it is mentioned that: "The largest increase in the use of renewables has come in the power sector, where their share of global electricity consumption reached 24.7% in 2017, surpassing the share of renewables in the heating sector for the first time." [90]. This rapid expansion is likely to continue in the coming years, particularly in light of the European Union's goal of becoming the first climate-neutral continent by 2050 [57]. Moreover, as envisaged in the 2030 Climate Target Plan of the European Green Deal, the European Union plans to reduce its carbon emissions by 55% by 2030 [57]. These European objectives have driven the continuous increase of the share of renewable production in Belgium. Indeed, around 800MW of wind production capacity along with about 1000MW of solar were installed in 2020 in Belgium [4].

However, even if renewable resources support countries in their journey to become increasingly sustainable, they are exerting pressure on the existing electrical system by being the cause of technical concerns. In fact, renewables are disruptive in the sense that they are currently injecting power whenever it becomes available without coordination with the remaining parts of the network. This phenomenon creates technical problems such as voltage issues, reactive power flows and an increased need for grid support services. This situation has accordingly intensified the need for the incorporation of flexibility in worldwide electricity systems so as to balance the variability of renewable supplies. Although storage devices can act as a source of flexibility, their investment cost is a limitation for providing a straightforward solution to this problem. Besides, they are not sufficient to cover the entire need of the system for flexibility. Furthermore, the variability of renewable resources could also be dealt with

by means of fast-response generators but this suggestion would lead to a rise in operational costs and carbon emissions. These alternatives unfortunately weaken the economical and environmental benefits of renewable resources.

In this context, it is worth noting that the part of the electrical power system operating in the most sophisticated fashion is the high-voltage portion of the grid (which is composed of high voltage transmission lines, to which large generators and industrial loads are connected). Consequently, a large amount of unused flexible resources connected to the low-voltage system persists, originating from flexible residential and commercial demand. This residential flexibility can be exploited efficiently in order to break the current barriers that are bounding the growth of renewable energy integration. Residential demand response has recently received increasing consideration in the scientific literature since it is viewed as a viable solution for mobilizing this unused residential flexible consumption. This dissertation therefore focuses on the application of a residential electricity tariff and its generalized form based on the premise that electricity is now viewed as a service with different degree of quality. Comparisons between the proposed electricity tariffs are performed, with a focus on quantifying the impact of these tariffs on system efficiency and costs incurred by different types of households.

The following opening chapter aims at presenting the motivations and contributions of the present work along with a general introduction on demand response. This chapter is divided as follows. Section 1.2 describes demand response programs from a broad perspective by presenting their benefits and challenges along with an exposition of several existing schemes. The current status of European countries regarding residential demand response is also depicted. In section 1.3, the electricity tariff proposed in this dissertation is outlined. Finally, section 1.4 presents the organization of this thesis by highlighting the contributions of the author that are associated with each chapter.

1.2 Demand Response

Demand response represents intentional adjustments in electricity usage by end-use consumers from their usual consumption profile in reaction to the time variation of the price of electricity [3]. In this section, the benefits but also the challenges linked with the integration of demand response in power systems are highlighted. A description of known residential demand response programs is also provided along with current practice in terms of demand response in Europe.

1.2.1 Benefits and Potential

Demand response can be highly beneficial for power system operations in different respects. Its different benefits along with its estimated potential, based on numerous pilot programs, are exposed in the following paragraphs of the present section.

Reduced Needs for Peak Capacity Generators

Over the past years, residential electricity prices have not revealed the intrinsic variation in prices characterizing the electrical industry. Electricity has therefore been consumed by customers without regards to the current stress of power systems at certain periods during the day, which has led to large consumption during peak hours [66]. Since peak hours correspond to a small portion of the year, some peaking and flexible plants are built only to be used for a few hours annually. Demand response programs can help by moving peak consumption to off-peak hours in order to reduce the capacity requirements of the system and thus, in the meantime, the need for investing in peaking units such as open cycle gas turbines (OCGT) [17, 128]. Since these units are generally characterized by high marginal cost, this phenomenon can also enable a reduction in electricity prices during peak periods due to a more efficient use of the existing installed capacity [63].

Reduction in Network Investments

Reduction in new investments to support the network may also be envisioned with demand side management. Indeed, such schemes can be employed at the distribution level in order to efficiently operate power networks. Operations such as frequency regulation, mitigation of voltage issues, and reduced congestion can benefit from the direct adaptation of residential and commercial electricity consumption. This can enable a reduced need for reinforcement and upgrade of the existing electricity network [63, 128, 139, 161].

Support for Large-Scale Renewable Energy Integration

As emphasized in the first part of this chapter, demand response is seen as a simple solution for coping with the uncertainty and variability of renewable generation. Indeed, demand side management can contribute towards meeting the large amount of reserve capacity required for an extended penetration of renewables [17,128,167]. For example, in the case of a wind generation increase, it has been proven in [106] that demand side management can reduce the increase in operation cost resulting from wind integration while also increasing the amount renewable power capacity that can be installed.

Demonstrations of Demand Response Potential in Pilot Programs

A large number of diverse pilot experiments and studies have already proven the usefulness of demand response in the residential sector, such as [66,101,127,163]. For example, Faruqui *et al.* presents an analysis of 63 pilot programs in 9 different countries in [67] and provides an overview in [66] of 15 experiments that quantify the benefits of demand response based on dynamic pricing. In [64], it is demonstrated that the benefit of a large-scale adoption of dynamic tariffs by consumers could amount to 67 billion euros in Europe. The authors also show that a peak reduction of 20 to 30% can be achieved for certain rate designs. In the US, Faruqui [65] estimates a reduction of 5% in demand peak, which translates to an economic saving of 3 billion dollars per year. Moreover, another analysis realized in the United Kingdom estimates a reduction in system costs that ranges between 7.1 and 8.1 billion pounds per year for a deeply decarbonized system that can be achieved with the large-scale mobilization of demand response. Even though these experiments and studies provide different quantitative estimates, there is a general agreement on the fact that demand response can largely decrease system cost, notwithstanding the fact that consumer response depends on climate, seasons, countries and other characteristics [63].

The literature on demand response further explores in detail the benefit of applying these programs to a particular device in the house. Such devices include electric heating, air conditioners, water heaters, and others. For example, the LINEAR project realized in Belgium [21, 34] quantifies the flexibility that can be gained from wet appliances (washing machines, tumble dryers and dishwashers). Electric vehicles and heat pumps are also an interesting option for mobilizing flexibility, as demonstrated in an analysis of the UK system [135]. The potential of thermostatically controlled loads such as air conditioners and fridges has also been studied carefully [18, 19, 100, 109]. Finally, regarding electric heating, a Danish study concludes that a reduction of 6% of the Danish peak load can be operated if 50% of the households in Denmark using electric heating were to be placed under demand response programs [167].

This wide range of pilots and studies demonstrates the significant potential gains that can be achieved by having demand response replacing flat residential tariffs. They also highlight the substantial opportunity to harness the potential of a growing number of flexible appliances such as electric vehicles, air conditioners, home batteries, ... that can provide useful support for power grid operations and the integration of renewable resources [145].

1.2.2 Challenges

Whereas the engagement of demand side flexibility in the commercial and industrial sector has been increasing steadily, the mobilization of residential flexibility lags behind. This is despite increasing evidence of substantial benefits related to the use of residential flexibility in power grids as shown in the previous section. Moreover, Gils *et al.* also observes that the residential sector is characterized by higher levels of flexibility than the commercial and industrial sector [78] (also observed in [62]). This gap between the existing proliferation of industrial and residential flexibility can be explained by several barriers and challenges that are limiting or slowing down the mobilization of residential demand flexibility.

Consumer Requirements and Behaviour

First of all, certain barriers to the large-scale integration of residential demand response are related to consumer requirements and behaviour regarding the consumption of electricity. Indeed, a crucial feature of residential consumers is their limited attention span. Customers are thus not willing to monitor constantly electricity tariffs and adapt their consumption accordingly. In order to account for this concern, the direct management of appliances has been considered in the literature. However, this violates the general principles of decentralizing power system operations through electricity markets and is additionally viewed as being too intrusive by consumers [179].

Furthermore, according to realized pilot projects and experiments, it has been proven that the education and awareness of consumers play an important role on the benefits that can be achieved by residential demand response [179]. In order to maximize the gain of its introduction, the aggregator should focus on the creation of accessible and simple tariffs for consumers [64]. Moreover, informing consumers about their electricity consumption and the need for demand response through media campaigns, more detailed electricity bills, and other measures, is essential for consumers to understand the importance of engaging in such programs [64, 128].

Finally, the system operator is currently the only entity responsible for maintaining the quality of electricity service in the form of reliable access to power supply. However, if demand response is mobilized so as to support power networks, this shifts the responsibility towards the end-user which may be viewed as an excessive burden by the consumer [128].

In view of the previous arguments, it is therefore crucial for demand response aggregators to formulate business models that are capable of mobilizing residential flexibility while respecting the needs of consumers for control over their equipment, privacy and simplicity in the pricing of electricity [86]. It is

also essential to propose several demand response tariffs at the same time to account for the variety of consumer profiles [30, 125, 154].

Challenges Related to Establishing a Business Case

A consensus emerges from the literature concerning the difficulty of establishing a business case for demand response [128, 161]. Indeed, Strbac in [161] argues that consumer response to changing electricity prices is heavily dependent on price differences or provided incentives. Therefore, a small change may not be enough for harnessing sufficient residential demand response to the extent that can prove useful for system operators. Poor judgement in the pricing of residential flexibility is best exemplified through a recent backlash against net metering [133]. Net metering was introduced in a number of US States, including Arizona, Hawaii and California in recent years. It has recently been retracted due to adverse distributional effects [61, 75] and due to the inability of the existing distribution infrastructure to support the roll-out of solar panels that has been induced by net metering.

Furthermore, despite the fact that demand side management allows a more efficient operation of power systems compared to traditional solutions, it results in an increased complexity of operating power systems [161]. To deal with this issue, the most common proposal in the literature for enabling its efficient use is through an aggregator that will serve as an interface between the system and a large number of residential consumers [128].

Uncertain Response of Demand Side Flexibility

Even though there is a large number of pilot projects that investigate the gain provided by certain demand response programs, it is challenging to quantify in advance their tangible benefits. The aggregate reaction of consumers to such programs depends on a large number of heterogeneous households that exhibit changing behaviours and different living conditions. It makes it complex to arrive at a common estimate for the potential of demand response [161]. Moreover, pilot studies are conducted by considering that consumers are price-taking, but do not analyze the impact that this price responsiveness can have on the determination of the price itself. Therefore, it is difficult to assess the real benefit of its massive introduction [128]. Finally, for the moment, only demand response programs for which the aggregator directly controls consumer appliances are seen by system operators as viable techniques for grid support such as frequency regulation because the reduction in demand can only be forecast precisely in that case [128].

Deployment of Enabling Technologies

As emphasized by Faruqui *et al.* in [64–66] and by Yan *et al.* in [179], the installation of enabling technologies for demand response - such as smart meters,

communication infrastructures, smart thermostats, in-home displays and so on - is essential for facilitating residential participation in power system operations. Indeed, home energy management systems are expected to become central technologies in households that will help consumers account for price signals while taking into consideration their requirements in terms of comfort [161]. However, the deployment of such ICT infrastructure has been slow [161,167], although it is advancing more rapidly recently owing to a number of research and industry initiatives [54, 56, 61].

1.2.3 Residential Demand Response Programs

Various demand response paradigms have been proposed and analyzed extensively in the scientific literature for mobilizing residential flexibility. These different designs can be clustered into two main groups: *price-based* and *quantity-based* (or incentive-based) methods [94]. *Price-based* programs, including time-of-use, real-time and critical peak pricing, are based on the premise that consumers are considered as sophisticated agents that react to changes in electricity prices. In this way, these schemes seek to decrease the pressure on power system operations in times when the balance between supply and demand is precarious by providing economic incentives to end-user consumers [17]. In contrast, *quantity-based* methods, such as direct load control, assume that an aggregator can shed residential load and, even for some programs, override residential consumers by directly controlling their appliances.

Price-Based Methods

As discussed previously, price-based programs include time-of-use, critical peak and real-time pricing. Yan *et al.* [179] reviews and compares these three demand response options through the results of pilot experiments. Time-of-use (TOU) rates are the most common since they have already been employed for several years to better take advantage of installed nuclear power plants [161]. This scheme considers a fixed electricity price for pre-defined time periods within a day. Its traditional version consists in a low electricity rate for power consumed during the night between, e.g., 10pm and 6am while the daytime consumption is subject to a higher price. Time-of-use pricing is already a significant progress relative to flat tariffs because it drives flexible electricity consumption to low-price time periods. However, this type of tariff only captures the expected long-run conditions of the system and does not reflect the high variability of renewable electricity supply [62]. As it is emphasizes in section 1.2.4, where we review residential demand response tariffs in Europe, time-of-use pricing is widely developed, especially for households with electric heating/cooling or electric vehicles [17].

Compared to time-of-use pricing, critical peak pricing (CPP) aims at accounting for the short-run conditions of the system as it is an event-based

tariff with the aim of reducing residential consumption in events of peak demand [128]. This program attempts to better depict system energy costs by charging an expensive electricity price for a certain number of hours during which the system is stressed. During other periods, the consumer is rewarded by having access to a discount on its electricity price. In such a setting, flexible consumption will therefore be directed to less expensive hours in order to lower consumer electricity bills [64]. This demand response paradigm better corresponds to modern power systems in which the generation of electricity is increasingly unpredictable due to renewable resources. Indeed, in the past, traditional approaches such as time-of-use pricing were sufficient to provide the flexibility required by the system [128]. A similar idea to critical peak pricing inspires peak-time rebates (PTR), where consumers are offered a rebate for delayed consumption based on a baseline usage during periods of critical system operations [3]. The fundamental weakness of this technique is that it requires the correct approximation of consumer baselines in order to estimate the actual reduction in consumption, which is a central but challenging aspect in the pricing of this paradigm [17, 31, 64].

The most "pure" form of dynamic pricing is achieved by real-time pricing (RTP) [155]. This paradigm considers the consumer as a real-time participant to the electricity market that reacts instantaneously to prices, for example, by reducing consumption during period of peak demands. The prices are revealed on a short-term (e.g. hourly) basis and change from day to day and hour to hour. Although real-time pricing represents the economic golden standard of demand response, the risk linked with the variability of electricity price may discourage consumers from enlisting [17]. This risk is best exemplified through the 2021 Texas electricity crisis during which wholesale market electricity prices reached 9$ per kWh (roughly 300 times the typical electricity price). Two electricity providers (Griddy and Octopus Energy) using real-time pricing understood the impact that the storm will have on electricity prices and urged their consumers to switch to providers with fixed-rate plans to avoid incredibly high electricity bill during the outage period. Indeed, even though this retailers encourage more consumers to see and feel the real-time price, they don't include a price hedge for protecting consumers during shortage events [33]. Moreover, while sophisticated industrial consumers can participate directly to the wholesale market by virtue of size and significant economic opportunities, real-time pricing may require an excessive amount of attention for small consumers [64].

Time-of-use, critical peak and real-time pricing techniques are focused on the application of an energy charge. Indeed, consumer is charged a certain price for the energy consumed during a certain period. These methods can be combined with a *demand charge*. In this framework, the maximum amount of simultaneous kilowatts withdrawn by a consumer during a certain time period is charged even if the adequate supply of power in that particular time period may not be at risk [17].

Quantity-Based Methods

In this category, direct load control (DLC) appears as the most common technique. In this setting, consumer appliances are controlled by an aggregator [99]. This aggregator has the authority to switch consumer appliances anytime there is a need to regulate the power demand in the system. This concept is more appropriate for appliances that can be easily shut down or cycled for short periods of time with minimal impact on consumer comfort, such as domestic air-conditioners, water heaters and swimming pool pumps [161]. System operators prefer these techniques to price-based methods for providing ancillary services since the effect of such a scheme can be better predicted [128]. Nonetheless, this concept is considered as being too intrusive by consumers in terms of privacy.

Another form of quantity-based scheme is based on capacity limits, i.e. limits on the maximum power that can be withdrawn anytime from the grid by a consumer. The consumer therefore retains control on its own appliances and decides what consumption to delay, taking into account the applied capacity limit [161].

1.2.4 Application of Demand Response in Europe

An overview of the application of demand response programs in Europe is presented in this section. As explained by Torriti *et al.* [167], Europe does not have harmonised demand response programs. Indeed, even though the European Commission recognizes demand response to be a central point in future power systems, the electricity markets of certain European countries are not yet prepared for integrating demand response. In that respect, Bertoldi *et al.* [11] presents the progress of European Member States towards opening their electricity markets for demand response as of the beginning of 2016.

Table 1.1 presents the different retail tariffs that are offered to residential consumers for 30 countries in Europe. From this table, we can observe that almost every European country is proposing some form of time-of-use pricing. Most of the time, this consists of a two-part tariff with cheap electricity during the night that may be useful for households with electrical heating. Sometimes, this tariff takes the form of a three-part charge with a cheap price during the night, a normal rate during the day, and an expensive price during peak consumption hours from 5pm to 10pm. France is the only country in Europe to propose a form of critical peak pricing. The Electricité de France (EDF) operator introduced the TEMPO tariff in 1993. In this scheme, the year is split into three types of days: white, blue and red. Most of the days in a year are blue (300). During blue days, consumers are charged with a cheap price. On the white days (43 a year), the electricity is charged at a higher rate. Finally, on red days (22 a year), the consumer is charged with the most expensive price in

Table 1.1: Residential electricity tariff structures in European countries. Updated and extended version of Table 1.1 in [117]. FT: flat tariff; TOU: time-of-use tariff; FT-D: flat tariff with demand charge; TOU-D: time-of-use tariff with demand charge; CPP: critical peak pricing; RTP: real-time pricing.

Countries \ Tariffs	FT	TOU	FT-D	TOU-D	CPP	RTP
Austria [59, 172]	✓	✓				
Belgium [45, 49, 110]	✓	✓	✓	✓		✓
Bulgaria [22]	✓	✓				
Croatia [88]	✓	✓				
Cyprus [39]	✓	✓				
Czech [143]	✓	✓				
Denmark [156]	✓	✓				✓
Estonia [37]	✓					✓
Finland [87, 102]	✓	✓				✓
France [97, 147]			✓	✓	✓	
Germany [120]	✓	✓				
Greece [148]			✓	✓		
Hungary [42]	✓	✓				
Ireland [48]	✓	✓				
Italy [157]			✓	✓		
Latvia [46]	✓					✓
Lithuania [53]	✓	✓				
Luxembourg [50]	✓	✓				
Malta [47]	✓					
Netherlands [171]	✓	✓				
Norway [80]	✓					✓
Poland [44]	✓	✓				
Portugal [162]			✓	✓		
Romania [38]	✓					
Slovakia [159]	✓	✓				
Slovenia [40]	✓	✓				
Spain [43]			✓	✓		✓
Sweden [107]	✓					✓
Switzerland [174]	✓	✓				
United Kingdom [129]	✓	✓				✓

order to face the incentive of moving a flexible part of consumption to cheaper days [3]. The color of a day is only revealed the day before. Finally, we can observe that only a small number of European countries offer the possibility to their residential consumers to choose real-time pricing [56]. Note that certain countries use some form of demand charge, which is a fixed monthly or yearly charge based on the capacity of the meter installed in the household. In Bel-

gium, this demand charge is only applied to prosumers. Moreover, note that, in Belgium, hourly real-time pricing is only proposed in Flanders for consumers with smart meters [32].

1.3 Priority Service

With the desire of respecting the requirements of residential consumers for control over their equipment, privacy and simplicity, this dissertation focuses on an alternative approach for mobilizing residential demand response at a massive scale, referred to as priority service pricing (PSP) [26]. This design aims at combining the strengths of price-based and quantity based methods. In this paradigm, electricity is treated by residential consumers as a service with attributes that can be differentiated, as opposed to a commodity that is traded in real time. This point of view has inspired various levels of differentiation in electricity delivery [15, 16, 28, 124, 126]. Service differentiation in the electrical industry is inspired from the successful implementation of this idea in other deregulated industries such as telecommunications.

Priority service pricing was first proposed by Chao and Wilson in [26] and by Oren in [132]. The feature of service that differentiates quality in priority service pricing is reliability. Concretely, an aggregator proposes a set of options for procuring *capacity strips* by means of a priority service menu in the form of price-reliability pairs. Each option is characterized by a different level of reliability. More reliable options are more expensive to procure. As a demand response paradigm, priority service recently received renewed attention in the theoretical literature [20, 23, 24, 108, 117–119, 131], as well as in practical applications [5, 136, 182] with a recent ARPA-E grant being awarded to develop priority service for use by US ISOs [7].

In the present study, we consider the specific implementation of priority service pricing with three options of different reliability following the ColorPower concept [136]. According to this method, an aggregator uses a color-tagging system based on traffic lights that consumers can set for each of their appliances: **(i)** *Green*: indicates cheap power that can be interrupted frequently; **(ii)** *Yellow*: indicates power that can be interrupted under emergency conditions; **(iii)** *Red*: indicates expensive power that cannot be interrupted [5, 77, 117–119, 131, 136]. Based on the offered menu, the household subscribes to a particular amount of capacity for each option, and enrolls in a long-term (e.g. annual) contract for electricity service. Once a household subscribed, the consumer allocates particular devices within the house to strips of different colors by ensuring that the mean power within an interval under a certain option does not exceed the subscribed amount of kilowatts for that particular color. In practice, this form of demand response can be implemented in households by means of fuse limits and color tags for plugs, whereby the

consumer can attribute a color to a specific appliance either manually or by means of a home energy management system. The described setup is presented in Figure 1.1. Figure 1.2 depicts how the interruption of colors affects the consumption pattern of a household along with the specific plug needed to implement priority service.

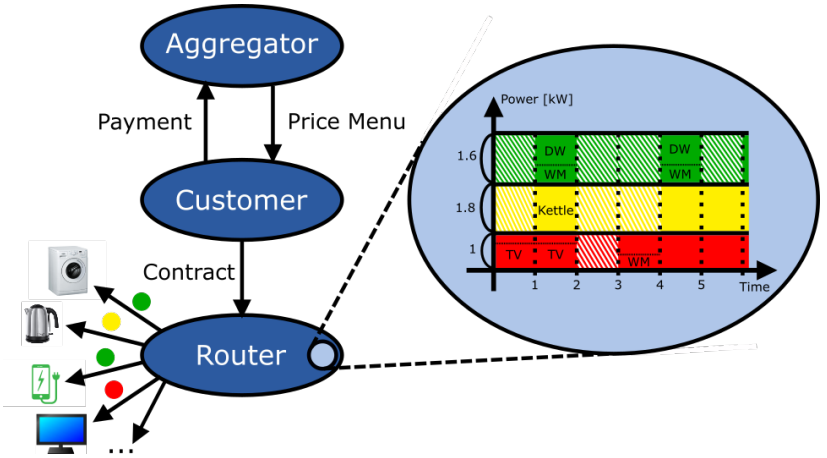

Figure 1.1: Setup of a home energy management router for priority service.

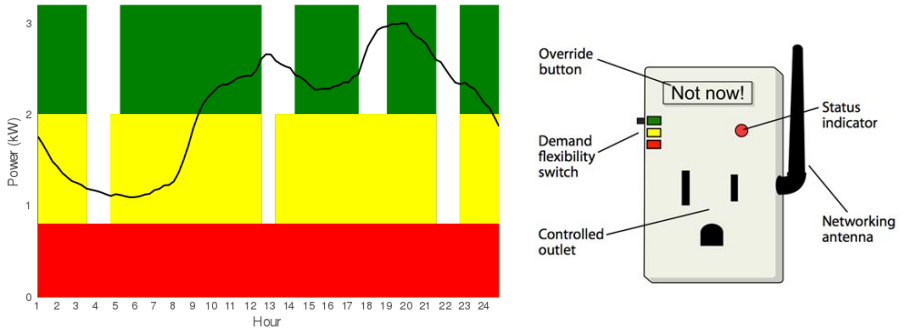

Figure 1.2: Illustration of the practical implementation of priority service pricing. The black line represents the total consumption of a household. The color blocks represent the amount of power available for each reliability option contracted by the consumer over a certain time period. Consumers can decide how to allocate major appliances through outlets equipped with switches and select a particular level of reliability. Source: [160].

In offering priority service contracts to residential consumers, the utility commits to a certain level of reliability for each option. This level of reliability

must be respected on average over an extended period of service (e.g. annually), even if certain periods of service may be characterized by fluctuations around this average [119]. In a central dispatch setting, the utility interrupts colors in order of decreasing reliability, since the menu is designed so that higher-valuation consumers self-select higher levels of reliability. The selection of one option from the menu by each consumer determines the service order or priority of the consumer. The aggregator is then tasked with designing a menu of services, such that consumers self-select reliability levels consistent with the reliability that the inherently stochastic supply mix of the aggregator can deliver. In doing so, the information asymmetry challenge is that the aggregator is not aware of the valuation of each individual consumer for power, as this is private information. The utility can only estimate aggregate statistical information about the consumer population [26, 119] in the form of demand functions. Note that, by subscribing to certain options of the menu, consumers reveal information about their valuation for power. Therefore, the aggregator belief of the system represented by the system level demand function can be updated in order to reflect the new information. Therefore, the aggregator can use this new belief about the system in order to design a new menu for the next subscription cycle. This cycling process presents certain similarities with the literature on incentive regulation [2, 95].

The pricing of priority service contracts is characterized by a menu of options $M = \{(p, s, r)\}$. For each option, p is the priority charge (payable in advance), s is the service charge (payable as service is provided), and r is the service reliability which is the probability of receiving the product or service. Although priority service theory is developed extensively, the literature is relatively terse in analyzing the role of service charges [131]. In our work, we demonstrate that service charges can play an instrumental role in decreasing the cost of priority service contracts to consumers, and thereby mitigate the capacity-based nature of priority service pricing. Multilevel demand subscription, a generalization of priority service that further differentiates electricity service in the dimension of duration, is also examined in this dissertation as an alternative to priority service with an energy component and is presented in the next section. The trade-off of simplicity versus the price of the contract and the efficiency of system operation are studied. The results of our analysis highlight the need for a demand response tariff composed of an energy and capacity charge for future power systems, as also advocated in [61].

1.3.1 Multilevel Demand Subscription

Multilevel demand subscription (MDSP) [25] generalizes priority service by allowing the aggregator to differentiate service along reliability *and* duration. From the point of view of consumers, kilowatts of different priority levels (i.e. colors) are "topped up" with credits. More credits entitle customers to use more hours of power of a certain quality, but cost more. The envisioned in-

terface used by consumers for such a service is depicted in Figure 1.3. The proposed contract is a forward contract. This implies that there is an inherent "override" option (which is activated automatically when the customer exceeds the capacity and duration limits of the contract), however in that case the customer would need to procure any additional consumption at the prevailing real-time price. Thus, the energy router within the home needs to respect not only the power limit of each color, but also the total number of credits over the service period (e.g. over the week or day). Clearly, this service offering presents increased complexity from the point of view of the household. However, it also allows the utility to better discriminate among consumer types. This contributes towards a more efficient allocation of power to flexible demand.

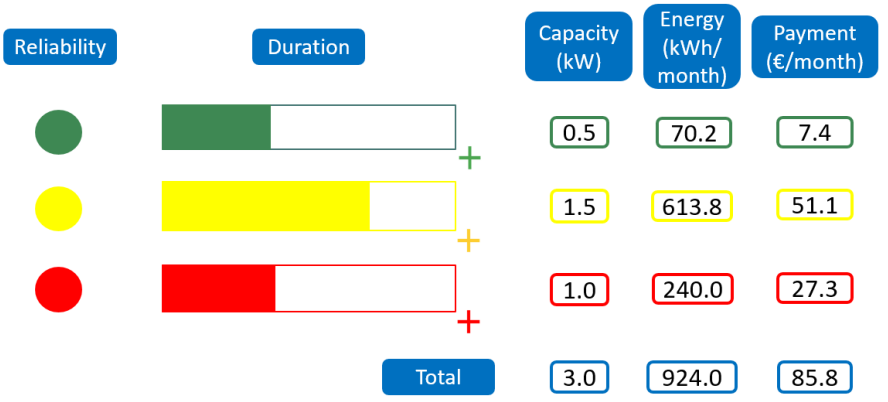

Figure 1.3: Envisioned interface for consumers to subscribe to multilevel demand subscription. Users can sign up for different reliability levels while defining the desired duration for each option. Source: [117].

Accordingly, the utility commits not only to honoring the reliability of each service option as in priority service, but also to honoring the duration of that option. The task of pricing the menu also becomes more challenging. Although the utility can still rely on aggregate statistical information about the population, it is now required to estimate a load duration curve for the population, parametric on a retail price. Therefore, the challenge of information asymmetry remains, with consumer types now characterized by a privately known index corresponding to their position on the system load duration curve. The aggregator uses this information in order to design a service offering that differentiates prices as a function of both reliability and duration. Note that, after subscribing to a service offering (for multilevel demand subscription or for priority service), the consumer satisfaction can be surveyed by the utility. This creates the possibility for the utility to improve the design of the menu through iterative communication with consumers and adaption of the offered menu.

1.3.2 Comparison to Alternative Methods for Engaging Consumers

Before advancing to the structure and contributions of the present dissertation, we briefly comment on how priority service and multilevel demand subscription compare to real-time pricing and direct load control. The latter are reasonable candidates for comparison, respectively belonging to price-based and quantity-based methods.

Although real-time pricing sets the efficient benchmark for engaging demand response, it stumbles upon a major difficulty. Residential consumers face fundamental challenges in assessing their real-time valuation for power. Under real-time pricing, every device within the household would be facing complex economic trade-offs at every balancing interval. By contrast, the goal of priority service and multilevel demand subscription is to simplify these economic trade-offs. The complexity of device scheduling is then transferred to a home energy router, which can gradually learn the preferences of the household. Moreover, as aforementioned in section 1.2.2, since consumer response to a change in price is uncertain and hard to predict with great precision [17], grid operators tend to prefer interruptible demand response programs than price-based methods for balancing supply and demand. This phenomenon is avoided with priority service since the aggregator has full control over the interruption of colors which are represented by a certain amount of kilowatts. The comparison between real-time pricing versus priority service is largely analogous to the standard dilemma between quantity versus price control in economics. This is a long-standing debate in the economics literature [175], and one argument in favor of quantity control is that it provides better insurance. Note that, in this work, the performance of real-time pricing may be over-estimated since we consider an ideal scenario where consumers are rational agents that react instantaneously to prices. This assumption may be too optimistic in practice, which would result in a degradation of the performance of real-time pricing.

On the other hand, direct load control is perceived as being overly intrusive [123]. Consumers prefer to maintain control over their devices, instead of handing that control over to a utility. In priority service and multilevel demand subscription, this is achieved by the color tagging system: if the household prefers to prioritize a certain device over another, it can swap the colors of the devices. Another important weakness of direct load control relates to lack of privacy. Privacy is a major concern in demand response, and has been a blocking point for the roll-out of demand response programs [134]. In the context of priority service and multilevel demand subscription, the utility is only aware of the aggregate kilowatts assigned to different service levels, as opposed to knowing which devices specifically constitute those kilowatts at any given balancing interval. Moreover, the literature on non-intrusive load monitoring allows an aggregator to infer the devices that are present in a household merely by ob-

serving the total consumption of this household. However, in order for these techniques to be effective, the power consumption of the household should be observed at a high frequency, typically larger than 1Hz. In the analysis of this thesis, the consumption of the household for each option will only be observed every 15 minutes by the aggregator, which allows the household to safeguard privacy with respect to electricity consumption.

Finally, it is worth commenting on how priority service may interact with different types of market structures. Traditional retailers typically expose themselves to risk in the wholesale electricity market, because they are required to serve consumers by buying energy from that market. However, consumers may require large amounts of power during periods with high prices, which can force retailers to procure expensive power. With priority service, the retailer is hedged since it can interrupt service to consumers during periods of high prices.

Demand response providers interact with capacity mechanisms as well as the enhancement of capacity mechanisms with reliability options [13] in order to extract another stream of revenue when launching demand response programs. Aggregators providing priority service contracts can specifically qualify for capacity markets. It is common in capacity mechanisms to only consider a portion of the bid capacity as qualifying for remuneration, since there is some uncertainty regarding the amount of demand response capacity that can be provided in real time. For example, if the aggregator is using a price-based demand response paradigm, the response of the consumers to changes in price can be highly uncertain. With priority service, the aggregator can always provide the qualified capacity with a considerable level of certainty, since consumers engage in capacity subscription. A remaining risk for the aggregator in this context is to match the offered reliability to the one promised during the menu design phase.

The literature in demand response has recently expanded in the field of transactive energy markets. Transactive energy markets are defined by [1] as 'the economic and control methodologies for managing the rate of consumption and generation resources and the energy trading within a power distribution network based on market mechanisms'. They aim at balancing supply and demand in electricity power networks while simplifying the large-scale integration of distributed resources [27]. Indeed, different parties can engage in transactions in these markets, in order to balance supply and demand. These parties include network operators, suppliers, aggregators, end-users, ... with each maximizing their individual profit. Different types of transactive mechanisms have been studied throughout these years, among them we can highlight peer-to-peer energy systems [114–116, 169] which are usually employed for engaging end-users in microgrids or small neighbourhoods. In this setting, we can envision a transactive energy market where aggregators providing priority service pricing to consumers may bid to provide demand response in order to

contribute towards balancing supply and demand at that particular level of the power network by interrupting certain options when needed.

1.4 Structure and Contributions

The research presented in this dissertation aims at exploring the effects of retail tariffs based on service quality differentiation for mobilizing residential flexible demand on power system operations and households electricity costs. This analysis only accounts for priority service pricing and multilevel demand subscription as candidates for demand response schemes. The conclusions of these studies are presented through five chapters which are linked to the particular contributions of the author to the existing literature.

- **Chapter 2: Combining Energy-Based Service Charges with Priority Service**
  In this chapter, a realistic consumer-centric analysis of several priority service pricing settings is provided along with a comparison against real-time pricing in terms of consumer comfort and expenditures. This analysis also demonstrates that service charges are a crucial element for the successful practical application of priority service in households. The content of this chapter relies on the following works:

  ◇ C. Gérard and A. Papavasiliou, "A comparison of priority service versus real-time pricing for enabling residential demand response", *2019 IEEE Power & Energy Society General Meeting (PESGM)*, IEEE, 2019.

  ◇ C. Gérard and A. Papavasiliou, "The role of service charges in the application of priority service pricing", *Energy Systems*, 2021. https://doi.org/10.1007/s12667-021-00471-7

- **Chapter 3: Designing Multilevel Demand Subscription Menus**
  This chapter investigates multilevel demand subscription as an alternative to priority service at the macroscopic scale. We first inspire ourselves by recent research on priority service [119] to cast the multilevel demand subscription menu design problem of Chao [25] as a Stackelberg game, which we express equivalently as a mixed integer linear program. Then, this reformulation is used to compare the two paradigms on nine types of households in a realistic model of the Belgian market. This study has led to the following publication:

  ◇ Y. Mou, C. Gérard, A. Papavasiliou and P. Chevalier, "Designing menus for multilevel demand subscription", *Proceedings of the 54th Hawaii International Conference on System Sciences*, 2021.

- **Chapter 4: Comparison of Priority Service with Multilevel Demand Subscription**
  This chapter develops a simulation framework based on the results of the previous chapter for comparing priority service, multilevel demand subscription, and real-time pricing on a system-wide level during real-time operations. The provided framework is used for developing the comparison on a model of the Belgian electricity system. The results described in this part of the dissertation are the focus of the following journal paper:

  ◇ *Submitted to IEEE Transactions on Smart Grid.* C. Gérard, D. Ávila, Y. Mou, A. Papavasiliou and P. Chevalier, "Comparison of priority service with multilevel demand subscription", *IEEE Transactions on Smart Grid*, 2021.

- **Chapter 5: Hierarchical Coordination of Medium and Low Voltage Distribution Grid in the Presence of Demand Response**
  This chapter describes preliminary research on how an aggregator that is responsible for several households under priority service can interact with the rest of the electricity network. The importance of integrating the network constraints in the computation of an aggregate residual demand function is illustrated on a simple example. The impact of different network constraint formulations on the resulting demand function is also highlighted using the same example.

- **Chapter 6: Conclusion and Future Perspectives**
  This chapter highlights the main insights of this dissertation and concludes the present document by outlining the future perspectives of the performed analysis.

2 Combining Energy-Based Service Charges with Priority Service

2.1 Introduction

As pointed out in section 1.3, priority service is a demand response aggregation paradigm that intends to combine the strengths of both real-time pricing and direct load control. In the original theory of priority service, it is proven that priority service and real-time pricing are equivalent in terms of consumer expenditures (Proposition III in [26]). However, we observe by means of a simple illustrative example [77] that this result can be violated under very reasonable relaxations of the assumptions employed by [26]. Intuitively, the reason why this equivalence result can break down is that the consumer needs to procure strips of service which need to be 'filled in' with jobs due to the capacity-based nature of priority service. This creates "holes" in the use of the contract, and effectively a non-concave incremental benefit function for households. This observation implies an increased cost of priority service for households, and motivates the addition of an energy component to the priority service scheme, so as to moderate the cost of the the total contract. This energy component is represented by the service charge of the priority service of the original theory. Even though this service charge was meant to be used as an added capacity component in order to decompose the settlement of consumers bills, our interpretation of service charges as energy charges provides increasing flexibility. Concretely, this component is required in realistic models of system operation in order to mitigate the cost of priority service for households that follow peaky consumption patterns.

What our analysis uncovers is that, although priority service theory is developed extensively, the literature on priority service is relatively terse in analyzing the role of service charges [131]. A specific proposal for service charges which is based on the marginal cost of supply is set forth by Chao [26]. In this chapter we revisit the theorems and proofs described in [26] for *any* non-zero service charge. The point of re-deriving these formulas is that they provide a useful starting point for the creation of a reasonable menu offering, even if the ideal

consumer who we assume is selecting menus in the original theory is much simpler than the inter-temporally constrained household model considered in this chapter. Consequently, we extend the theory by providing the following theoretical contributions in the present chapter:

- We propose a generalized version of the price menu constructed in [26] that accounts for *any* non-zero service charge function. We further prove that this menu is optimal in the sense that it induces a socially efficient choice of options from consumers.
- The equivalence proof regarding real-time pricing with priority service is extended to the mentioned generalized version of the price menu.
- We clarify the findings of [26] regarding the impact of a cutoff valuation on the equivalence proof between priority service and real-time pricing.
- We propose a way to compute service charges for a finite number of classes since finite menus are only provided in [26] in the case of a zero service charge.

After deriving generalized results for service charges in priority service contracts, we use these findings in order to develop practically viable offerings of priority service contracts with energy-based service charges that aim at not overwhelming the residential consumer with subscription fees. Accordingly, our work provides a realistic end-to-end analysis of several priority service pricing settings with energy-based service charges. The analysis aims at matching the level of rigor that has been devoted by the literature on real-time pricing. Our approach, which is consumer-centric and focuses specifically on consumer comfort and expenditures, is developed along the following four axes:

1. Designing priority service contracts with energy-based service charges.
2. Modeling the choice of an optimal contract by the household.
3. Simulating the dispatch of devices *given* a chosen contract.
4. Comparing several priority service schemes on a realistic case study.

We strive to integrate all of these axes in a single framework. By contrast, past literature on priority service [20, 23, 26, 108, 131, 136] is often limited to a subset of these dimensions, for example contract design [23, 26, 131], contract choice [23, 26, 108], or device dispatch [108, 136]. Note that the device dispatch model proposed in Margellos and Oren [108] is represented through a convex model. In our realistic representation of households, we considered non-convexities related to the power ratings of appliances. These non-convexities are represented by binary variables. We use our simulation framework to conduct a detailed analysis about the practical potential of demand response. This framework is also employed in order to provide insights on the interplay between priority service contracts with energy-based service charges and the incentive

to invest in home energy storage.

Concretely, in this chapter, we demonstrate that energy-based service charges become a crucial element for the successful practical application of priority service, especially for households that are characterized by peaky seasonal demand (e.g., as related to air conditioning loads in summer months). This energy component allows us to mitigate the capacity-based nature of priority service pricing, while preserving its simplicity relative to more complex contract offerings based on energy and capacity, such as multilevel demand subscription. Multilevel demand subscription is studied in Chapters 3 and 4.

The chapter is divided as follows. Section 2.2 generalizes the theory that characterizes priority service pricing in order to include non-zero service charges. Subsequently, section 2.3 is dedicated to the formulation of mathematical programs for scheduling appliances in a household subject to priority service or real-time pricing. In section 2.4 we present the data sources that we rely on for our case study. We also explain the procedure that we use for generating counterfactual real-time prices, and for designing a priority service menu with energy-based service charges that is comparable to real-time pricing. In section 2.5 we present our results on a case study of a typical household in Texas and compare them to a typical household in Belgium. Furthermore, we develop the main policy messages that emerge from the analysis of these results. Section 2.6 concludes the analysis of this chapter. Notation is summarized in the appendix 2.A.

2.2 Priority Service Pricing Theory

As discussed in section 1.3, priority service refers to an array of contingent forward contracts offered by an electricity supplier [26]. The selection of one option from the menu by each consumer determines the service order or priority of the consumer. Under each contingency, the seller rations supplies by serving customers in the order of their selected priorities. In the basic priority service model, v represents the valuation of a consumer for power. This valuation can equivalently be interpreted as a *ranking* of consumers, in the sense that under conditions of scarcity, consumers with higher valuation v should be entitled to higher-priority access to power. The function $D(v)$ corresponds to the demand function of the system. Information asymmetry means that the menu designer has access to *aggregate* system information (i.e., $D(v)$), but does not know which individual consumer corresponds to which type v *a priori* (i.e. when the contract is designed). This information is revealed ex post (i.e. after contracts are selected), following the revelation principle of mechanism design.

The key element of priority service pricing is the priority service menu $M = \{(p, s, r)\}$. The menu consists of (i) a priority charge p, which is payable

regardless of the usage of electricity, (ii) a service charge s, which is payable only when electricity is actually consumed, and (iii) a service reliability level r, which corresponds to the probability of receiving the product or service [26]. It is important to point out that the priority and service charges that are considered in the original theory as capacity-based. The role of the service charge s in the original theory is to decouple the settlement into two parts. In our work, we see the added value of using this service charge as an energy charge, so as to reduce the cost of priority service for households in a multi-temporal realistic case study. This is especially crucial for households with peaky consumption profiles. Concretely, in our interpretation of the original theory, if a consumer buys 2 kW and only consumes 1 kWh during hour 1, we assume that the service charge payment is s, not $2s$. Therefore, in this section, we revisit the original priority service theory presented in [26] in order to include service charges in a generalized form since the original theory proposes a specific formulation of the service charges based on marginal generator costs. The section is structured as follows. Section 2.2.1 restates Theorems I and II of [26] which characterize how consumers choose priority classes. Afterwards, section 2.2.2 presents an alternative to the priority service pricing menu in [26] that includes a general functional expression for service charges. Subsequently, in section 2.2.3, we show that the equivalence between priority service and spot pricing is maintained for a generalized form of service charge. Then, in section 2.2.4 we discuss the resulting effects in the priority service menu and the equivalence with spot pricing of adding a cutoff valuation. Finally, section 2.2.5 proposes a formula for service charges in the case of a menu with a finite number of classes. This final point is required for the practical implementation of priority service contracts in the case study of section 2.4.

2.2.1 Choice of Priority Classes by Consumers

As detailed previously, a priority service menu is composed of a set of options. The consumer chooses from the menu a priority option and assigns it to an increment of consumption. Concretely, we consider a continuum of consumers, with privately known types v. Each consumer engages in a forward agreement with an aggregator, according to which it pays a reservation charge p, in order to gain access to electricity service with reliability r. Additionally, the consumer pays a service charge s whenever it actually consumes power. As in the case of [26], without loss of generality, we characterize each consumer by a single unit of demand with an associated marginal willingness-to-pay v ($\in [0, V]$). Consequently, the objective of the consumer will be to choose from the menu M a priority option that maximizes its expected surplus. Therefore, for each v, the consumer solves the following problem:

$$Surplus(v) = \max\{\, r \cdot (v - s) - p \mid (p, s, r) \in M\}. \tag{2.1}$$

$Surplus(v)$ represents the surplus of a consumer with privately known type v when that consumer optimizes over the set of options offered in menu M. We

denote the optimal choice of a consumer of type v for the above problem as $\{p(v), s(v), r(v)\}$. Based on this consumer objective, two theorems are stated and proven in [26].

Theorem 2.1. *The optimal consumer choices satisfy the following conditions:* ***(A)*** *$r(v)$ is nondecreasing in v;* ***(B)*** *$p(v) + s(v) \cdot r(v)$ is nondecreasing in v; and* ***(C)*** *$p(v) + r(v) \cdot s(v) = \int_0^v [r(v) - r(u)]du$, for every v.*

Theorem 2.2. *If $p(\cdot)$, $s(\cdot)$, and $r(\cdot)$ satisfy conditions* ***(A)*** *and* ***(C)*** *stated in Theorem 2.1, and $M = \{(p(v), s(v), r(v)) \mid 0 \leq v \leq V\}$, then for each v, $(p(v), s(v), r(v))$ is an optimal solution to Problem (2.1).*

2.2.2 Priority Service Menu

In Chao [26], an optimal priority service menu with a specific formulation of service charge based on marginal cost of supply is presented. However, since this definition is restrictive, we present in this section a generalized version of this priority service menu by accounting for any form of service charge function. We further prove that this menu remains optimal according to the original theory.

Throughout this section, the representation of uncertainty used in [26] will be adopted. Therefore, all random variables are represented as a function of $\omega \in \Omega$, an abstract sample space associated with a σ field, and a probability measure. Following the standard theory [26], we denote by $\hat{p}(\omega)$ the instantaneous equilibrium price (or spot price) for electricity associated with a given random outcome ω. Then the service reliability of a type v consumer experiencing real-time pricing can be expressed as:

$$R(v) = \Pr[\hat{p}(\omega) \leq v]. \tag{2.2}$$

Eq. (2.2) indicates that the consumer is served in the events for which the spot price is less than its willingness to pay. Given this definition, we propose the following price menu M^*, and then show that it is equivalent to real-time pricing in section 2.2.3:

$$r^*(v) = R(v) \tag{2.3}$$

$$s^*(v) = S(v) \tag{2.4}$$

$$p^*(v) = \int_0^v [r^*(v) - r^*(u)]du - s^*(v)r^*(v) \tag{2.5}$$

$$M^* = \{(p^*(v), s^*(v), r^*(v)) \mid 0 \leq v \leq V\} \tag{2.6}$$

In our proposed menu, $S(v)$ can be any function of v and represents the mapping from consumer valuation to service charges. Note that this priority service menu is different from the one presented in [26]. Indeed, it does not consider any specific form of service charge and does not take a cutoff valuation into

account, whereas [26] defines a menu by specifying a service charge linked with the marginal cost of the supply side and a cutoff valuation.

Using Theorem 2.2, we can show that our priority service menu M^* induces optimal consumer choices.

Proof. In order to prove that M^* will induce optimal consumer choices, from Theorem 2.2, only conditions **(A)** and **(C)** must hold for M^* to be optimal.

Condition (A): By definition of $R(v)$, $r^*(v)$ is nondecreasing in v.

Condition (C): By definition of $p^*(v)$, it follows that:

$$\begin{aligned} p^*(v) + s^*(v) \cdot r^*(v) &= \left[\int_0^v [r^*(v) - r^*(u)]du - s^*(v) \cdot r^*(v) \right] + s^*(v) \cdot r^*(v) \\ &= \int_0^v [r^*(v) - r^*(u)]du \end{aligned}$$

Since conditions **(A)** and **(C)** hold, the price menu M^* induces optimal consumer choices for Problem (2.1). □

Note that this result implies that any form of service charge can be used (positive, negative, increasing, constant, decreasing, ...) while preserving the optimality of the menu. Under the ideal conditions presented in the original theory, the service charge does not have an essential impact, since $p(v) + s(v) \cdot r(v)$ can be aggregated into a new priority charge $\pi(v)$ with a 0 service charge. However, in practical settings which consider a multi-period framework and realistic assumptions for appliances leading to non-convexities, this service charge function can be useful in order to decrease the cost of priority service for households. Note that interpreting service charges as an energy-based component does not imply that information asymmetry is sacrificed.

2.2.3 Equivalence between Priority Service and Spot Pricing

An important practical attribute of priority service is that it should not overburden consumers. The natural benchmark of comparison is the consumer bill that would be incurred under real-time pricing. The practically relevant question is whether consumers pay a premium for the added simplicity of priority service pricing. Chao [26] proves that there is no such premium. Therefore, having proposed a priority service menu M^* with a general service charge and having proven its optimality, we are interested in exploring next to what extent the newly proposed menu retains the equivalence to real-time pricing proven in [26]. In this section, we are therefore able to establish that *any* service charge function can be used for designing a priority service menu that maintains the

theoretical equivalence of priority service and real-time pricing.

As emphasized by [26], the key difference between real-time pricing and priority service pricing is in the time frame. Indeed, any consumer experiencing real-time pricing will be subject to a price that is revised instantaneously as the status of supply and demand changes. Instead, under priority service, the consumer subscribes to a forward contract over a longer period of time. These two pricing schemes are closely related, and indeed spot pricing can be viewed as a limiting case of priority service as the pricing period is reduced to zero [26]. Proposition 2.3 in [26] establishes a close relation between the two pricing schemes. We now show that the proof holds for the case of a more general service charge function $s^*(v) = S(v)$ (see Eq. (2.4) above).

Proposition 2.3. *Under the assumption of risk neutrality, priority service pricing and spot pricing are equivalent from the perspective of individual consumers. The expected expenditures and the expected surplus of each consumer under the two pricing schemes are identical. That is,*

$$p^*(v) + s^*(v) \cdot r^*(v) = \mathbb{E}\{\hat{p}(\omega) \cdot I_{\{\hat{p}(\omega) \le v\}}(\omega)\}$$

and

$$[v - s^*(v)] \cdot r^*(v) - p^*(v) = \mathbb{E}\{[v - \hat{p}(\omega)] \cdot I_{\{\hat{p}(\omega) \le v\}}(\omega)\}$$

where $I_{\{\hat{p}(\omega) \le v\}}(\omega)$ is an indicator function, which takes on value 1 or 0 depending on whether ω belongs to the set $\{\omega : \hat{p}(\omega) \le v\}$.

Proof. The expected expenditure of a consumer of type v under spot pricing can be written as follows:

$$\begin{aligned}
&\mathbb{E}\{\hat{p}(\omega) \cdot I_{\{\hat{p}(\omega) \le v\}}(\omega)\} \\
&\quad = \int_{-\infty}^{+\infty} x \cdot \Pr[\hat{p}(\omega) \cdot I_{\{\hat{p}(\omega) \le v\}}(\omega) = x]\, dx \qquad \text{(by definition of operator } \mathbb{E}) \\
&\quad = \int_{0}^{v} x \cdot \Pr[\hat{p}(\omega) \cdot I_{\{\hat{p}(\omega) \le v\}}(\omega) = x]\, dx \qquad \text{(because } 0 \le x \le v) \\
&\quad = \left[x \cdot \Pr[\hat{p}(\omega) \cdot I_{\{\hat{p}(\omega) \le v\}}(\omega) \le x]\right]_0^v - \int_0^v \Pr[\hat{p}(\omega) \cdot I_{\{\hat{p}(\omega) \le v\}}(\omega) \le x]\, dx \\
&\qquad\qquad \text{(integration by parts[1])} \\
&\quad = v - \int_0^v \Pr[\hat{p}(\omega) \cdot I_{\{\hat{p}(\omega) \le v\}}(\omega) \le x]\, dx \\
&\quad = v - \int_0^v \left[1 - \Pr[\hat{p}(\omega) \cdot I_{\{\hat{p}(\omega) \le v\}}(\omega) \ge x]\right] dx \\
&\quad = \int_0^v \Pr[\hat{p}(\omega) \cdot I_{\{\hat{p}(\omega) \le v\}}(\omega) \ge x]\, dx \\
&\quad = \int_0^v \Pr[x \le \hat{p}(\omega) \le v]\, dx
\end{aligned}$$

$$
\begin{aligned}
&= \int_0^v \left[\Pr[\hat{p}(\omega) \leq v] - \Pr[\hat{p}(\omega) \leq x] \right] dx \\
&= \int_0^v \left[R(v) - R(x) \right] dx && \text{(by definition of } R(v)\text{)} \\
&= r^*(v) \cdot v - \int_0^v r^*(x)\, dx && \text{(by definition of } r^*(v)\text{)} \\
&= \int_0^v \left[r^*(v) - r^*(x) \right] dx \\
&= p^*(v) + s^*(v) \cdot r^*(v) && \text{(by Theorem 2.1)}
\end{aligned}
$$

□

The general intuition behind this equivalence proof lies in the fact that real-time pricing implies a certain profile of consumption for the system. In a static framework, the valuation of each consumer is fixed. This allows the aggregator to rank the priority of service of different consumers based on their valuation. Knowing the priority of service of each consumer, when a continuum of priority service options is considered, allows the aggregator to compute the reliability that a particular consumer (i.e. valuation) is entilted to. A crucial observation in the above proof is that the argument does not depend on any particular service charge. Thus, the general service charge that we propose in Eq. (2.4) above is valid for this proof, and therefore the equivalence between real-time pricing and priority service that is expressed in Proposition II of [26] still holds. Note that the choice of the service charge is left to the menu designer. Concretely, this result allows us to determine a procedure for computing an *optimal* menu (as opposed to comparing real-time pricing to an arbitrary priority service menu that allocates resources in the system suboptimally). Note that we show in [77] that this proposition does not hold in practical settings with non-concave demand functions that emerge due to inter-temporal dependencies and non-convexities related to the operation of devices. The illustrative example used in [77] is detailed in appendix 2.B.

2.2.4 Role of Cutoff Valuation

In this section we analyze the interplay of the non-zero service charge with the cutoff valuation v_0. We are specifically interested in analyzing whether the equivalence between real-time pricing and priority service remains valid. Indeed, it is not clear from the proof of Proposition II in [26] whether this equivalence result still holds for a positive cutoff valuation. Therefore, we propose the following priority service pricing menu, M^{**}, that uses a cutoff

[1] Integration by parts on x and $\Pr[\hat{p}(\omega) I_{\{\hat{p}(\omega) \leq v\}}(\omega) = x]$ where the indefinite integral of the second term is $\Pr[\hat{p}(\omega) I_{\{\hat{p}(\omega) \leq v\}}(\omega) \leq x]$ by definition of the cumulative distribution and probability density function.

valuation v_0 and a general form of service charge:

$$r^{**}(v) = \begin{cases} R(v) & \text{if } v \geq v_0 \\ 0 & \text{if } v < v_0 \end{cases} \tag{2.7}$$

$$s^{**}(v) = \begin{cases} S(v) & \text{if } v \geq v_0 \\ 0 & \text{if } v < v_0 \end{cases} \tag{2.8}$$

$$p^{**}(v) = \int_0^v [r^{**}(v) - r^{**}(u)]du - s^{**}(v) \cdot r^{**}(v) \tag{2.9}$$

$$M^{**} = \{(p^{**}(v), s^{**}(v), r^{**}(v)) \mid 0 \leq v \leq V\} \tag{2.10}$$

Similarly to the menu presented in section 2.2.2, M^{**} can be shown to induce optimal consumer choices. Indeed, priority service menu M^{**} verifies conditions **(A)** and **(C)**.

Having established the optimality of the priority service menu M^{**}, we discuss the influence of the presence of a cutoff valuation on the equivalence result between real-time pricing and priority service. We show that the equivalence holds only for $v_0 \in [0, V]$ such that:

$$\int_0^{v_0} R(x)\, dx = 0.$$

Since $R(x) \geq 0$, this condition is equivalent to:

$$R(x) = 0 \; \forall x \in [0, v_0].$$

Proof. For the priority menu M^{**}, we can keep the equivalence proof until the step where the function $R(x)$ is introduced in the equation. We have:

$$\begin{aligned}
\mathbb{E}\{\hat{p}(\omega) \cdot I_{\{\hat{p}(\omega) \leq v\}}(\omega)\} &= \int_0^v \left[R(v) - R(x)\right] dx \\
&= R(v) \cdot v - \int_0^v R(x)\, dx \\
&= r^{**}(v) \cdot v - \left[\int_0^{v_0} R(x)\, dx + \int_{v_0}^v r^{**}(x)\, dx\right] \\
&= \int_0^v [r^{**}(v) - r^{**}(x)]\, dx - \int_0^{v_0} R(x)\, dx \\
&= p^{**}(v) + s^{**}(v) \cdot r^{**}(v) - \int_0^{v_0} R(x)\, dx
\end{aligned}$$

Therefore, the equivalence is only verified when the integral part of the sum is equal to 0. □

2.2.5 Priority Service Pricing for a Finite Number of Classes

In order to implement priority service in a practical setting, it is necessary to consider a finite number of priority classes instead of a continuum of options. Chao [26] only provides results for designing a menu with a finite set of options, in which the service charge is zero. In this section, we relax this assumption. First, we demonstrate that Proposition VI of [26] holds for a non-zero service charge. Furthermore, we propose a way to compute service charges for a finite number of classes. In doing so, we closely follow the original theory, but adapt it to the needs of our analysis for performing a simulation on a realistic case study. In this setting, consumers are divided into n priority classes based on their willingness to pay, say $[0, v_1]$, $[v_1, v_2]$, ..., $[v_{n-1}, V]$, where $0 = v_0 < v_1 < ... < v_{n-1} < v_n = V$. Service is provided to consumers such that consumers in a higher value class enjoy a higher priority (and pay more), however, within each class, all consumers are treated equally and therefore are served in a random order. Then, the probability that a consumer with valuation v between v_i and v_{i+1} will be served is:

$$r(v) = r_i = \int_{v_i}^{v_{i+1}} \left[\frac{D(v) - D(v_{i+1})}{D(v_i) - D(v_{i+1})} \right] dR(v) + R(v_i). \tag{2.11}$$

We propose, in this section, a formula that can be used in order to create a unique service charge per class:

$$s(v) = s_i = \int_{v_i}^{v_{i+1}} \left[\frac{D(v) - D(v_{i+1})}{D(v_i) - D(v_{i+1})} \right] dS(v) + S(v_i) \tag{2.12}$$

The total payment of a consumer in priority class i is computed as:

$$\begin{aligned} p(v) + r(v) \cdot s(v) = p_i + s_i \cdot r_i &= \int_0^v [r(v) - r(u)]du \\ &= v_0 \cdot r_0 + \sum_{j=1}^{i} v_j \cdot (r_j - r_{j-1}) \end{aligned} \tag{2.13}$$

Given the proposed transformation of a continuum of priority classes to a finite number, we can revisit the result presented in [26] regarding the surplus obtained with a finite number of priority classes. Indeed, the authors in [26] prove the following proposition, which considers a priority service menu with no service charge and additional assumptions.

Proposition 2.4. *The surplus that is unrealized due to a finite number n of priority classes is of order $\frac{1}{n^2}$. That is, $S_n \geq S_\infty - O(\frac{1}{n^2})$.*

Our analysis allows us to conclude that this proposition can be extended to the case where the service charge is represented by *any* function. Indeed, the proof linked with this proposition does not depend on the form of the service

charge. Therefore, this result can be used in order to demonstrate that, even with a non-zero service charge, nearly 90% of the potential benefit of priority service pricing can be captured by offering just three priority classes, as in the ColorPower approach that we describe in section 1.3 and specifically analyze in this dissertation.

2.3 Household Decision Model

In order to quantify the impact of real-time pricing and the influence of adding energy-based service charges to priority service on consumers, we describe mixed integer linear programming formulations for scheduling appliances efficiently in the house under each scheme. These scheduling problems proxy the behavior of a home energy management system. Such a home energy management system places minimum decision-making requirements on residential consumers, by automating electricity consumption in the house, so that this consumption reacts to utility pricing signals. An extensive review of home energy management systems is provided in [181].

Most of the work in the field of home energy management systems is focused on real-time pricing [8, 29, 35, 83, 89, 168, 173, 176]. Notably, a limited amount of the recent literature analyzes the impact of alternatives to real-time pricing. For example, Hayn [85] compares the impact of a flat tariff, a variable energy tariff, a variable capacity tariff and a combination of energy with capacity tariffs.

Whereas the majority of the home energy management system literature is devoted to real-time pricing, the modeling approach that is used for solving the appliance scheduling problem is wide. Reinforcement learning has been considered as a viable approach for adaptive real-time home energy systems [83, 130, 176]. Jin *et al.* [93] employs model predictive control. Mathematical programming formulations based on mixed integer linear programs (MILP) are widespread in the literature [8, 29, 77, 85, 89, 105, 122]. Due to computational considerations, certain papers adopt a relaxed formulation of MILP programs [168]. For a broad review on modeling approaches applied to home energy management systems, we refer the reader to Beaudin and Zareipour [9]. To a large extent, the aforementioned research assesses the impact of different tariffs on the operation of the system [79, 85]. By contrast, the impact of demand response schemes on consumer comfort and monthly electricity bills often receives less consideration. Instead, this chapter is focused on the impact of demand response on *consumers*, rather than the system.

The notable growth of the literature on home energy management systems has in part been possible due to large demand response pilot programs that have been deployed recently. Such demand response programs increase the

amount of available data that is accessible to the research community, even at the level of individual appliances. For instance, the LINEAR demand response pilot provides insights about the flexibility of wet appliances in Belgium [34]. The availability of appliance-level consumption data and consumer features allows the research community to generate synthetic load profiles for residential consumers [150]. This is expected to proliferate further analysis for understanding the impact of demand response on consumers.

In this work, we consider a household that contains a battery, solar panels, an electric vehicle, and several appliances that can be considered as being flexible or inflexible loads. Flexible loads correspond to "jobs" with specific execution deadlines and power consumption profiles, which are assumed to be known in advance. These include wet appliances (dishwashers, washing machines and tumble dryers). Cycling appliances such as HVAC, fridges and freezers are not considered as being flexible in this work due to computational reasons. This direction may be interesting to consider in further developments of this work. Finally, no uncertainty regarding arrival times, deadlines, consumption profiles, etc. is considered in the present model.

Several assumptions are used in our analysis, following [77]:

(A1) An appliance can change color (i.e. move to a different reliability tier) while in the middle of executing a power consumption profile in the priority service setting;

(A2) An appliance can be interrupted at any stage of its operation and be started on again at the stage it was interrupted;

(A3) An appliance arrives with a deadline by which the task of the appliance must be completed, in order for the consumer to avoid any frustration;

(A4) The power consumption footprint of each appliance is known.

(A5) Any unused solar power is wasted. No payment is made by the grid to buy that extra solar power.

A footprint of an appliance is defined as the usual consumption pattern of the appliance. The estimation of these consumption patterns is the focus of an extensive body of literature on non-intrusive load monitoring [84].

We now proceed with the mathematical programming formulations of the device scheduling problems. The formulation is inspired from [85], but modified in order to include features that are particular to priority service. Note that binary variables are often used in the optimization demand response literature [94] which is the case here since both formulations are mixed integer linear programs (MILP). Section 2.3.1 presents the real-time pricing setting. In section 2.3.2 we describe the changes that are required in order to represent priority service.

2.3.1 Real-Time Pricing

In this section, we describe a mathematical program that schedules appliances under real-time pricing in a household. In this setup, the consumer is facing a real-time price for electricity and chooses which appliances to turn on or off by reacting to electricity prices. In the following model, we assume perfect foresight on the realization of real-time prices. We divide the description of the mathematical program into different elements that are present in the household.

Solar Panels and Inflexible Load

Solar production at time step t is represented by S_t, and s_t corresponds to the solar supply actually used. Inflexible load consumption in period t is denoted by B_t, and corresponds to inflexible appliances. The consumer may decide to serve only a portion b_t of its inflexible load, and incurs a cost of ϕ per unit of discarded energy. The following constraints are thus added to the overall program:

$$0 \leq s_t \leq S_t \ \ \forall t \in \mathcal{T}, \tag{2.14}$$

$$0 \leq b_t \leq B_t \ \ \forall t \in \mathcal{T}. \tag{2.15}$$

Electric vehicle

The state of charge of the home electric vehicle is denoted by soc_t^{EV} and its maximum capacity is EV^{max}. The charge efficiency is denoted by η^{EV}. The charge and discharge decisions are represented respectively by ch_t^{EV} and dis_t^{EV}, and are limited by the maximum rates, which are expressed respectively by Ch_{EV}^{max} and Dis_{EV}^{max}. Since the electric vehicle is either charging or discharging at any given moment, we use a binary indicator variable u_t^{EV} in order to represent the charge/discharge state of the vehicle. Finally, charging or discharging requires the vehicle to be plugged in. The parameters T_A and T_D represent, respectively, the time of arrival and departure of the vehicle. The parameters EV_A and EV_D express, respectively, the state of charge at arrival and departure. The operation of the electric vehicle can therefore be represented by the following constraints, based on [52, 73, 76]:

$$0 \leq ch_t^{EV} \leq Ch_{EV}^{max} \cdot u_t^{EV} \ \ \forall t \in \mathcal{T}, \tag{2.16}$$

$$0 \leq dis_t^{EV} \leq Dis_{EV}^{max} \cdot (1 - u_t^{EV}) \ \ \forall t \in \mathcal{T}, \tag{2.17}$$

$$0 \leq soc_t^{EV} \leq EV^{max} \ \ \forall t \in \mathcal{T}, \tag{2.18}$$

$$soc_t^{EV} = soc_{t-1}^{EV} + \Delta t \cdot \left[\eta^{EV} ch_t^{EV} - dis_t^{EV}\right] \ \ \forall t \in [T_A + 1; T_D], \tag{2.19}$$

$$ch_t^{EV} = dis_t^{EV} = 0 \ \ \forall t \notin]T_A; T_D[, \tag{2.20}$$

$$soc_t^{EV} = 0 \ \ \forall t \notin [T_A; T_D], \tag{2.21}$$

$$soc_{T_A}^{EV} = EV_A, \tag{2.22}$$

$$soc_{T_D}^{EV} = EV_D, \tag{2.23}$$
$$soc_0^{EV} = EV^{max}, \tag{2.24}$$
$$u_t^{EV} \in \{0,1\} \ \ \forall t \in \mathcal{T}, \tag{2.25}$$

Here, Δt corresponds to the number of hours present in a time period, e.g. 0.25 in the case of 15-minute intervals.

Flexible Appliances

As explained previously, flexible appliances are modeled as power demand arrivals with specific deadlines and interruptible power consumption profiles. A consumption profile is divided into one power level/part per time period. The binary variable $x_{t,j,\beta,\tau}$ is 1 if part τ of appliance j that arrives at time β is scheduled to run at time t. The flexible appliances are modeled by the following set of constraints:

$$1 \geq \sum_{\tau \in \mathcal{T}_j} x_{t,j,\beta,\tau} \ \ \forall t \in \mathcal{T}, \ j \in \mathcal{J}, \ \beta \in \mathcal{B}_j, \tag{2.26}$$
$$1 \geq \sum_{t \in \mathcal{T}} x_{t,j,\beta,\tau} \ \ \forall j \in \mathcal{J}, \ \beta \in \mathcal{B}_j, \ \tau \in \mathcal{T}_j, \tag{2.27}$$
$$\sum_{t<t_{ON}} x_{t,j,\beta,\tau} \geq x_{t_{ON},j,\beta,\tau+1} \ \ \forall t_{ON} \in \mathcal{T}, \ j \in \mathcal{J}, \beta \in \mathcal{B}_j, \tau \in \mathcal{T}_j \setminus \{\tau_{end}\}, \tag{2.28}$$
$$1 = \sum_{t<\beta+1} x_{t,j,\beta,\tau_{end}} \ \ \forall j \in \mathcal{J}, \ \beta \in \mathcal{B}_j, \tag{2.29}$$
$$x_{t,j,\beta,\tau} \in \{0,1\} \ \ \forall t \in \mathcal{T}, \ j \in \mathcal{J}, \ \beta \in \mathcal{B}_j, \ \tau \in \mathcal{T}_j. \tag{2.30}$$

Eq. (2.26) expresses the fact that only one part of the profile of an appliance j can be served during a certain time period. The fact that a part of an appliance can only be served once in the entire horizon is represented by Eq. (2.27). Furthermore, the order of the parts of the consumption profile of each appliance must be respected. For example, the first hour of the washing machine has to be served before the second one. This is described in Eq. (2.28). Finally, an appliance must finish before the next arrival of that appliance see Eq. (2.29).

Battery

The constraints representing the operation of the household battery are given by Eqs. (2.31)-(2.36). The notation follows the exposition of the electric vehicle model.

$$0 \leq ch_t^B \leq Ch_B^{max} \cdot u_t^B \ \ \forall t \in \mathcal{T} \tag{2.31}$$
$$0 \leq dis_t^B \leq Dis_B^{max} \cdot (1 - u_t^B) \ \ \forall t \in \mathcal{T} \tag{2.32}$$

$$0 \leq soc_t^B \leq B^{max} \ \ \forall t \in \mathcal{T} \tag{2.33}$$

$$soc_t^B = soc_{t-1}^B + \Delta t \cdot \left[\eta^B ch_t^B - dis_t^B\right] \ \ \forall t \in \mathcal{T} \tag{2.34}$$

$$u_t^B \in \{0,1\} \ \ \forall t \in \mathcal{T} \tag{2.35}$$

$$soc_0^B = 0 \tag{2.36}$$

Power Balance and Objective Function

The goal of the household is to minimize the sum of the expenditures in the real-time market and consumer discomfort:

$$\sum_{t\in\mathcal{T}} \Delta t \cdot \left[\lambda_t \cdot y_t + \phi \cdot (B_t - b_t)\right] + \sum_{\substack{j\in\mathcal{J},\beta\in\mathcal{B}_j,\\ t>D_j+\beta}} F_j \cdot (t - D_j - \beta) \cdot x_{t,j,\beta,\tau_{end}} \tag{2.37}$$

The first term of the sum represents the payments to the real-time market. Here, λ_t corresponds to the real-time price of electricity, and y_t to the total electricity consumption. The second term is linked with the extra cost due to shedding of inflexible consumption. Finally, the last term represents the frustration of the consumer for any delay in serving a flexible appliance beyond its deadline D_j, where F_j is a measure for this frustration.

The total device scheduling model under real-time pricing can then be expressed as follows:

$$\begin{aligned}
\min_{\substack{x_{t,j,\beta,\tau}, y_t, s_t, b_t, u_t^B,\\ ch_t^B, dis_t^B, soc_t^B, u_t^{EV},\\ ch_t^{EV}, dis_t^{EV}, soc_t^{EV}}} \quad & (2.37) \\
\text{s.t.} \quad & (2.14) - (2.36) \\
& y_t = b_t - s_t + ch_t^{EV} - dis_t^{EV} + ch_t^B - dis_t^B \\
& \qquad + \sum_{j,\beta,\tau} \rho_{j,\tau} \cdot x_{t,j,\beta,\tau} \ \ \forall t \in \mathcal{T} \quad (2.38) \\
& y_t \geq 0 \ \ \forall t \in \mathcal{T} \quad (2.39)
\end{aligned}$$

The total consumption of the household is thus the sum of the consumption of each flexible appliance along with inflexible load, battery charge/discharge, and electric vehicle charge/discharge at every time period. The parameter $\rho_{j,\tau}$ represents the consumption pattern of part τ of appliance j.

2.3.2 Priority Service Pricing

In this section, the mathematical program which schedules appliances by means of priority service pricing combined with energy-based service charges is presented. As pointed out in section 1.3, we consider a priority service price menu

that contains three options corresponding to colors [136]. Each color corresponds to a different level of reliability for serving electricity and is represented by an additional index i contained in set $\mathcal{I}$. The priority service pricing scheme is different from the real-time approach because the consumer subscribes for a certain amount of *capacity* to each option of the menu at the beginning of the horizon instead of facing variable prices at each time period. After subscribing, the consumer is entitled to the requested *capacity* for each color and faces the reliability of the corresponding option. The objective function in the case of priority service pricing combined with energy-based service charges is therefore given by Eq. (2.40).

$$\sum_{i\in\mathcal{I}} \Delta t \cdot \left[|\mathcal{T}| \cdot \lambda_i^P \cdot P_i^{max} + \sum_{t\in\mathcal{T}} \lambda_i^S \cdot y_{t,i} \right] + \sum_{t\in\mathcal{T}} \phi \cdot \Delta t \cdot \left[B_t - \sum_{i\in\mathcal{I}} b_{t,i} \right] + \sum_{\substack{i\in\mathcal{I}, j\in\mathcal{J}, \\ \beta\in\mathcal{B}_j, \\ t>D_j+\beta}} F_j \cdot (t - D_j - \beta) \cdot x_{t,j,\beta,\tau_{end},i} \tag{2.40}$$

The first term in the sum represents the expenditure of the consumer for subscribing to an amount of power P_i^{max} with a *priority charge* λ_i^P for each option i at the beginning of the horizon. The second term corresponds to the cost due to the actual consumption of electricity. Here, λ_i^S is the energy-based *service charge* for option i. Finally, the two last terms are similar to the ones presented for the real-time pricing model. Note that any inflexible load shedding incurred by the household due to unreliable service is not planned, and its cost is captured by Eq. (2.40).

The total consumption under each option i is bounded by the amount of power procured in the beginning of the horizon. The additional constraints of the priority service model are given by Eq. (2.41).

$$0 \leq y_{t,i} \leq profile_{t,i} \cdot P_i^{max} \quad \forall t \in \mathcal{T},\ i \in \mathcal{I} \tag{2.41}$$

Here, $profile_{t,i}$ is a binary parameter that records if color i is interrupted or not at time period t. The mathematical program that schedules appliances based on priority service with energy-based service charges can be obtained from the real-time pricing model, using the same procedure as in [77], by: (i) adding a summation over the different colors to every equation of the model; (ii) using the new objective function given in Eq. (2.40); (iii) adding Eq. (2.41) to the model.

2.4 Case Study

We apply our model of priority service with energy-based service charges and real-time pricing to realistic household models. We rely on three categories

of data, which we now present. In section 2.4.1 we describe the data used for populating the household models. Section 2.4.2 is devoted to the construction of a series of real-time prices in a forward-looking scenario of widespread demand response adoption. This is needed in order to create a priority service menu on the basis of meaningful real-time prices for a system considering a large penetration of demand response. It is also essential to realize a meaningful comparison between the two demand response schemes. Finally, in section 2.4.3 we describe how we design a priority service menu which is consistent with the real-time prices of the market.

2.4.1 Household Data

We use the Texas household with identity number 661 from the Pecan Street data set [141]. The total electricity consumption of the household, along with several appliance consumption profiles, is available at a 15-minute resolution. The electricity production of the solar panel in the household for 2018 is also part of the data set.

Solar and Inflexible Load

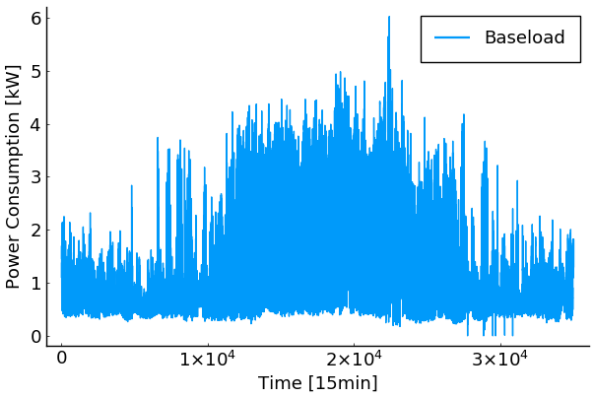

Figure 2.1: Inflexible load consumption (referred to as baseload in the graph) of the considered Texas household for the year 2018. Source: Pecan Street Inc. Dataport.

We obtain the inflexible load of the household by subtracting the consumption of flexible appliances from the total load. The appliances defined in this work as being flexible are the washing machine, the dishwasher, and the tumble dryer. The inflexible load and solar production of our chosen household for the year 2018 are presented in Figure 2.1. The total energy corresponding to inflexible demand amounts to 10777 kWh over the year. The total solar energy produced throughout the year corresponds to approximately 70% of the inflexible load (7762 kWh). However, the lack of synchronization between solar production and inflexible consumption implies that solar power can only

serve 30% of the inflexible demand. The annual energy consumption for the electric vehicle and the flexible appliances is equal to 3284 kWh and 380 kWh, respectively.

Flexible Appliances

The deadline is computed as the average flexibility window observed for each wet appliance in [34]. Following [34], disutility values are assumed to be constant over time. This assumption cannot capture the growing frustration of a consumer that is subject to several consecutive delays, as this level of detail is out of scope for the present work.

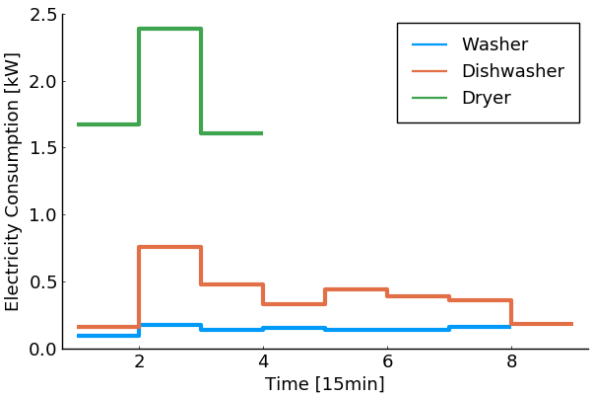

Figure 2.2: Washing machine, dishwasher and tumble dryer electricity consumption profiles for the Texas household. Source: Pecan Street Inc. Dataport.

Electric Vehicle

We consider a Chevy Volt with a battery capacity of 16 kWh [52]. The maximum charging and discharging power amounts to 3.3 kW. We assume a charging efficiency of 95%. The data concerning the use of the electric vehicle are based on a German study [111]. The results of the study show that electric vehicles are mostly used during weekdays, in order to drive to work, which is our assumption for this case study. Based on [111], we assume a typical departure and arrival time of 8am and 5:30pm respectively. Concerning the arrival and departure state of charge, the electric vehicle is ensured to be fully charged right before departure, and returns from work after traveling a distance of 60 km per day with an assumed consumption of 0.2 kW/km [111].

Battery

The battery specifications are based on the Tesla Powerwall 2 [166]. The total capacity of the battery is equal to 13.5 kWh. The maximum charging and

discharging power is considered to be 5 kW and the charging efficiency is 90%. The annual battery investment cost is sourced from [117] and ranges from 85 to 496$/year. This cost range accounts for potential future improvements in battery manufacturing costs (1110 to 3330$), varying lifespan of the battery (15 to 20 years), and varying annual discount rates (3 to 10%).

2.4.2 Real-Time Prices

We consider households that are exposed to the wholesale market of the Electric Reliability Council of Texas (ERCOT) [51]. Note that the real-time prices that have transpired in ERCOT in the past are based on a relatively inelastic demand function. The goal of this section is to use these observed real-time prices in order to estimate a new price series that accounts for the flexibility of residential consumers. This is needed in order to create input for Eqs. (2.3)-(2.6), which are required for determining an *optimal* priority service menu which allocates system resources efficiently to consumers.

The generation of this new time series of real-time prices uses as input the historically realized real-time prices, the historically realized demand, and the wind and solar production of each 15-minute period of 2018. The process of obtaining counterfactual real-time prices is described as follows:

1. Form groups of 15-minute periods with similar solar and wind production, by means of clustering.

2. For each group, create a piecewise linear supply function. Assume a zero cost for wind and solar production, and use a linear regression over the set of historically observed market clearing prices and quantities. We assume that the system has a maximum production capacity of 110 GW.

3. For each 15-minute period, estimate an isoelastic demand function with an elasticity of -0.5 based on the observed price-quantity data point. The curve is shifted by the amount of industrial demand, which is assumed to be inflexible.

4. For each 15-minute period, compute a new real-time price by using the intersection of the estimated demand function and the respective supply function of the group to which the period belongs.

Summary statistics of the new real-time prices, compared to the old ones, are presented in Figure 2.3.

2.4.3 Priority Service Menu

As we note in Eqs. (2.3)-(2.6), the design of an *optimal* priority service menu requires as input the time series of equilibrium real-time prices. In this chapter, we have generalized the theory of [26] in order to account for *optimal* menus

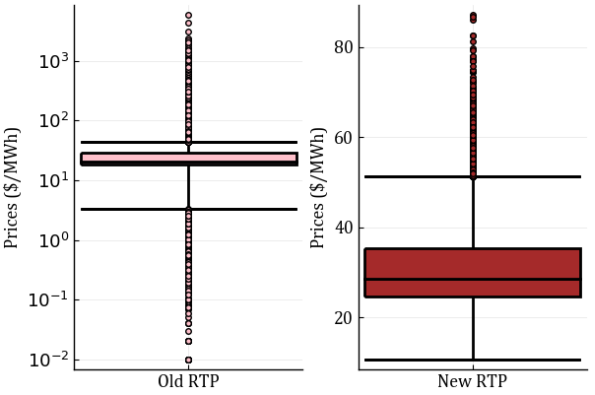

Figure 2.3: Summary statistics of historically observed real-time prices, versus counterfactual prices based on a market with an elastic residential sector.

with service charges. This extension gives us a reasonable starting point for creating a priority service menu with non-zero service charges based on real-time prices. The procedure can be summarized as follows:

1. Create an optimal reliability curve $R(v)$ using Eq. (2.2), which indicates the proportion of time that a consumer with a certain valuation should be served under efficient real-time dispatch.

2. Decide on a service charge function $S(v)$. In this work, the service charge is considered to be a constant function of consumer valuation. Four values of service charge are analyzed: 0, 10, 20 and 25\$/MWh, in order to assess the impact of the service charge level on the electricity bill of households. Thus, we create 4 priority service menus, one for each service charge.

3. Use Eqs. (2.11)-(2.12) to transform the continuum of options into only 3 options. Concretely, we use the reliability levels that are indicated in Table 2.1 in order to compute the valuation breakpoints from Eqs. (2.11)-(2.12).

4. Compute the priority charge of each option for each choice of service charge, using Eq. (2.13).

The priority charge of each menu is presented in Table 2.1. Each column corresponds to a different service charge.

The interruption profile of each option is created as follows. For each option, each 15-minute period belonging to the x% lowest real-time prices is considered to be a period when that option has access to electricity service. Here, x corresponds to the reliability of the option. For example, the 60% lowest real-time prices are the periods when the green color will be ON.

Table 2.1: Priority service menus for different levels of energy-based service charges.

Colour	Reliability [%]	p_0 [$/MWh]	p_{10} [$/MWh]	p_{20} [$/MWh]	p_{25} [$/MWh]
Green	60	15.08	9.08	3.06	0.06
Yellow	85	24.54	16.04	7.54	3.29
Red	99	30.8	20.9	10.98	6.03

2.5 Results and Discussions

Numerical experiments are performed using the **JuMP** package [36] in the **Julia** programming language [12]. The optimization program presented in section 2.3 is solved for every week of an entire year. Therefore, the analysis is dynamic, as it accounts for inter-daily and inter-seasonal variations. Breaking the device scheduling into weekly sub-problems lowers computation time and permits efficient use of parallel computing. The mathematical programs are solved using the **Gurobi** optimization solver [81]. We run our programs on the high performance computing Lemaitre3 cluster hosted at UCLouvain and part of the CECI facility. We present the results of these simulations in Table 2.2.

Two simulations are performed regarding priority service:

1. One simulation for which the consumer subscribes to a single contract for the entire year.
2. One simulation where the consumer can change its subscription from one week to the next. Allowing the consumer to update its choice on a weekly basis reduces the amount of power that is procured without being used by taking into account the impacts of a varying weekly consumption profile.

The first simulation is motivated by the premise that priority service combined with energy-based service charges offers a simple alternative to real-time pricing, by not requiring consumers to update their contracts too often. The results for the first simulation are presented in the lines of Table 2.2 corresponding to "yearly" for the subscription type. The results of the second simulation are presented in the other lines of the table. Note that the best contract for the first simulation is chosen among the set of best weekly contracts generated by the second simulation.

From the results that are presented in Table 2.2, we can provide the following observations, which are discussed in detail in the following sections:

- Adding energy-based service charges is essential in keeping costs manageable for priority service pricing.
- Priority service pricing is significantly more expensive for households than real-time pricing.

Table 2.2: Consumer costs [$/year] for real-time and priority service pricing for different energy-based service charge levels (0, 10, 20, and 25$/MWh).

Dataset	Subscription Type	Pricing Scheme Battery	RTP No	RTP Yes	PSP-0 No	PSP-0 Yes	PSP-10 No	PSP-10 Yes	PSP-20 No	PSP-20 Yes	PSP-25 No	PSP-25 Yes
Texas	Weekly	Electricity Bill	290.95	203.97	606.99	334.33	510.52	297.59	408.06	257.17	350.79	224.64
		Discomfort	0.0	0.0	401.21	0.0	393.32	0.0	387.78	0.0	387.78	0.0
		Total	**290.95**	**203.97**	**1008.2**	**334.33**	**903.84**	**297.6**	**795.85**	**257.17**	**738.57**	**224.65**
	Yearly	Electricity Bill	290.95	203.97	1111.61	838.55	854.69	646.67	644.83	484.72	387.79	361.47
		Discomfort	0.0	0.0	475.45	32.07	475.45	32.07	413.9	0.0	519.19	11.08
		Total	**290.95**	**203.97**	**1587.06**	**870.62**	**1330.15**	**678.74**	**1058.73**	**484.72**	**906.98**	**372.56**
Belgium	Weekly	Electricity Bill	139.52	103.45	354.62	146.64	302.12	141.07	236.39	132.53	192.43	119.44
		Discomfort	0.0	0.0	61.57	0.0	40.96	0.0	26.88	0.0	26.88	0.0
		Total	**139.52**	**103.45**	**416.19**	**146.64**	**343.08**	**141.07**	**263.27**	**132.53**	**219.31**	**119.44**
	Yearly	Electricity Bill	139.52	103.45	559.84	279.25	436.83	235.71	335.56	190.14	257.2	167.6
		Discomfort	0.0	0.0	80.76	24.3	80.76	24.3	49.11	39.94	49.1	4.85
		Total	**139.52**	**103.45**	**640.6**	**303.55**	**517.59**	**260.01**	**384.67**	**230.08**	**306.3**	**172.45**

- Batteries, when used for real-time pricing, can slash the retail bill by more than one fourth. However, procuring a battery is not a worthwhile investment under real-time pricing.
- If consumers are constrained to choose among priority service contracts with energy-based service charges, then a battery is a worthwhile investment.
- There is significant value added for households in updating subscriptions relatively frequently.

In order to clarify if these observations can be generalized, we consider a household that faces different weather and consumer behavior. We therefore rerun our analysis against a Belgian household, which is populated based on the LINEAR dataset [34]. We specifically assume that the Belgian household is subject to the same priority service menu as the Texas household. The results of these two simulations are presented in Table 2.2.

2.5.1 Significance of Service Charge

Table 2.2 highlights the fact that adding energy-based service charges to priority service pricing is *essential* for a viable implementation in a practical setting. This is due to the fact that, under priority service pricing, consumers pay for reserving *capacity* that may not be used entirely at any given time interval. We present an example of this difference in Figure 2.4 for the Texas household. The blue surface in the figure corresponds to the electric power that is consumed by the household. By contrast, the red and yellow surfaces represent the amount of power that is reserved by the consumer for week 21 of year 2018 when the household does not include a battery and when the contract is updated on a weekly basis. The energy which is booked but not actually used amounts to 325.2 kWh over the whole week. This corresponds to a significant cost when the energy-based service charge is low compared to the priority charge in the priority service menu.

Higher energy-based service charges allow a reduction in "wasted expenditures" for booking capacity that is not actually used, and thus decrease the cost of priority service pricing for residential consumers. When a consumer procures a priority service contract, it has to pay a priority charge for the reserved capacity of each priority tier and a service charge for each unit of energy that is actually consumed. We can observe from Table 2.1 that the priority charge is decreasing when the service charge is increasing. Therefore, if we increase the service charge, the bill is decreasing because we pay less for unused energy, as indicated in Figure 2.4. However, this service charge cannot be increased arbitrarily in a practical setting, since we require the priority charge to be non-negative.

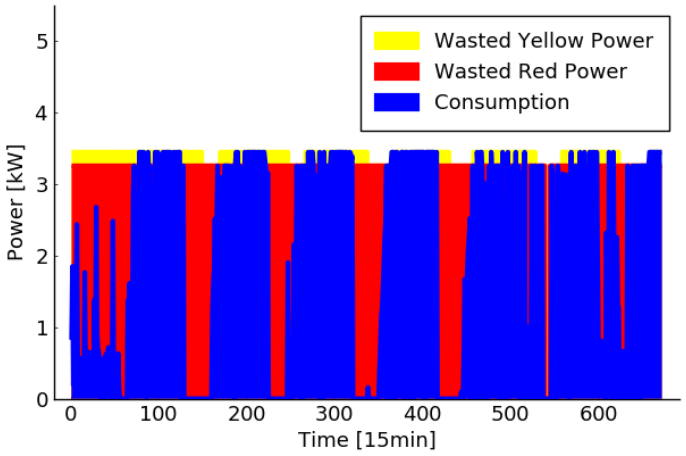

Figure 2.4: Texas household power consumption profile for week 21. The energy that is procured but not used amounts to 325.2kWh.

2.5.2 Priority Service versus Real-Time Pricing

Table 2.2 indicates that priority service pricing is substantially more expensive for households than real-time pricing. This is due to the fact that, under real-time pricing, consumers only pay for electricity that they actually use. Under priority service pricing, consumers pay for reserving *capacity* that may not be used entirely at any given time interval. This leads to wasted power, as shown in the example of Figure 2.4 for the Texas household.

As we discuss in section 2.2.3, Chao [26] establishes an equivalence between priority service and real-time pricing in terms of consumer expenditures. The proof relies on the concavity of the marginal benefit function of the consumer, as explained in [77]. This result is clearly violated in the present context. The essential difference between our realistic setting and the more simplified setting considered by Chao in [26] is that devices can only consume power if they have access to a level of capacity which at least covers their power rating. This results in total benefit functions (which map the fuse limit of the household to a total benefit over the subscription horizon) which are non-concave, and thus violate the necessary conditions for the equivalence result of [26] to hold. In intuitive terms, the fact that a device needs a minimum amount of power to operate creates "holes" of unused priority service capacity. This effect has been explained in a stylized example in [77]. It is reaffirmed in the realistic simulations in the present work, and motivates the need for employing energy-based service charges effectively in order to keep consumer costs for priority service contracts as low as possible.

2.5.3 Interaction between Real-Time Pricing and Storage

The results of Table 2.2 indicate a reduction of the total electricity bill by 29.9% under real-time pricing when a battery is considered for the Texas household, while it accounts for 25.9% for the Belgian household. This indicates a substantial benefit in home energy storage under real-time pricing. However, deploying storage is still costly. Recall, from section 2.4, that the annual investment cost of a battery ranges from 85 to 496$/year. This cost exceeds the yearly gain in the electricity bill of the consumer. Therefore, when a consumer is exposed to real-time pricing, the procurement of a battery is not a worthwhile investment.

2.5.4 Interaction of Priority Service Pricing with Storage

If residential consumers are limited to priority service contracts, then an investment in home energy storage becomes interesting for the Texas household. Observe that, for example, in the case of weekly subscription and a service charge of 25$/MWh, the bill decreases by 69.58% (net decrease of 513.92$/year). Insofar as the Belgian household is concerned, the difference between the results obtained with and without a battery is not sufficient for deducing that it can cover its investment cost. Note, however, that the battery that we consider in our analysis is large. As we can observe from the total cost in Table 2.2, the Texas household consumes a significantly larger amount of energy compared to the Belgian household. Therefore, this particular battery may not be the best choice for the Belgian household.

2.5.5 Yearly versus Weekly Contract

Another notable observation that can be drawn from Table 2.2 is the significant difference between consumer costs for weekly versus annual priority service contracts. This can be explained by observing the large variations in the load in Figure 2.1. Indeed, renewing subscription on a weekly basis allows consumers to better adapt their contract to the weekly fluctuations of load. As we observe in Figure 2.4, when too much capacity is booked, the consumer incurs an unnecessary cost for power that is not used. We can observe that this significant difference is reduced for the Belgian household, but remains high. Indeed, without a battery, the mean of this difference passes from 38% for the Texas household to 33% for the Belgian household. With a battery, it reduces from 51% to 43%.

The reduction of the difference between costs linked with weekly and yearly contracts for the Belgian household compared to the Texas one can be explained by observing Figure 2.5, where we present the inflexible load of the Belgian household. Compared to the Texas household, the Belgian consumer has a relatively flat inflexible load profile, with fewer seasonal variations. This allows the Belgian household to choose a yearly subscription that better represents its needs during the entire year. Instead, the Texas household buys

a higher yearly subscription, in order to satisfy its inflexible load during the summer. This leads to a large amount of unused energy credits during the winter. Note that considering HVAC as a flexible appliance may enable the Texas household to reduce its annual subscription.

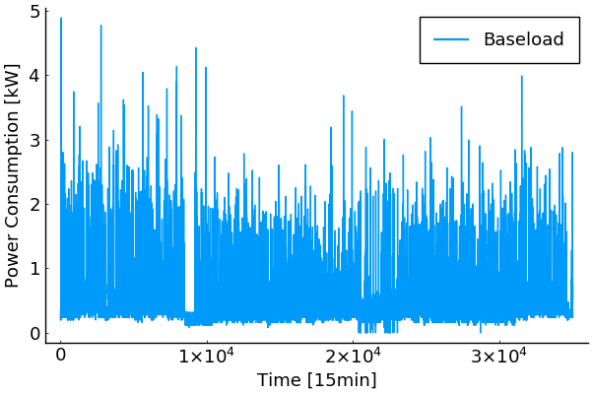

Figure 2.5: Inflexible load (referred to as baseload in the graph) of the Belgian household.

This observation is further validated by Figure 2.6. This figure presents a boxplot of the weekly total cost incurred by each household when the consumers are able to update subscriptions weekly, with no service charges considered. We can detect larger fluctuations for the Texas household due to seasonal variations in its inflexible load. As mentioned in section 2.2.3, real-time pricing is the limit case of priority service pricing when a new contract is signed every 15 minutes. Even though changing subscriptions relatively frequently can be advantageous in terms of better tailoring the contract to consumption that can be adapted by the growing use of sophisticated automatic energy management systems, the simplicity of priority service is sacrificed by having to subscribe to a new contract very frequently.

2.6 Conclusion

In this chapter, we develop a consumer-centric methodology for analyzing the impact of quality differentiation for mobilizing residential demand response. Our analysis focuses on quantifying the impact of demand response on consumer comfort and bills. We apply the methodology to the simplest instance of quality differentiation, namely priority service. We design a priority service menu which is consistent with real-time prices and extend the existing priority service theory to include a general form of service charges. Simulations are conducted on households from Texas and Belgium.

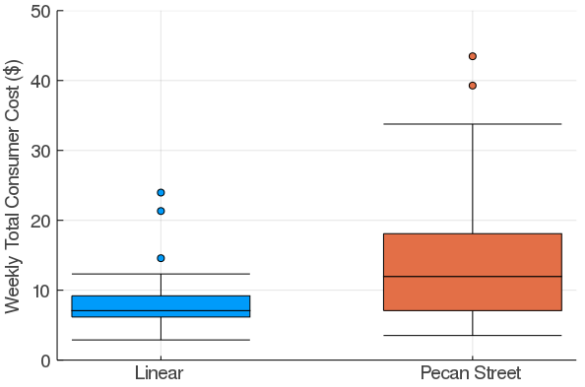

Figure 2.6: Boxplot of the weekly total cost incurred by the Texas and Belgium household when weekly subscriptions are allowed, and no service charges are considered.

Our case study quantifies the role played by adding energy-based service charges to priority service in the performance of this scheme in terms of consumer payments and comfort. Indeed, our work highlights the importance of combining priority service with energy-based service charges in a practical implementation of priority service, where "wasted payments" are minimized by shifting charges from the capacity to the energy component of the service. Furthermore, we also assess the performance wedge between real-time pricing and priority service in terms of consumer payments and comfort. The conclusions drawn for real-time pricing in this work are based on an idealized version of reality, since consumers are considered as rational agents who react instantaneously to prices. This assumption may not be valid in practice, which would imply a degradation on the performance of real-time pricing. We analyze the dependency between the load profile and the benefit for households to invest in batteries under priority service pricing combined with energy-based service charges. In the real-time pricing setting, even though a battery allows a reduction in the electricity bill by 25%, the consumer fails to recover the cost of investing in home energy storage. Finally, we note that there is significant added value for households to changing their priority service contract frequently, in order to better target their weekly needs.

2.A Notations

Notations used throughout this chapter are summarized in this section.

Sets and Indices

$\mathcal{I}, i$	Set of colors/priority service options and its corresponding index.
$\mathcal{T}, t$	Set of time periods and its corresponding index.
$\mathcal{J}, j$	Set of flexible appliances present in the household and its corresponding index.
$\mathcal{B}_j, \beta$	Set of starting times of flexible appliance j and its corresponding index.
$\mathcal{T}_j, \tau$	Set of part of flexible appliance j and its corresponding index.

Parameters

M	Priority service pricing menu of options.
p, $p(v)$, p_i	Priority charge of an option in the priority service pricing menu [\$/MWh].
s, $s(v)$, s_i	Service charge of an option in the priority service pricing menu [\$/MWh].
r, $r(v)$, r_i	Reliability of an option in the priority service pricing menu.
v	Consumer valuation for power.
$\hat{p}(\omega)$	Real-time price in the original priority service theory.
Δt	Number of time periods present in an hour.
S_t	Total solar production of the household at time period t [kW].
B_t	Total inflexible load of the household needed to be served at time period t [kW].
Ch_{EV}^{max}	Maximum charging power for the electric vehicle [kW].
Dis_{EV}^{max}	Maximum discharging power for the electric vehicle [kW].
EV^{max}	Maximum capacity of the electric vehicle [kWh].
η^{EV}	Electric vehicle charging efficiency ($\in [0, 1]$).
T_A, EV_A	Arrival time period of the electric vehicle and its respective state of charge.
T_D, EV_D	Departure time period of the electric vehicle and its respective state of charge.
Ch_B^{max}	Maximum charging power for the battery [kW].
Dis_B^{max}	Maximum discharging power for the battery [kW].
B^{max}	Maximum capacity of the battery [kWh].
η^B	Battery charging efficiency ($\in [0, 1]$).
ϕ	Unflexible load shedding cost [\$/kWh].
F_j	Marginal frustration cost for delaying the end of flexible appliance j of one time period after its deadline [\$/time period].
D_j	Deadline of flexible appliance j.
$\rho_{j,\tau}$	Part τ of the Power consumption footprint of flexible appliance j to be served [kW].
λ_i^P	Priority charge of option i in the priority service menu [\$/kWh].

λ_i^S Service charge of option i in the priority service menu [$/kWh].

$profile_{t,i}$ Binary indicator if option i is available or not at time period t.

Variables

$s_{t,i}$ Used solar production at time period t by option i [kW].

$b_{t,i}$ Served inflexible load at time period t by option i [kW].

u_t^{EV} Binary variable indicating if the household electric vehicle is charging or not at time period t.

$ch_{t,i}^{EV}$ Electric vehicle charging power at time period t from option i [kW].

$dis_{t,i}^{EV}$ Electric vehicle discharging power at time period t into option i [kW].

soc_t^{EV} State of charge of the electric vehicle at time period t [kWh].

u_t^B Binary variable indicating if the household battery is charging or not at time period t.

$ch_{t,i}^B$ Power from color i used to charge the battery at time period t [kW].

$dis_{t,i}^B$ Power discharged from the battery into option i at time period t [kW].

soc_t^B State of charge of the battery at time period t [kWh].

$y_{t,i}$ Total household power consumption at time period t for option i in the priority service pricing setting [kW].

$x_{t,j,\beta,\tau,i}$ Binary decision for part τ of flexible appliance j arrived at time period β to be turned ON at time period t with option i.

P_i^{max} Amount of power subscribed by consumer to option i in the priority service menu [kW].

Functions

$Surplus(v)$ Surplus of a consumer with privately known type v.

$R(v)$ Function exploited to represent the reliability for a consumer with valuation v.

$S(v)$ Function used to represent the service charge for a consumer with valuation v.

$D(v)$ System demand function for a certain valuation v.

2.B Example Where Priority Service is Not Equivalent to Real-Time Pricing

The equivalence result of Chao [26] which is extended in section 2.2.3 is established under idealized conditions in a static framework. We find in [77] that this result can be violated under very reasonable relaxations of these assumptions that occur in practice. This is demonstrated by means of a simple example. The example, along with the conclusions following its exposition, are repeated in this section. For additional details, the reader is referred to [77]. The selected example is constructed for a period of 10 hours, with a time step of one

hour. During this 10-hour period, the real-time prices faced by the consumer for each hour are presented in Table 2.3.

Table 2.3: Real-time prices faced by the consumer during the 10-hour period and the interruption pattern of colors for the priority service pricing scheme.

Hour	Real-time Price [/€kWh]	Green	Orange	Red
1	0.02	ON	ON	ON
2	0.05	OFF	OFF	ON
3	0.086	OFF	OFF	OFF
4	0.06	OFF	OFF	ON
5	0.04	OFF	ON	ON
6	0.09	OFF	OFF	OFF
7	0.032	OFF	ON	ON
8	0.055	OFF	OFF	ON
9	0.08	OFF	OFF	ON
10	0.01	ON	ON	ON

As explained in section 2.4.3, in order to design a priority service pricing menu from this set of real-time prices, we fix the reliability levels of each option as follows:

- Green: 20% reliability
- Orange: 40% reliability
- Red: 80% reliability

By using the procedure presented in section 2.4.3, the priority service menu is obtained and presented in Table 2.4. The third, fourth and fifth columns of Table 2.3 record if a certain color is interrupted or not during a certain time period, given the levels of reliability.

Table 2.4: Price menu obtained for 3 options of priority service.

Option Color	Price [/€kWh]	Reliability [%]	Range Valuation
Green	0.004	20	[0.02;0.0305[
Orange	0.01010	40	[0.0305;0.058[
Red	0.0333	80	[0.058; →

Finally, the two mathematical programs presented in section 2.3 are applied to a single household that contains only one appliance. This appliance has a duration of 4 hours and the deadline imposed by the consumer for its end is hour 5. The footprint of the appliance is presented in Table 2.5. If this

appliance finishes on time, then the consumer achieves a reward equal to 1€. On the other hand, for every hour that the appliance is delayed beyond its deadline, the consumer incurs a cost of 0.5€. If the appliance job is not complete before the end of the 10-hour horizon, then the consumer incurs a cost of 3€. These three values quantify the frustration or satisfaction of the consumer.

Table 2.5: Footprint representing the electrical consumption of the single appliance of the household.

Part Footprint [h]	1	2	3	4
Footprint Consumption [kW]	1.1	3.05	2.5	0.43

Given the aforementioned setup, the two mathematical programs are solved respectively presented in sections 2.3.1 and 2.3.2. The objective value obtained for each scheme along with the best set of actions at a given time period are presented in Table 2.6. It is important to note that the optimal policy for each approach is identical. This is the case because, in time period 3, the red color is off so the consumer cannot use it to serve his appliance and the real-time pricing scheme chooses also not to use the appliance considering the high price of that time period.

Table 2.6: Objective function value and optimal policy obtained by solving the mathematical program belonging to each approach.

	Objective Value [€]	Best Policy
Real-time	0.6583	Serve-Serve-Not-Serve-Serve
Priority Service	-0.01565	Red-Red-Not-Red-Red

Before comparing the objective value of both approaches, we first note that the consumer will subscribe to 3.05 kW of red power for 10 hours. To see why this is the case, note that this amount of power corresponds to the highest power consumption of the appliance (the second part). Therefore, if the second part of the appliance footprint is not served at time period 2 or with red color, this implies that the appliance cannot finish before at least time period 8, which is far beyond the deadline. Moreover, the loss incurred by finishing the job after the deadline for the consumer is not balanced by a subscription to a less reliable option.

Consumer net benefits can now be compared for the two different approaches. According to Table 2.6, we observe that the priority service pricing scheme is causing a notable reduction in the net benefit of the consumer. This is largely due to the fact that priority service implies that the consumer is obliged to procure a capacity strip. This is how the service is defined: according to priority service, consumers procure increments of capacity. As a result,

the consumer subscribes for 10 hours of power and only uses its subscription for 5 hours. This conclusion is consistent with the observations drawn made in this chapter regarding more realistic households.

3 Designing Multilevel Demand Subscription Menus

3.1 Introduction

As we discuss in section 1.3.1, multilevel demand subscription [25] is a generalization of priority service pricing which allows the aggregator to further differentiate service by *duration*. This added component induces the idea of an energy-based component added to priority service, which is developed in the previous chapter by means of service charges. Since it is observed in that chapter that service charges are essential for achieving a practical implementation of priority service pricing, studying multilevel demand subscription in detail allows us to explore further options for retail tariffs that combine an energy component with a capacity component compared to purely capacity-based tariffs.

Whereas the theory of quality differentiation [25, 26] is a valuable starting point for investigating priority service and multilevel demand subscription, it is limited to analytical models that rely on stringent assumptions (e.g. synchronization of loads, idealized and abstract representations of households). In order to analyze multilevel demand subscription and compare it with priority service on a system-wide perspective, a modeling framework for designing multilevel demand subscription menus for realistic case studies is developed in this chapter and detailed in section 3.2. Firstly, inspired by recent research on priority service [119], the multilevel demand subscription menu design problem of Chao [25] is cast as a Stackelberg game which is then transformed into a mixed integer linear program. For this purpose, a mapping from time sorted in a load duration curve to real time is proposed. The entire process is developed in section 3.4. In order to account for realistic household demand functions, section 3.3 presents a fuse limit model in the spirit of Margellos [108] for computing demand functions for individual household types. These demand functions are then aggregated into a concave system demand function. Then, an optimization problem is described in section 3.5 which describes how a household optimizes its subscription choice. Ultimately, the entire process is applied to two realistic

models of the Belgian market, which are detailed in section 3.6. Section 3.7 presents and compares the results that are obtained for both demand response programs. Finally, section 3.8 concludes the analysis. Appendix 3.A gathers all notations used in the employed models of this chapter.

3.2 Process Overview and Models

In order to assess the performances of priority service and multilevel demand subscription on a system-wide perspective, we propose a three-step menu design framework which is presented in Figure 3.1. It is aimed at comparing the two demand response schemes with an explicit consideration of the storage capability and local supply uncertainty of prosumers. We briefly introduce each block as follows:

1. **Household Type Model:** In order to be able to price and design these demand response services for consumers, the aggregator needs an estimation of either the demand function of the system in the case of priority service pricing or the load duration curve for multilevel demand subscription. We consider different types of households that are equipped with rooftop PV panels, but differ in the size of batteries and consumption profiles. The valuation of power increments is calculated and extrapolated for each *type* of household by means of a stochastic optimization program, in order to derive a system-level demand function. This demand function is used as an ingredient for the design of a reliability-duration menu.

2. **Menu Design Model:** When the system-level load duration curve is available, the aggregator can design a menu of options for each demand response scheme from which consumers can select a particular contract with the most suitable reliability-price trade-off. This menu design is realized by solving a bilevel optimization program that computes the equilibrium solution of a Stackelberg game between the aggregator and consumers which integrates day-ahead unit commitment constraints and forecast scenarios of system-level renewable production.

3. **Household Subscription Selection Model:** Given the price menu designed in the previous step, households decide on their subscription based on a stochastic scheduling model. In this model, the interruption of different options and the rooftop PV production are modeled as a scenario tree. The management of the battery is optimized as well.

Each block is presented in detail in the following sections, respectively sections 3.3, 3.4 and 3.5.

During this process, two types of uncertainty related to renewable supply are accounted for: long-term and short-term. Long-term uncertainty is represented

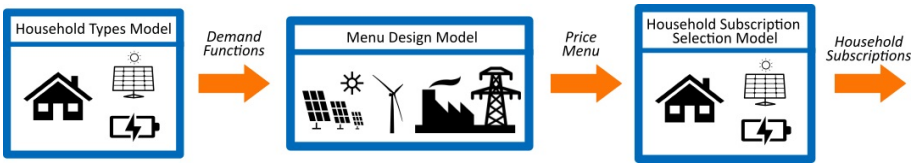

Figure 3.1: General framework that is employed for comparing multilevel demand subscription and priority service.

by a set of scenarios that correspond to seasonal variations. In the case study of section 3.6, the set $\mathcal{S}$ consists of weekdays and weekends for each season of the year. Each scenario $s \in \mathcal{S}$ occurs with a probability P^s. For each scenario, short-term uncertainty, which corresponds to the real-time production of renewable energy, is modeled by a scenario tree with different outcomes of renewable production for each time stage of the day.

3.3 Characterizing Household Types

In order to design the multilevel demand subscription menu that is offered to consumers, the utility must quantify the valuation of an increment of power for a certain duration. The idea of our proposed approach is to estimate the marginal value of an increment in the fuse limit of a household in the same spirit as [108]. To form the system load duration curve used by the utility to design menus, the obtained marginal value curves of each household are combined into one system load duration curve. However, due to the combination of different household types which do not consume power in a synchronized way due to their respective characteristics (storage and/or solar panels), there is no guarantee that this obtained aggregated system marginal value is a concave function of the duration of consumption. Therefore, in a second phase, we compute the closest concave approximation of this estimate. We use this function as input to the menu design problem of section 3.4.

In order to estimate the valuation of an increment of power for a certain duration, we propose a stochastic optimization program for each type of household. This mathematical program allows us to represent battery and load shedding decisions over a day, while enforcing a fuse limit on the household that is equipped with solar panels and must serve a mix of flexible and inflexible load. As mentioned earlier, two types of uncertainty are represented, long-term and short-term. For each scenario, short-term uncertainty is denoted by $\omega_{[t]}^{S,s} \in \Omega_{[t]}^{S,s}$ which represents the sequence of solar panel production up to stage t, while in scenario s. Moreover, $P^s_{t,\omega_{[t]}^{S,s}}$ denotes the probability that is linked with the realization of this solar production sequence up to time stage t. For each household type $h \in \mathcal{H}$, the household model employed for creating a system

load duration curve is therefore given as follows:

$$(HV_h)\colon \min_{\substack{\mathbf{ls},\mathbf{nd},\\ \mathbf{e},\mathbf{bc},\mathbf{bd}}} V_{cut} \cdot \left(\sum_{s\in\mathcal{S}} \sum_{t\in\mathcal{T}} \sum_{\omega_{[t]}^{S,s}\in\Omega_{[t]}^{S,s}} P^s \cdot P^s_{t,\omega_{[t]}^{S,s}} \cdot ls_{t,s,\omega_{[t]}^{S,s}} \right) \tag{3.1}$$

$$\text{s.t.} \quad 0 \le bd_{t,s,\omega_{[t]}^{S,s}} \le BD_h, \;\; t\in\mathcal{T}, s\in\mathcal{S}, \omega_{[t]}^{S,s}\in\Omega_{[t]}^{S,s} \tag{3.2}$$

$$0 \le bc_{t,s,\omega_{[t]}^{S,s}} \le BC_h, \;\; t\in\mathcal{T}, s\in\mathcal{S}, \omega_{[t]}^{S,s}\in\Omega_{[t]}^{S,s} \tag{3.3}$$

$$0 \le e_{t,s,\omega_{[t]}^{S,s}} \le E_h, \;\; t\in\mathcal{T}, s\in\mathcal{S}, \omega_{[t]}^{S,s}\in\Omega_{[t]}^{S,s} \tag{3.4}$$

$$e_{t,s,\omega_{[t]}^{S,s}} = e_{t-1,s,\omega_{[t]}^{S,s}} - \frac{bd_{t,s,\omega_{[t]}^{S,s}} \cdot \Delta t}{\eta_h^d} + bc_{t,s,\omega_{[t]}^{S,s}} \cdot \eta_h^c \cdot \Delta t, \quad t\in\mathcal{T}, s\in\mathcal{S}, \omega_{[t]}^{S,s}\in\Omega_{[t]}^{S,s} \tag{3.5}$$

$$DP_{h,s,t} - ls_{t,s,\omega_{[t]}^{S,s}} + bc_{t,s,\omega_{[t]}^{S,s}} - PV_h \cdot \omega_t^{S,s} - bd_{t,s,\omega_{[t]}^{S,s}} = nd_{t,s,\omega_{[t]}^{S,s}}, \;\; t\in\mathcal{T}, s\in\mathcal{S}, \omega_{[t]}^{S,s}\in\Omega_{[t]}^{S,s} \tag{3.6}$$

$$\left(\lambda_{t,s,\omega_{[t]}^{S,s}}\right)\colon nd_{t,s,\omega_{[t]}^{S,s}} \le FL, \;\; t\in\mathcal{T}, s\in\mathcal{S}, \omega_{[t]}^{S,s}\in\Omega_{[t]}^{S,s} \tag{3.7}$$

$$ls_{t,s,\omega_{[t]}^{S,s}} \ge 0, \;\; t\in\mathcal{T}, s\in\mathcal{S}, \omega_{[t]}^{S,s}\in\Omega_{[t]}^{S,s} \tag{3.8}$$

The goal of the household is to minimize its economic damage from not serving part of its load. The parameter V_{cut} represents the risk-adjusted cost of consumers for accessing the spot market. Constraints (3.2), (3.3) and (3.4) represent, respectively, the discharge power, charge power and storage capacity limits of the household battery. Constraint (3.5) describes the dynamics of the battery, with η_h^c and η_h^d expressing respectively the charge and discharge efficiency of the household battery. Note that household batteries are assumed to be empty at the beginning of the day, i.e. $e_0 = 0$. The power balance in the household is represented by Constraint (3.6), where parameter $DP_{h,s,t}$ corresponds to the inflexible load of household type h at time t for scenario s, while PV_h corresponds to the the rooftop solar capacity installed in the household. The parameter $PV_h \cdot \omega_t^{S,s}$ indicates the rooftop solar supply sample production for that time stage. Finally, Constraint (3.7) limits the power that can be drawn from the grid by the household using parameter FL (i.e. the fuse limit of the household).

The dual multiplier $\lambda_{t,s,\omega_{[t]}^{S,s}}$ of Constraint (3.7) is used for quantifying the incremental value of the fuse limit. Concretely, the valuation for an additional unit of power in period t of actual operations, given fuse limit FL, is computed as follows

$$\sum_{s\in\mathcal{S}} \sum_{\omega_{[t]}^{S,s}\in\Omega_{[t]}^{S,s}} \lambda_{t,s,\omega_{[t]}^{S,s}}, \;\; t\in\mathcal{T}.$$

This valuation is then derived for different levels of fuse limit. We use this information in order to create a demand function for increments of power for each household type at a given operating interval.

3.4 Multilevel Demand Subscription Menu Design MILP Reformulation

The multilevel demand subscription pricing problem can now be cast as a bilevel optimization program. The problem has been formulated and solved in the literature as a Stackelberg equilibrium [25]. We depart from the classical description of the problem that is developed in [25], in order to allow for a more general representation of uncertainty and production constraints which are typically encountered in production simulation models. In this respect, we follow the approach described in [119], where the Stackelberg equilibrium formulation of priority service pricing [26] is cast as a bilevel optimization program. Bilevel formulations were already adopted in the literature for designing other demand response contracts, e.g. in [74]. We reformulate the problem as a mixed integer linear program by exploiting its structure. The exposition here focuses on multilevel demand subscription pricing, with priority service pricing being a special case.

3.4.1 Bilevel Mathematical Structure

Chao [25] casts the multilevel demand subscription pricing problem as a Stackelberg equilibrium. The leader of this Stackelberg game is the utility that designs a multilevel demand subscription menu which is offered to consumers, who are the followers. Due to information asymmetry (see section 1.3.1), the leader integrates in the bilevel program the optimal reaction of the followers to the menu design problem[1]. This gives rise to a mathematical program with equilibrium constraints that also integrates menu design with unit commitment. Note that, following the literature [25], we do not consider transmission or distribution constraints in our model. This bilevel model can be represented abstractly as follows, and is further illustrated in Figure 3.2.

$$\max_{\mathbf{m},\mathbf{n},\mathbf{o},\mathbf{p},\mathbf{r},\boldsymbol{\pi}} \quad SW(\mathbf{m},\mathbf{n},\mathbf{o},\mathbf{p},\mathbf{d},\mathbf{r}) \tag{3.9}$$

$$\text{s.t.} \quad (\mathbf{m},\mathbf{n},\mathbf{o},\mathbf{p},\mathbf{d}) \in \mathbf{X} \tag{3.10}$$

$$\mathbf{r} = \psi(\mathbf{d},\boldsymbol{\sigma}^\star) \tag{3.11}$$

$$\boldsymbol{\sigma}^\star \in \arg\max_{\sigma}\{CS(\mathbf{r},\boldsymbol{\pi}) : \sigma \in \Sigma\} \tag{3.12}$$

[1] In the absence of information asymmetry, the surplus generated is collected by the aggregator, since the aggregator can target the exact valuation of consumers for power.

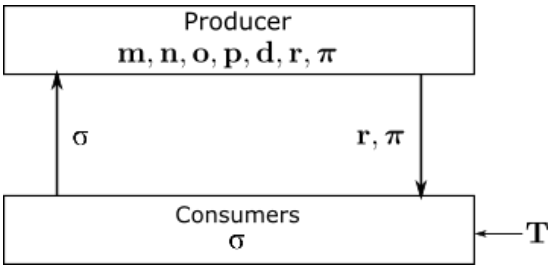

Figure 3.2: Interaction between the producer and consumers in the multilevel demand subscription bilevel model.

In this model, the variables $\mathbf{m}, \mathbf{n}, \mathbf{o}, \mathbf{p}$ correspond respectively to startup and shutdown decisions, unit commitment and power generation. The subscription quantity of each consumer to each option of the multilevel demand subscription menu is indicated by $\boldsymbol{\sigma}$, while the supply to each option is indicated by $\mathbf{d}$. The reliability, duration and price of the options in the menu are denoted by $\mathbf{r}$, $\mathbf{T}$ and $\boldsymbol{\pi}$ respectively. We assume that the duration is an exogenous parameter, and is therefore not a variable in the model.

The objective of the utility in this mathematical program is to maximize social welfare, as represented by function SW in Eq. (3.9). The technical constraints of the producer are captured in Eq. (3.10). Constraint (3.11) indicates that the designed price menu is required to deliver a promised level of reliability during a certain duration, which is influenced by the way consumers react to the offered menu. Finally, consumers decide on their subscription by maximizing their individual surplus (represented by the function CS), as shown in Eq. (3.12).

3.4.2 Representation of the Household by the Utility

From the point of view of the utility who is designing a service menu, the population of households can be represented by a distribution over valuations. This distribution is encoded in the parameters $(D_l, V_l(t))$. The function $V_l(t)$ is a non-decreasing function of t, since more hours of consumption increase the benefit of the household. Note that the formulation of the consumer problem below implicitly assumes that $V_l(t)$ is further a concave function of t, otherwise it would be needed to sum over time periods in the first term of the objective function. Section 3.3 describes how the utility can estimate this function based on information about the distribution of installed equipment in residential households.

Given a set of consumer types $\mathcal{L}$, each of them as a follower subscribes to service options from a menu with $|\mathcal{I}| \cdot |\mathcal{J}|$ options. The set $\mathcal{I}$ expresses the

offered reliability, while the set $\mathcal{J}$ includes the set of duration options. Each consumer type l then solves the following problem for choosing an option from the menu, given the reliability r_i, duration T_j, and price $\pi_{i,j}$ of each option from the upper-level problem:

$$(CP_l)\colon \max_{\sigma_{l,i,j}} \sum_{\substack{i\in\mathcal{I},\\ j\in\mathcal{J}}} \sigma_{l,i,j}\Big(r_i \cdot V_l(T_j) - \pi_{i,j}\Big) \tag{3.13}$$

$$\text{s.t.} \quad \sigma_{l,i,j} \geq 0, \;\; i \in \mathcal{I},\; j \in \mathcal{J} \tag{3.14}$$

$$(\gamma_l): \sum_{i\in\mathcal{I}, j\in\mathcal{J}} \sigma_{l,i,j} \leq D_l \tag{3.15}$$

The goal of the consumer is to maximize its profit from procuring an option (i, j). The first term in the objective function of Eq. (3.13) is the expected benefit from procuring option (i, j). The constraint of Eq. (3.15) expresses the fact that options are stacked up to the amount of kilowatts that the household wishes to procure.

The optimality conditions of the consumer model are employed as constraints for the producer model to account for the optimal reaction of consumers. By exploiting to the linearity of the consumer model, the optimality conditions can be described as a compilation of primal and dual feasibility and strong duality conditions [119]. The dual (CD_l) of the menu selection problem for the consumer is given as follows:

$$(CD_l)\colon \min_{\gamma_l} \;\; \gamma_l \cdot D_l \tag{3.16}$$

$$s.t. \quad \gamma_l \geq r_i \cdot V_l(T_j) - \pi_{i,j}, \;\; i \in \mathcal{I},\; j \in \mathcal{J} \tag{3.17}$$

$$\gamma_l \geq 0 \tag{3.18}$$

Strong duality is expressed by Eq. (3.19):

$$\gamma_l \cdot D_l = \sum_{\substack{i\in\mathcal{I},\\ j\in\mathcal{J}}} \sigma_{l,i,j}\Big(r_i \cdot V_l(T_j) - \pi_{i,j}\Big), \;\; l \in \mathcal{L} \tag{3.19}$$

By exploiting further the particular structure of the consumer problem, we demonstrate in Proposition 3.1 that any consumer type l may as well limit its choice to a unique option out of the menu offered by the utility. This observation is an essential tool that allows the formulation of the Stackelberg equilibrium as a mixed integer linear program.

Proposition 3.1. *There exists* $(\tilde{\sigma}_{l,i,j}, i \in \mathcal{I}, j \in \mathcal{J})$ *with* $\tilde{\sigma}_{l,i,j} \in \{0, D_l\}$ *which attains the optimal objective function value.*

Proof. The proof of this proposition follows the approach of [119]. The KKT conditions of (CP_l) are given by (3.20) and (3.21):

$$0 \leq \sigma_{l,i,j} \perp -r_i \cdot V_l(T_j) + \pi_{i,j} + \gamma_l \geq 0 \tag{3.20}$$

$$0 \leq \gamma_l \perp D_l - \sum_{\substack{i \in \mathcal{I}, \\ j \in \mathcal{J}}} \sigma_{l,i,j} \geq 0 \tag{3.21}$$

Two cases are to be considered:

Case 1: If $D_l - \sum_{i,j} \sigma^\star_{l,i,j} > 0$, then $\gamma_l = 0$. This implies that consumer l derives zero net benefit at the optimal solution. Thus, $\tilde{\sigma}_{l,i,j} = 0$ for all $i \in \mathcal{I}, j \in \mathcal{J}$ is optimal.

Case 2: If $D_l - \sum_{i,j} \sigma^\star_{l,i,j} = 0$, then it suffices to show that if two options are 'active' (in the sense that $\sigma > 0$) then they have an equal payoff, and can therefore be equivalently replaced by a single option. Applying this argument for all options that are active gives the desired conclusion. Consider any two options (i, j) and (i', j') for which $\sigma^\star_{l,i,j} > 0$ and $\sigma^\star_{l,i',j'} > 0$. Then $-r_i \cdot V_l(T_j) + \pi_{i,j} + \gamma_l = 0$ and $-r_{i'} \cdot V_l(T_{j'}) + \pi_{i',j'} + \gamma_l = 0$, and substituting out γ_l, we have $r_i \cdot V_l(T_j) - \pi_{i,j} = r_{i'} \cdot V_l(T_{j'}) - \pi_{i',j'}$.

□

3.4.3 Utility

The utility acts as the leader in the Stackelberg game, and aims at pricing the menu so as to maximize system welfare, while accounting for the optimal response of the households to the offered menu. Thus, the utility solves a unit commitment model by accounting for the individual choice of options $\sigma^\star_{l,i,j}$ by each consumer type, which is the optimal solution to model (CP_l) described in section 3.4.2.

In addition, the utility owns a set of renewable assets. Their production is characterized by a set of scenarios. The uncertainty taken into account in the menu design program only corresponds to long-term uncertainty, such as seasonal variations, and is represented by the scenario set $\mathcal{S}$ (see section 3.3). Due to practical concerns related to the scalability of the model scalability, we assume that the additional short-term uncertainty considered in section 3.3 is not integrated in this model. This assumption is supported by the fact that menu design is a long-term problem. This optimization program is treated as a two-stage problem (menu design in the first stage, operation of the grid in the second stage). The non-negative vector $\mathbf{d}$ corresponds to the amount of power that is offered to different options under different time periods and scenarios. The optimization is carried out over a horizon $|\mathcal{T}|$. In the test case of section 3.6, this horizon corresponds to 24 hours.

The menu design problem of the utility can be summarized as follows:

$$(MD): \max_{\substack{\mathbf{m},\mathbf{n},\mathbf{o}, \\ \mathbf{d},\mathbf{p},\boldsymbol{\pi},\mathbf{r}}} \; -\sum_{\substack{s \in \mathcal{S},\ g \in \mathcal{G}, \\ t \in \mathcal{T}}} P^s \cdot h_g(m_{g,t,s}, n_{g,t,s}, o_{g,t,s}, p_{g,t,s})$$

$$+ \sum_{\substack{i\in\mathcal{I}, l\in\mathcal{L},\\ j\in\mathcal{J}}} \sigma^{\star}_{l,i,j}(\mathbf{r},\boldsymbol{\pi}) \cdot V_l(T_j) \cdot r_i \tag{3.22}$$

$$\text{s.t.} \quad f_g(m_{g,t,s}, n_{g,t,s}, o_{g,t,s}, p_{g,t,s}) \leq 0, \;\; g \in \mathcal{G}, s \in \mathcal{S} \tag{3.23}$$

$$\sum_{\substack{i\in\mathcal{I},\\ j\in\mathcal{J}}} d_{i,j,t,s} = \sum_{g\in\mathcal{G}} p_{g,t,s} + R_{t,s}, \;\; t \in \mathcal{T}, s \in \mathcal{S} \tag{3.24}$$

$$d_{i,j,t,s} \leq N_{j,t} \sum_{l\in\mathcal{L}} \sigma^{\star}_{l,i,j}(\mathbf{r},\boldsymbol{\pi}), \;\; i \in \mathcal{I}, j \in \mathcal{J}, t \in \mathcal{T}, s \in \mathcal{S} \tag{3.25}$$

$$r_i \cdot T_j \sum_{l\in\mathcal{L}} \sigma^{\star}_{l,i,j}(\mathbf{r},\boldsymbol{\pi}) = \sum_{\substack{s\in\mathcal{S},\\ t\in\mathcal{T}}} P^s \cdot d_{i,j,t,s}, \;\; i \in \mathcal{I}, j \in \mathcal{J} \tag{3.26}$$

$$d_{i,j,t,s} \geq 0, \; i \in \mathcal{I}, j \in \mathcal{J}, t \in \mathcal{T}, s \in \mathcal{S} \tag{3.27}$$

$$p_{g,t,s} \geq 0, \;\; g \in \mathcal{G}, t \in \mathcal{T}, s \in \mathcal{S} \tag{3.28}$$

$$m_{g,t,s}, \; n_{g,t,s}, \; o_{g,t,s} \in \{0,1\}, \;\; g \in \mathcal{G}, t \in \mathcal{T}, s \in \mathcal{S} \tag{3.29}$$

The goal of the utility, which is expressed in the objective function of Eq. (3.22), is to maximize social welfare. The first term in the objective function corresponds to the expected production cost of the utility and the second term to the consumer benefit, as estimated from the utility based on the load duration curve that is estimated in section 3.3. The function $h_g(m_{g,t,s}, n_{g,t,s}, o_{g,t,s}, p_{g,t,s})$ expresses the production cost of a generator, while the vector of constraints in Eq. (3.23) encodes linear production constraints that relate to unit commitment and the dispatch of conventional units, such as ramp rates, minimum up and down times, and so on. Power balance is expressed in Constraint (3.24), where $R_{t,s}$ indicates the amount of renewable (system-level solar and wind) production in period t under scenario s. Constraint (3.25) expresses the fact that a consumer type can only be served if that type is requesting power at a given interval, and if that interval is served under option $j \in \mathcal{J}$. The binary parameter $N_{j,t}$ determines whether a certain duration option $j \in \mathcal{J}$ is being served in time period t of actual operations or not. Note that, given a duration option $j \in \mathcal{J}$ and a mapping from the time indexing of a load duration curve to the time indexing of actual operations, we can define this indicator. Moreover, by definition, $\sum_{t\in\mathcal{T}} N_{j,t} = T_j$. In other words, service option j corresponds to T_j time periods of service. Finally, Constraint (3.26) ensures that an option $i \in \mathcal{I}$ receives the requested reliability r_i.

3.4.4 Bilevel Formulation of Multilevel Demand Subscription Pricing

The Stackelberg game that is described in section 3.4.2 can be formulated equivalently as a mixed integer linear program, following a similar approach to [119]. Firstly, note that Proposition 3.1 allows us to represent the continuous variable $\sigma_{l,i,j}$ which corresponds to the subscription choice of type l consumers as the

following product, $\sigma_{l,i,j} = D_l \cdot \mu_{l,i,j}$, where $\mu_{l,i,j} \in \{0,1\}$ are binary variables.

In order to reduce the bilevel program to a single-level problem, we append the optimality conditions of the consumer model to the utility menu design program. Here, we consider the reliability r_i, price $\pi_{i,j}$ and subscription to each option as variables. Moreover, we replace the subscription variables $\sigma_{l,i,j}$ by the previously mentioned product. These optimality conditions correspond to primal feasibility (Eqs. (3.14) and (3.15)), dual feasibility (Eqs. (3.17) and (3.18)) and strong duality (Eq. (3.19)).

We now tackle the non-convex constraints resulting from the products $r_i \cdot \mu_{l,i,j}$ and $\pi_{i,j} \cdot \mu_{l,i,j}$. Using McCormick envelopes, we linearize these products. In particular, note that reliability is naturally within the interval $0 \leq r_i \leq 1$, and price is within the interval $0 \leq \pi_{i,j} \leq \Pi^+$, where Π^+ corresponds to a price limit. This allows us to replace $\pi_{i,j} \cdot \mu_{l,i,j}$ by a new variable $y_{l,i,j}$, and $r_i \cdot \mu_{l,i,j}$ by another one $w_{l,i,j}$. Therefore, the strong duality Constraint (3.19) for each load type $l \in \mathcal{L}$ can be rewritten as follows:

$$\gamma_l = \sum_{i \in \mathcal{I}, j \in \mathcal{J}} w_{l,i,j} \cdot V_l(T_j) - \sum_{i \in \mathcal{I}, j \in \mathcal{J}} y_{l,i,j} \tag{3.30}$$

$$0 \leq y_{l,i,j} \leq \Pi^+ \cdot \mu_{l,i,j}, \;\; i \in \mathcal{I}, j \in \mathcal{J} \tag{3.31}$$

$$y_{l,i,j} \leq \pi_{i,j}, \;\; i \in \mathcal{I}, j \in \mathcal{J} \tag{3.32}$$

$$y_{l,i,j} \geq \Pi^+ \cdot \mu_{l,i,j} + \pi_{i,j} - \Pi^+, \;\; i \in \mathcal{I}, j \in \mathcal{J} \tag{3.33}$$

$$0 \leq w_{l,i,j} \leq \mu_{l,i,j}, \;\; i \in \mathcal{I}, j \in \mathcal{J} \tag{3.34}$$

$$w_{l,i,j} \leq r_i, \;\; i \in \mathcal{I}, j \in \mathcal{J} \tag{3.35}$$

$$w_{l,i,j} \geq \mu_{l,i,j} + r_i - 1, \;\; i \in \mathcal{I}, j \in \mathcal{J} \tag{3.36}$$

$$0 \leq r_i \leq 1, \;\; i \in \mathcal{I} \tag{3.37}$$

$$0 \leq \pi_{i,j} \leq \Pi^+, \;\; i \in \mathcal{I}, j \in \mathcal{J} \tag{3.38}$$

$$\mu_{l,i,j} \in \{0,1\}, \;\; i \in \mathcal{I}, j \in \mathcal{J} \tag{3.39}$$

The final mixed integer linear program is expressed as a single-level MILP:

$$(MILP): \max_{\substack{\mathbf{m},\mathbf{n},\mathbf{o},\mathbf{d},\\ \mathbf{p},\boldsymbol{\pi},\mathbf{r},\\ \boldsymbol{\mu},\boldsymbol{\gamma},\mathbf{y},\mathbf{w}}} - \sum_{\substack{s \in \mathcal{S},\\ g \in \mathcal{G}}} P^s \cdot h_g(m_{g,t,s}, n_{g,t,s}, o_{g,t,s}, p_{g,t,s}) + \sum_{\substack{i \in \mathcal{I}, l \in \mathcal{L},\\ j \in \mathcal{J}}} D_l \cdot V_l(T_j) \cdot w_{l,i,j} \tag{3.40}$$

$$\text{s.t.} \quad f_g(m_{g,t,s}, n_{g,t,s}, o_{g,t,s}, p_{g,t,s}) \leq 0, \; g \in \mathcal{G}, s \in \mathcal{S} \tag{3.41}$$

$$\sum_{i \in \mathcal{I}, j \in \mathcal{J}} d_{i,j,t,s} = \sum_{g \in \mathcal{G}} p_{g,t,s} + R_{t,s}, \;\; t \in \mathcal{T}, s \in \mathcal{S} \tag{3.42}$$

$$d_{i,j,t,s} \leq \sum_{l \in \mathcal{L}} D_l \cdot N_{j,t} \cdot \mu_{l,i,j}, \; i \in \mathcal{I}, j \in \mathcal{J}, t \in \mathcal{T}, s \in \mathcal{S} \tag{3.43}$$

$$T_j \sum_{l \in \mathcal{L}} D_l \cdot w_{l,i,j} = \sum_{s \in \mathcal{S},\ t \in \mathcal{T}} P^s \cdot d_{i,j,t,s}, \quad i \in \mathcal{I}, j \in \mathcal{J} \tag{3.44}$$

$$d_{i,j,t,s} \geq 0, \quad i \in \mathcal{I}, j \in \mathcal{J}, t \in \mathcal{T}, s \in \mathcal{S} \tag{3.45}$$

$$p_{g,t,s} \geq 0, \quad g \in \mathcal{G}, t \in \mathcal{T}, s \in \mathcal{S} \tag{3.46}$$

$$m_{g,t,s},\ n_{g,t,s},\ o_{g,t,s} \in \{0,1\}, \quad g \in \mathcal{G}, t \in \mathcal{T}, s \in \mathcal{S} \tag{3.47}$$

$$\sum_{i \in \mathcal{I}, j \in \mathcal{J}} \mu_{l,i,j} \leq 1, \quad l \in \mathcal{L} \tag{3.48}$$

$$\gamma_l \geq r_i \cdot V_l(T_j) - \pi_{i,j}, \quad i \in \mathcal{I}, j \in \mathcal{J}, l \in \mathcal{L} \tag{3.49}$$

$$\gamma_l \geq 0, \quad l \in \mathcal{L} \tag{3.50}$$

$$(3.30) - (3.39)$$

3.5 Household Subscription

Once the menu design program of section 3.4.4 is solved in order to obtain a multilevel demand subscription menu, each household must determine which specific option to procure. Thus, each household type $h \in \mathcal{H}$ solves a menu subscription problem.

Following the model of section 3.3, we account for short and long-term uncertainty. Long-term uncertainty corresponds to seasonal variations and is represented by the set of scenarios $\mathcal{S}$. However, the household now faces short-term uncertainty related to two different sources. These are the real-time production of solar panels, and the availability of each multilevel demand subscription option. Short-term uncertainty is modeled as a scenario tree which now accounts for these two sources of uncertainty. This is depicted in Figure 3.3 in the case of only two solar power production possibilities per time period. The nodes of the scenario tree are named according to the realization of renewable supply (with 'L' indicating *low* solar supply, and 'H' indicating *high* solar supply) as well as the service interruption (with 'R' indicating that only the red color is served, 'RY' indicating that only the red and yellow colors are served, and 'RYG' indicating that all colors are served). We depict short-term uncertainty by $\omega^s_{[t]} = (\omega^{S,s}_{[t]}, \omega^C_{[t]}) \in (\Omega^{S,s}_{[t]} \times \Omega^C_{[t]}) = \Omega^s_{[t]}$, where $\omega^{S,s}_{[t]}$ and $\omega^C_{[t]}$ correspond respectively to a sequence of rooftop solar production and to a sequence of ON/OFF states for each option in the multilevel demand subscription menu up to stage t.

The level of subscription to each option is represented by variable $\sigma_{h,i,j}$. This decision is not indexed by scenario, because this choice does not depend on each scenario (i.e. it remains the same over all seasons and weekdays/weekends). Daily operational decisions, represented by the following variables $(\mathbf{ls}, \mathbf{nd}, \mathbf{bd}, \mathbf{bc}, \mathbf{e})$, are indexed by $s \in \mathcal{S}$ and $\omega^s_{[t]} \in \Omega^s_{[t]}$, because long-term and short-term realizations of uncertainty influence household operational deci-

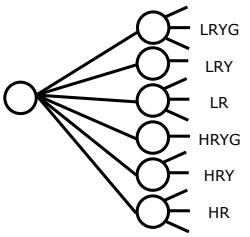

Figure 3.3: Illustration of a portion of the scenario tree for the household model (HC_h) of section 3.5 in the case of only two solar panel production possibilities per time period.

sions. The entire optimization of the household is modeled using the following stochastic program:

$$(HC_h)\colon \min_{\substack{\boldsymbol{\sigma},\mathbf{ls},\mathbf{nd},\\ \mathbf{bd},\mathbf{bc},\mathbf{e}}} \; V_{cut}\cdot\left(\sum_{s\in\mathcal{S}}\sum_{t\in\mathcal{T}}\sum_{\omega^s_{[t]}\in\Omega^s_{[t]}} P^s\cdot P^s_{t,\omega^s_{[t]}}\cdot ls_{t,s,\omega^s_{[t]}}\right) + \sum_{i\in\mathcal{I}}\sum_{j\in\mathcal{J}}\pi_{i,j}\cdot\sigma_{h,i,j} \tag{3.51}$$

$$\text{s.t. } 0\le bd_{t,s,\omega^s_{[t]}}\le BD_h,\;\; t\in\mathcal{T}, s\in\mathcal{S}, \omega^s_{[t]}\in\Omega^s_{[t]} \tag{3.52}$$

$$0\le bc_{t,s,\omega^s_{[t]}}\le BC_h,\;\; t\in\mathcal{T}, s\in\mathcal{S}, \omega^s_{[t]}\in\Omega^s_{[t]} \tag{3.53}$$

$$0\le e_{t,s,\omega^s_{[t]}}\le E_h,\;\; t\in\mathcal{T}, s\in\mathcal{S}, \omega^s_{[t]}\in\Omega^s_{[t]} \tag{3.54}$$

$$e_{t,s,\omega^s_{[t]}} = e_{t-1,s,\omega^s_{[t]}} - \frac{bd_{t,s,\omega^s_{[t]}}\cdot\Delta t}{\eta^d_h} + bc_{t,s,\omega^s_{[t]}}\cdot\eta^c_h\cdot\Delta t,\quad t\in\mathcal{T}, s\in\mathcal{S}, \omega^s_{[t]}\in\Omega^s_{[t]} \tag{3.55}$$

$$DP_{h,s,t} - ls_{t,s,\omega^s_{[t]}} + bc_{t,s,\omega^s_{[t]}} - PV_{t,s,\omega^{S,s}_t} - bd_{t,s,\omega^s_{[t]}} = \sum_{i\in\mathcal{I}} nd_{i,t,s,\omega^s_{[t]}},\;\; t\in\mathcal{T}, s\in\mathcal{S}, (\omega^{S,s}_{[t]},\omega^C_{[t]})\in\Omega^s_{[t]} \tag{3.56}$$

$$nd_{i,t,s,\omega^s_{[t]}}\le\sum_{j\in\mathcal{J}}\sigma_{h,i,j}\cdot 1_{[i,t,\omega^C_t]},\;\; i\in\mathcal{I}, t\in\mathcal{T}, s\in\mathcal{S}, (\omega^{S,s}_{[t]},\omega^C_{[t]})\in\Omega^s_{[t]} \tag{3.57}$$

$$\widetilde{nd}_{i,t,s,\omega^s_{[t]}}\le\sum_{j\in\mathcal{J}}\sigma_{h,i,j}\cdot 1_{[i,t,\omega^C_t]},\;\; i\in\mathcal{I}, t\in\mathcal{T}, s\in\mathcal{S}, (\omega^{S,s}_{[t]},\omega^C_{[t]})\in\Omega^s_{[t]} \tag{3.58}$$

$$nd_{i,t,s,\omega^s_{[t]}}\le\widetilde{nd}_{i,t,s,\omega^s_{[t]}}\;\; i\in\mathcal{I}, t\in\mathcal{T}, s\in\mathcal{S}, \omega^s_{[t]})\in\Omega^s_{[t]} \tag{3.59}$$

$$\sum_{t\in\mathcal{T}}\widetilde{nd}_{i,t,s,\omega^s_{[t]}}\le\sum_{j\in\mathcal{J}}T_j\cdot\sigma_{h,i,j},\;\; i\in\mathcal{I}, s\in\mathcal{S}, \omega^s_{[t]}\in\Omega^s_{[t]} \tag{3.60}$$

$$ls_{t,s,\omega^s_{[t]}}, \widetilde{nd}_{i,t,s,\omega^s_{[t]}}\ge 0,\;\; i\in\mathcal{I}, t\in\mathcal{T}, s\in\mathcal{S}, \omega^s_{[t]}\in\Omega^s_{[t]} \tag{3.61}$$

The notation and constraints of the model are similar to those in section 3.3. The goal of the household, depicted in Eq. (3.51), is to minimize the cost of load shedding along with the cost of subscribing to a particular option of the proposed menu. Constraints (3.52) to (3.55) detail the functioning of the battery in the household. The power balance constraint for the house is expressed in Eq. (3.56), where the net demand of the household which drawn from the grid, $nd_{i,t,s,\omega^s_{[t]}}$, is now indexed by the different reliability options of the proposed menu. Eq. (3.57) expresses the upper limit on net demand that the household is entitled to. The indicator variable $1_{[i,t,\omega^C_t]}$ indicates whether a certain reliability level i is being served at a given stage of a sequence of outcomes or not. A new variable named $\widetilde{nd}_{i,t,s,\omega^s_{[t]}}$ represents the positive part of variable $nd_{i,t,s,\omega^s_{[t]}}$ and therefore only the energy drawn by the household from the grid. Indeed, the household is able to export excess solar power to the grid but does not receive any payment from it. Moreover, this action does not allow the reliability energy counter to move backwards either. Thus, Eq. (3.58) and (3.59) allow us to describe this new variable. Constraint (3.60) imposes that the amount of energy consumed under a certain option cannot exceed the total energy credits that are topped up for that reliability option $i \in \mathcal{I}$.

3.6 Case Study Data

This section is dedicated to the description of the datasets that are used for populating the case study. This data includes household parameters, renewable supply scenarios, and system parameters for the Belgian system in a forward-looking scenario for the year 2050. Two simulations are presented in the next section, with differing levels of temporal resolution. The approach is built around representative days, each of which is split into (i) either six 4-hour time steps in the first simulation or (ii) 96 15-minute blocks in the second simulation. Section 3.6.1 is dedicated to the computation of the renewable production scenarios. Household parameters are then detailed in section 3.6.2. The parameters linked with the operation of the system along with details on generators are provided in section 3.6.3.

As already mentioned in section 3.2, the considered case study takes into account two types of uncertainty: long-term and short-term uncertainty. Long-term uncertainty is represented by seasonal variations captured by 8 reference day types that consist of weekdays and weekends for each season of the year. Then, for each scenario, short-term uncertainty is represented by the real-time production of solar panels and color interruption patterns via a scenario tree. For each day type we have correspondingly different profiles for households, generators, industrial load, and so on.

3.6.1 Renewable Supply Scenarios

Since two types of uncertainty are accounted for in this study, for each season, two types of data need to be generated for renewable supply:

- ◇ Short-term uncertainty: a scenario tree representing solar real-time production uncertainty.
- ◇ Long-term uncertainty: one daily profile that provides the forecast renewable supply (wind and solar) at every time period.

Only seasons are accounted for at this stage, because solar and wind production are not influenced by weekends and weekdays. Data from the website of the Belgian TSO Elia [41] for years 2013 to 2017 are collected in order to produce the required scenario tree and daily profiles. These data are then scaled up based on the EU 2050 reference scenario [55].

Short-Term Uncertainty: Real-time Production

In order to generate a scenario tree of solar supply for each season, we implement a methodology developed by [149] which aims at capturing inter-temporal uncertainty. This approach is developed in [96]. For the 4-hour case study, a scenario tree with 2 different outcomes per time stage is considered for both solar and wind power. For the 15-minute case study, we consider a more detailed version of the scenario tree, by allowing ten possible realizations of both solar and wind power for each time stage. Figure 3.4 depicts the lattice for a typical spring day in the case study with 15-minute resolution for solar and wind production. Note that the scenario tree encodes the normalized outcome for renewable production that must be scaled by the total installed capacity of renewable supply. Moreover, the wind lattice in this chapter is only used for computing long-term uncertainty (see below) but will be used for further analysis in the results of the next chapter (see section 4.4).

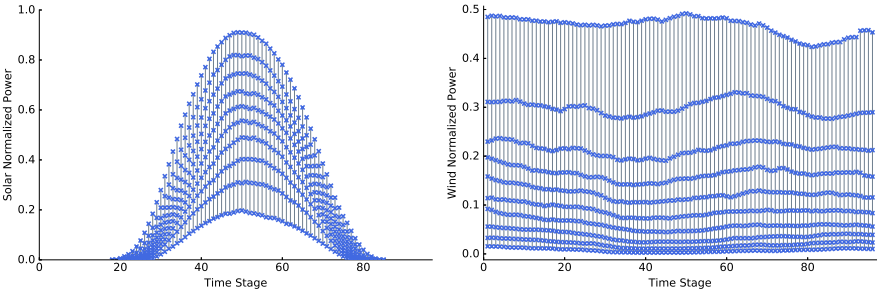

Figure 3.4: Scenario tree for solar (left) and wind (right) production with 15-minute resolution.

Long-Term Uncertainty: Forecast Production

Long-term uncertainty is represented by a daily production profile for both wind and solar production. This profile is obtained for each season by computing the mean production of the respective scenario tree. Figure 3.5 depicts the obtained forecast solar production for 4-hour and 15-minute resolution. Wind production is represented in Figure 3.6. In general, we can observe from these figures that wind is typically less available in summer and spring in comparison with winter and autumn while the inverse conclusion can be drawn for solar supply.

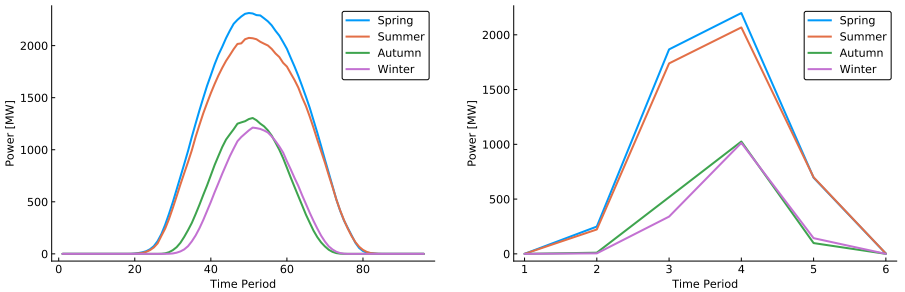

(a) 15-minute resolution (b) 4-hour resolution

Figure 3.5: Long-term system-level forecast solar production.

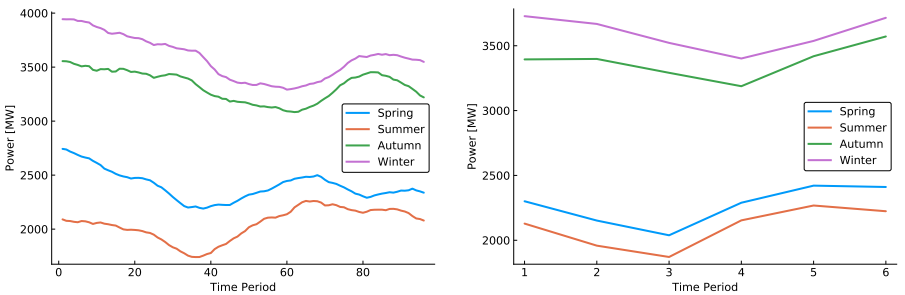

(a) 15-minute resolution (b) 4-hour resolution

Figure 3.6: Long-term system-level forecast wind production.

3.6.2 Household Parameters

Belgium is composed of households with different electricity consumption behaviours. In order to represent the different household types in terms of demand profiles realistically, we use data from the Belgian DSO Fluvius [69]. The data includes injection and production for approximately 100 households with a resolution of 15 minutes for the year 2016. The dataset consists of households

that are subject to a flat tariff, as well as others that subscribed to a two-part tariff (day/night tariff). Our goal is to group household profiles present in this dataset so as to generate three representative load profiles for Belgian households that can be used for populating our models. However, household profiles in this dataset are influenced by the tariff that they are subscribed to during the time when the data is collected. Therefore, we create a procedure in order to recover only the inflexible part of the load profile of each household. The steps used in order to obtain these three profiles are detailed hereafter:

1. Keep only households with daily load consumption between 2.5 and 40 kWh, in order to remove outliers [92].

2. For each day of a household under a flat tariff, find a day of a household under a two-part tariff with a comparable daily consumption and with a similar temporal profile. Compute an inflexible load profile from the minimum of the two daily profiles. This step allows us to approximate the part of the household consumption that is not dependent on the tariff, and can therefore be interpreted as being inflexible.

3. Cluster the resulting inflexible profiles in order to obtain 3 groups of households for each day type.

The mean profiles of each cluster for each day type are kept as the three representative load profiles for each day type. The averaged representative household daily load profiles are presented in Figure 3.7. In this figure, profile 1 (F1) corresponds to 67.78% of the population, profile 2 (F2) corresponds to 25.38%, and profile 3 (F3) corresponds to 6.84%.

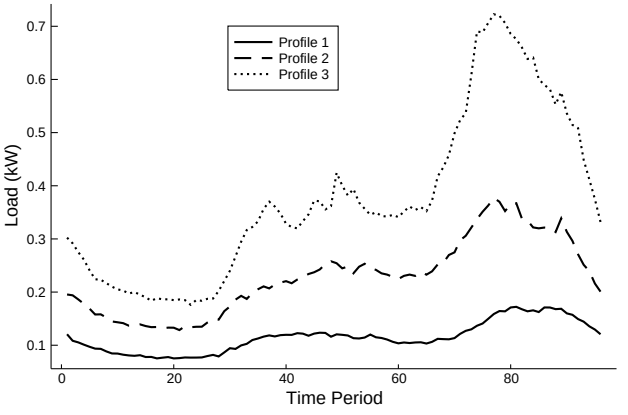

Figure 3.7: Household profiles, averaged over day types, that we consider in the case study. The data is based on Fluvius [69].

In order to account for the behaviour of households with batteries and local production (e.g. rooftop solar panels), we assume that (i) 16% of the households is equipped with a PV panel[2], (ii) one third of the households with a PV panel is equipped with a large battery (whose specifications we describe below), (iii) one third of the households with a PV panel is equipped with a smaller battery (whose specifications we describe below), and (iv) one third of the households with a PV panel is not equipped with a battery. Only types F2 and F3 are assumed to own PV panels. The installed capacity of PV panels is dimensioned so as to allow households to cover 100% of their annual consumption. Since 1kWc of PV panels produces 1000kWh on average per year [178], profile F2 is assumed to have an installed capacity of 2kWc, while profile F3 is assumed to have an installed capacity equal to 3.2kWc. We assign no PV to profile F1, because its annual consumption is considered too small to merit installing PV. The technical specifications of household batteries are presented in Table 3.1. In total, we model nine types of households. Their characteristics are presented in Table 3.2[3]. Even though only nine different types of households are considered in this work, the aggregator can apply the same menu design method to a different group of households by capturing the heterogeneity of the group via the representative aggregated demand function. The goal of considering these different types of households is to close the loop by observing the impacts of these two pricing schemes on these different types of households.

Table 3.1: Technical specifications of household batteries.

Battery Type	Large [166]	Small [113]
Energy Storage Limit [kWh]	13.5	3.84
Power Limit [kW]	5	0.85
Efficiency [%]	95	95

3.6.3 System Parameters

We now proceed to describe the configuration of the Belgian system. The fleet of conventional generators in the model consists of 55 units. The installed capacity of each technology follows the projected capacity of the year 2050,

[2]This percentage is computed by accounting for the fact that residential solar accounts for 64% of the total installed solar capacity in Belgium in 2018 [177]. Moreover 50% of the newly installed PV capacity up to 2030 will be residential solar capacity [58]. Therefore, in the foreseen scenario of 2050, residential solar production is projected to account for 56.94% of the total solar supply.

[3]Despite the fact that household types 2 to 7 represent a small fraction of the Belgian population, their contribution to system flexibility is not negligible (see section 4.4). Moreover, our analysis aims at analyzing the impact of demand response not only on the system but also on individual household types (see section 3.7.3 and 4.4), therefore we are interested in household heterogeneity (e.g. different load profiles, and possible differences in ownership of solar and/or storage), even if certain types of households represent a relatively small fraction of the total population.

Table 3.2: Characteristics of the different types of households.

Type	1	2	3	4	5	6	7	8	9
Category	F1	F2	F3	F2	F3	F2	F3	F2	F3
PV Panel	No	Yes	Yes	Yes	Yes	Yes	Yes	No	No
PV Installed [kW]	0	2	3.2	2	3.2	2	3.2	0	0
Battery Size	No	Large	Large	Small	Small	No	No	No	No
Proportion [%]	67.8	1.35	0.365	1.35	0.365	1.35	0.365	21.32	5.74

according to the EU 2050 reference scenario [55]. The technical and economic specifications of the units (maximum power production, marginal cost, heat rates, ...) are available from the website of the Belgian TSO Elia [41]. The installed capacity of conventional generators, which totals 15784 MW, can be broken down as follows: gas (14965 MW), oil (10 MW), biomass (542 MW), and waste (267 MW). Figure 3.8 compares the Belgian energy mix between year 2015 and our forward-looking scenario of 2050. The long-term maintenance schedule of units is accounted for by derating the maximum capacity of the units by a certain availability ratio. The availability ratio follows the hourly profiles of 2015 [41]. Import profiles for the year 2015 with hourly resolution are collected from [41]. These profiles are scaled up according to the projected value of the year 2050 of the EU 2050 reference scenario [55]. In order to create system and household level inflexible load profiles, the total load profile of year 2015 [41] is split into residential, industrial and commercial load, according to *Synthetic Load Profiles (SLPs)* [164]. Synthetic load profiles are normalized electricity consumption time series with 15-minute resolution that are publicly available for the residential and non-residential sectors. The load profiles are scaled up to the year 2050 according to the EU 2050 reference scenario [55]. Figure 3.9 represents the evolution for import and total load in Belgium from 2015 to our forward-looking scenario of 2050.

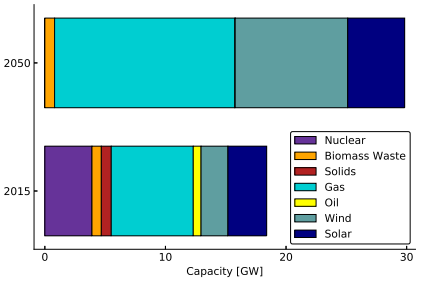

Figure 3.8: Installed capacity in Belgium (2015 and 2050).

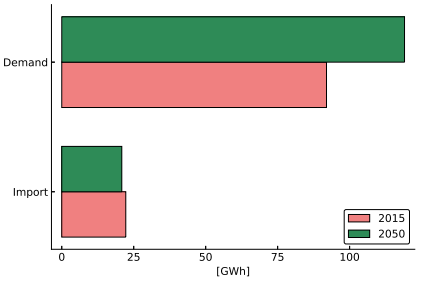

Figure 3.9: Comparison of import and demand for Belgium (2015 and 2050)

The pumped hydro storage in Belgium is assumed to have a pumping capacity amounting to 1200 MW, while the energy storage capacity of pumped

hydro amounts to 5700 MWh. Pumped hydro resources are assumed to have a roundtrip efficiency of 76.5% [138].

3.7 Application and Discussion

In this section, we continue by presenting the results obtained for each model presented in section 3.2 populated with the data given in section 3.6. Note that we consider two case studies, one with a 4-hour time step resolution and the other considering time periods of 15 minutes. First, the household characterization model is used (see section 3.3) to create a system load duration curve in section 3.7.1. Then, section 3.7.2 presents the resulting menus for both multilevel demand subscription and priority service. Finally, section 3.7.3 presents the subscription choices of households under both demand response schemes. Numerical experiments are performed using the **JuMP** package [36] in the **Julia** programming language [12]. The mathematical programs are solved using the **Gurobi** optimization solver [81]. The 4-hour resolution case study is solved on a DELL Latitude 7490 with 1.7GHz Intel Quad Core i5 processors, whereas the 15 minute resolution case study is run on the high performance computing Lemaitre3 cluster hosted at UCLouvain as part of the CECI facility.

3.7.1 System-Level Load Duration Curve

In order to create a menu of options, we approximate the system-level load duration curve using the model of section 3.3. This model is solved using the stochastic dual dynamic programming (SDDP) technique [144, 158] for the 15-minute resolution case study due to the large number of outcomes per time stage. We present the resulting demand functions for the first household type in Figure 3.10 under both resolutions. The demand functions of each type are then aggregated, according to the number of households in each type. We thus obtain a system-level demand function, which is generally not concave. In order to derive the concave functions $V_l(t)$ in Eq. 3.13 of problem (CP_l), which approximate the system-level demand function, we use a least-square fit that respects the concavity of $V_l(t)$. The concave approximation of this system-level demand function is presented in Figure 3.11 for both case studies. Note that the obtained load duration curves for other household types for both resolutions are presented in Appendix 3.B along with the non-concave version of the system-level demand functions.

3.7.2 Optimal Menus

After computing the system-level load duration curve, we solve the MILP formulation of the Stackelberg equilibrium presented in section 3.4.4 in order to derive both a priority service and a multilevel demand subscription menu. Indeed, since priority service is a special case of multilevel demand subscription,

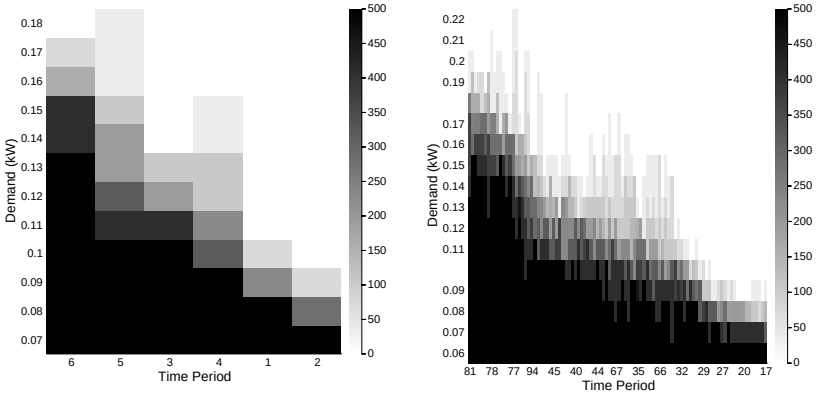

(a) 4-hour resolution (b) 15-minute resolution

Figure 3.10: Demand functions for the first household type. The x-axis corresponds to the time period of the load duration curve, the y-axis represents the fuse limit. The tone of grey indicates valuation for an increment of fuse capacity, ranging from 0 to 500 €/MWh.

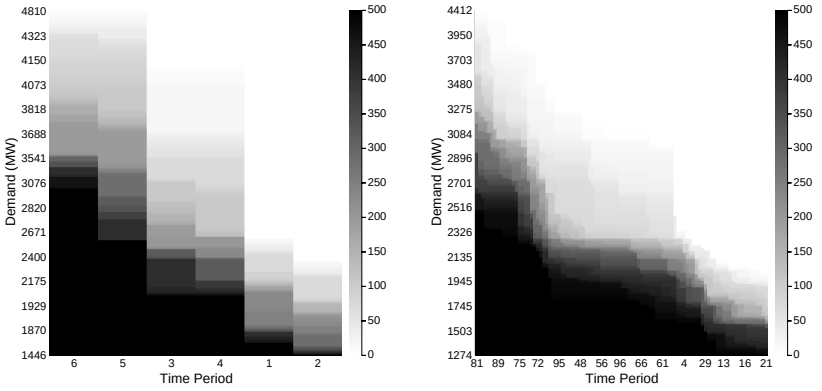

(a) 4-hour resolution (b) 15-minute resolution

Figure 3.11: Concave approximation of the system-level demand function.

the same MILP formulation can be used for designing a priority service menu. This optimal set of options is presented in Table 3.3 for the case studies with both resolutions.

In order to compare priority service and multilevel demand subscription consistently, we fix the price and reliability of multilevel demand subscription options that cover the full duration of service. By doing so, the set of options under multilevel demand subscription includes the set of options under pri-

Table 3.3: Optimal priority service menu for both resolutions.

Option	Reliability [%]		Price [€/kW-month]	
	4-hour	15-minute	4-hour	15-minute
Green	66.49	58.37	37.79	31.39
Yellow	90.32	89.38	69.93	66.78
Red	100	100	91.94	87.08

ority service. The resulting optimal multilevel demand subscription menu is presented in Table 3.4.

Table 3.4: Optimal multilevel demand subscription menu for both time resolutions.

Option	Duration [%]	Reliability [%]		Price [€/kW-month]	
		4-hour	15-minute	4-hour	15-minute
Green	33.33	66.49	58.37	21.52	17.69
	66.66			33.10	27.21
	100			37.79	31.39
Yellow	33.33	90.32	89.38	41.41	43.04
	66.66			63.14	61.72
	100			69.93	66.78
Red	33.33	100	100	53.43	52.64
	66.66			82.19	80.98
	100			91.94	87.08

3.7.3 Household Contract Choices

Figure 3.12 presents the optimal subscription of each household type to the priority service or the multilevel demand subscription menu for the 4-hour case study. Moreover, Figure 3.13 presents household subscriptions under both demand response schemes when time periods of 15 minutes are considered. These results represent the output of the model presented in section 3.5. For the 15-minute case study, due to the substantial number of potential realizations of uncertainty, this model is solved using stochastic dual dynamic programming (SDDP) [144, 158] as in the case of the other household model presented in section 3.3.

By observing Figure 3.14 that compares the total energy subscription of both schemes for both resolutions, we observe that the total subscribed energy of each household under multilevel demand subscription is lower than under priority service, despite the fact that the total subscribed capacity is higher. This observation is driven by the offer of options with shorter duration in multilevel demand subscription. Consequently, multilevel demand subscription is not only advantageous for households, by allowing higher peak capacity when

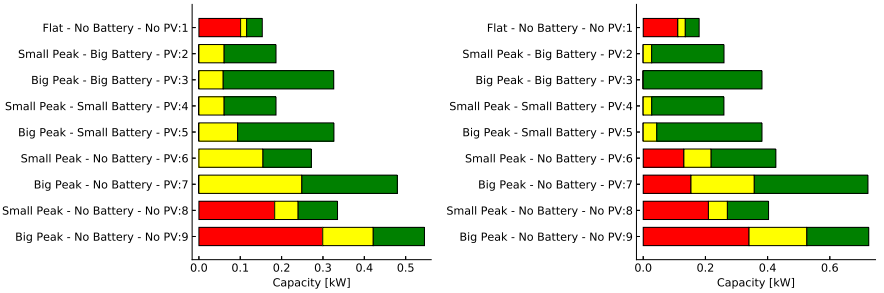

Figure 3.12: Capacity subscriptions of each household type to each option under priority service (left) and multilevel demand subscription (right) for the case study with 4-hour resolution.

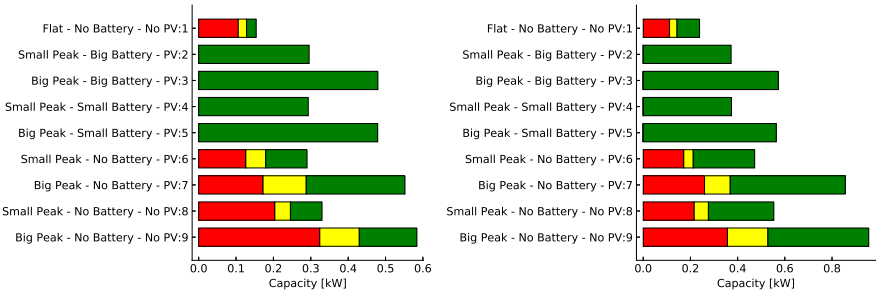

Figure 3.13: Capacity subscriptions of each household for each option under priority service (left) and multilevel demand subscription (right) for the case study with 15-minute resolution.

needed, but is also favorable for the producer, because the subscribed energy demand is closer to the real consumption of households.

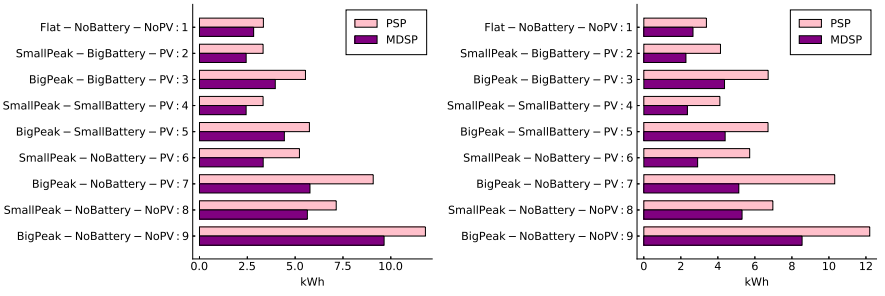

Figure 3.14: Comparison of the total energy subscription of households under priority service and multilevel demand subscription for the 4-hour case study (left) and the 15-minute case study (right).

Moreover, multilevel demand subscription allows the consumer to face a lower bill than under priority service pricing as it can be observed in Figure 3.15 for the 15-minute case study. This is due to the fact that multilevel demand subscription expresses the valuation of the consumer more accurately. However, the 4-hour results of Figure 3.15 indicate that the subscription cost for multilevel demand subscription is not always lower than for priority service, as it is the case with 15-minute resolution. This is due to the fact that a 4-hour resolution fails to capture the economic savings that a household achieves by subscribing to options with very short duration (e.g. 1 hour).

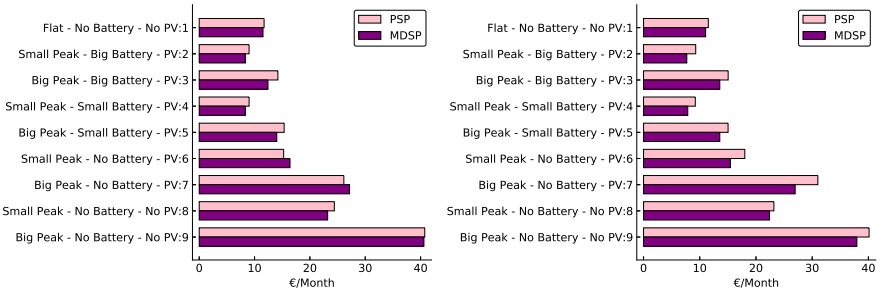

Figure 3.15: Comparison of the bill faced by households subscribing to priority service and multilevel demand subscription for the 4-hour case study (left) and the 15-minute case study (right).

Even though the electricity bill is not always lower under multilevel demand subscription, Figure 3.16 highlights that the total cost faced by every type of household is lower under multilevel demand subscription. The total cost accounts for the electricity bill along with the cost incurred by households due to involuntary curtailment of inflexible load. We can observe that, even though in certain cases multilevel demand subscription leads to a higher bill, it is still more beneficial to resort to it because the gain in terms of shortage cost balances this effect.

3.8 Conclusion

This chapter focuses on the design of priority service and multilevel demand subscription as two demand response options for mobilizing flexible residential demand. We present a method for the utility to approximate the system load duration curve. We then derive a MILP formulation of the bilevel Stackelberg equilibrium for designing the two menus. Finally, we express the menu selection problem of households. We perform a realistic case study of the Belgian market, and find that households can better match their energy consumption under multilevel demand subscription: they subscribe to less energy, and more capacity than under priority service pricing. Households also experience a lower bill

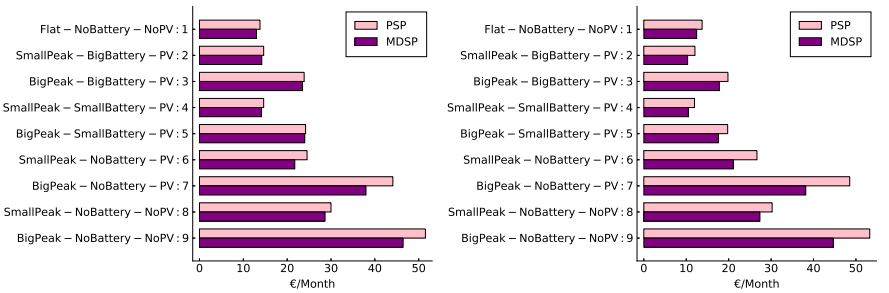

Figure 3.16: Comparison of the total cost (electricity bill and shortage cost) faced by households subscribing to priority service or multilevel demand subscription for the 4-hour case study (left) and the 15-minute case study (right).

and total cost for multilevel demand subscription than under priority service.

3.A Notations

All the notations used throughout this chapter are summarized in the different parts of this section.

Sets

$\mathcal{G}, \lvert\mathcal{G}\rvert$	Set of generators and its cardinality
$\mathcal{L}, \lvert\mathcal{L}\rvert$	Set of consumer types and its cardinality
$\mathcal{H}, \lvert\mathcal{H}\rvert$	Set of households and its cardinality
$\mathcal{T}, \lvert\mathcal{T}\rvert$	Set of time periods and its cardinality
$\mathcal{I}, \lvert\mathcal{I}\rvert$	Set of reliability options and its cardinality
$\mathcal{J}, \lvert\mathcal{J}\rvert$	Set of duration options and its cardinality
$\mathcal{S}, \lvert\mathcal{S}\rvert$	Set of long-term scenarios and its cardinality
$\Omega_{[t]}^{S,s}$	Set of sequences of solar panel production up to stage t for scenario s (representation of the solar scenario tree linked with the long-term scenario s)
$\Omega_{[t]}^{C}$	Set of sequences of color ON/OFF states up to stage t
$\Omega_{[t]}^{s}$	Set representing the cross product of solar panel production for scenario s and color ON/OFF states uncertainty given by $\Omega_{[t]}^{S,s} \times \Omega_{[t]}^{C}$

Parameters

V_{cut}	Penalty parameter if a shortage occurs for households, assumed to be equal to 500 €/kWh
P^s	Probability of occurrence of scenario s
$P^s_{t,\omega_{[t]}^{S,s}}$	Probability of occurrence of a sequence of normalized solar panel production $\omega_{[t]}^{S,s}$ up to stage t of the set of sample paths available from the scenario tree belonging to scenario s

$P^s_{t,\omega^s_{[t]}}$ Probability of occurrence of a sequence of uncertainty realization $\omega^s_{[t]}$ up to stage t of the set of sample paths available from the scenario tree belonging to scenario s multiplied by the probability of occurrence of a sequence of colors ON/OFF states up to stage t from the interruption pattern scenario tree

BD_h Battery charge capacity in household of type h [kW]

BC_h Battery discharge capacity in household pf type h [kW]

E_h Battery energy capacity in household of type h [kWh]

η^d_h Battery discharge efficiency for household of type h

η^c_h Battery charge efficiency in household h

Δt Number of time periods in an hour (e.g. 4 for the 4-hour case study and 0.25 for the 15-minute analysis)

$DP_{h,t,s}$ Load (Demand Profile) of household h at stage t in scenario s [kW]

PV_h Solar panel installed capacity for household type h [kW]

FL Fuse limit imposed on the household model [kW]

T_j Duration of option j

$V_l(T_j)$ Valuation of consumer type l for a duration T_j [€/MWh]

D_l Demand of consumer type l [MW]

$\sigma^*_{l,i,j}(\mathbf{r},\boldsymbol{\pi})$ Optimal subscription quantity of consumer l under option (i,j) [MW] for the menu defined by $(\mathbf{r},\boldsymbol{\pi})$

$R_{t,s}$ System-level renewable production (solar and wind) at time period t in scenario s [MW]

$N_{j,t}$ Binary parameters that determines whether a certain duration option j is being served in time period t of actual operations or not

Π^+ Upper bound of menu prices

Variables

$ls_{t,s,\omega^s_{[t]}}$ Load shedding at stage t in scenario s for the sequence of uncertainty $\omega^s_{[t]}$ up to stage t (given by the tuple $(\omega^{S,s}_{[t]},\omega^C_{[t]})$ representing respectively the solar production sequence and the ON/OFF states of reliability options)

$bd_{t,s,\omega^s_{[t]}}$ Discharge power of the battery at stage t in scenario s for the sequence of uncertainty $\omega^s_{[t]}$ up to stage t (given by the tuple $(\omega^{S,s}_{[t]},\omega^C_{[t]})$ representing respectively the solar production sequence and the ON/OFF states of reliability options)

$bc_{t,s,\omega^s_{[t]}}$ Charge power of the battery at stage t in scenario s for the sequence of uncertainty $\omega^s_{[t]}$ up to stage t (given by the tuple $(\omega^{S,s}_{[t]},\omega^C_{[t]})$ representing respectively the solar production sequence and the ON/OFF states of reliability options)

$e_{t,s,\omega^s_{[t]}}$ Energy stored in the battery at stage t in scenario s for the sequence of uncertainty $\omega^s_{[t]}$ up to stage t (given by the tuple $(\omega^{S,s}_{[t]},\omega^C_{[t]})$ representing respectively the solar production sequence and the ON/OFF states of reliability options)

$nd_{t,s,\omega^s_{[t]}}$ Net demand (positive and negative) from the grid at stage t in scenario s for the sequence of uncertainty $\omega^s_{[t]}$ up to stage t (given by the tuple $(\omega^{S,s}_{[t]}, \omega^C_{[t]})$ representing respectively the solar production sequence and the ON/OFF states of reliability options)

$\lambda_{t,s,\omega^{S,s}_{[t]}}$ Dual variable of the fuse limit constraint in the household demand function stochastic program at stage t in scenario s for the solar panel production sequence $\omega^{S,s}_{[t]}$ up to stage t

$\sigma_{l,i,j}$ The subscription quantity of consumer l under option (i,j) [MW]

r_i Reliability of option i [%]

$\pi_{i,j}$ Price of option (i,j) with reliability r_i and duration T_j [€/MW]

γ_l Dual variable of Constraint (3.15) representing the net surplus of consumer type l

$p_{g,t,s}$ Production of generator g at time period t in scenario s [MW]

$m_{g,t,s}$ Start up decision of generator g at time period t in scenario s

$n_{g,t,s}$ Shut down decision of generator g at time period t in scenario s

$o_{g,t,s}$ Unit commitment decision of generator g at time period t in scenario s

$d_{i,j,t,s}$ Supply to option (i,j) at time period t in scenario s [MW]

$\mu_{l,i,j}$ Binary subscription decision of consumer l for option (i,j)

$y_{l,i,j}$ Auxiliary variable to represent $\pi_{i,j} \cdot \mu_{l,i,j}$

$w_{l,i,j}$ Auxiliary variable to represent $r_i \cdot \mu_{l,i,j}$

$\mathbf{m}$ Compact form of $m_{g,t,s}$, similarly for $\mathbf{n}$, $\mathbf{o}$, $\mathbf{p}$, $\mathbf{d}$, $\mathbf{y}$, $\mathbf{w}$, $\boldsymbol{\gamma}$, $\mathbf{r}$, $\boldsymbol{\pi}$, $\boldsymbol{\sigma}$ and $\boldsymbol{\mu}$

$\sigma_{h,i,j}$ Subscription quantity under option (i,j) for household h kW]

$nd_{i,t,s,\omega^s_{[t]}}$ Net demand (positive and negative) from the grid for option i with reliability r_i at stage t in scenario s for the sequence of uncertainty $\omega^s_{[t]}$ up to stage t (given by the tuple $(\omega^{S,s}_{[t]}, \omega^C_{[t]})$ representing respectively the solar production sequence and the ON/OFF states of reliability options)

$\widetilde{nd}_{i,t,s,\omega^s_{[t]}}$ Net demand (only positive) from the grid for option i with reliability r_i at stage t in scenario s for the sequence of uncertainty $\omega^s_{[t]}$ up to stage t (given by the tuple $(\omega^{S,s}_{[t]}, \omega^C_{[t]})$ representing respectively the solar production sequence and the ON/OFF states of reliability options)

Functions

h_g Cost function of generator g, including production costs, startup and minimum load costs

f_g Constraints of unit commitment problems, including minimum up and down times, ramp rates and production limits

SW Social welfare function

CS Consumer surplus function

3.B Household Load Duration Curves

In section 3.7.1, the demand functions obtained for the first household type are presented. The demand functions obtained for all household types are presented in detail in this section. Figure 3.17 corresponds to the 4-hour case study and Figure 3.18 corresponds to the 15-minute case study.

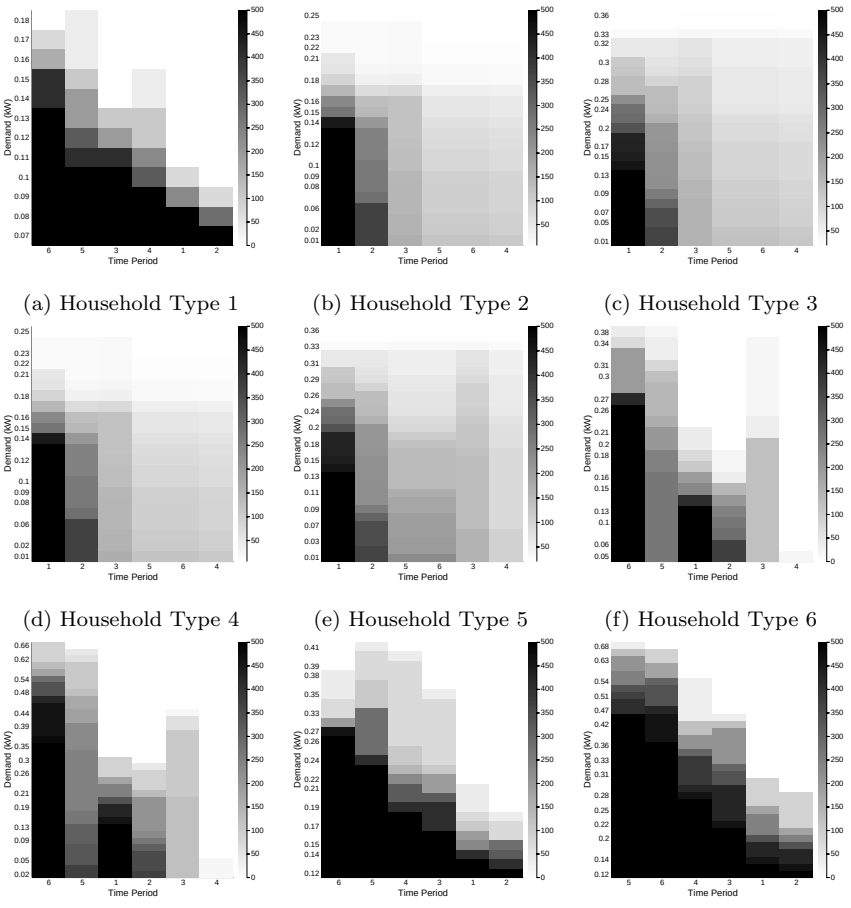

(a) Household Type 1 (b) Household Type 2 (c) Household Type 3

(d) Household Type 4 (e) Household Type 5 (f) Household Type 6

(g) Household Type 7 (h) Household Type 8 (i) Household Type 9

Figure 3.17: Demand functions obtained for each household type for the 4-hour case study. The x-axis corresponds to the time period of the load duration curve, while the y-axis represents the fuse limit. The grey tone indicates the valuation for an increment of fuse capacity, ranging from 0 to 500 €/MWh.

Figure 3.19 shows the non-concave system-level demand function obtained by the aggregation of load duration curves from each household type for both

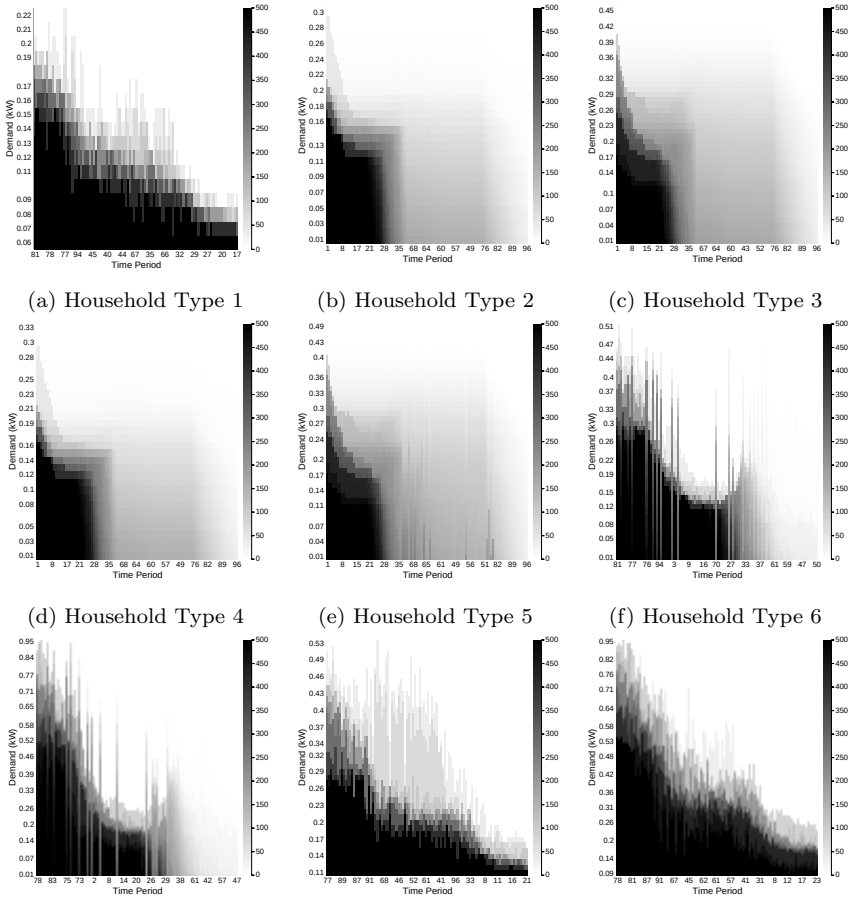

(a) Household Type 1 (b) Household Type 2 (c) Household Type 3

(d) Household Type 4 (e) Household Type 5 (f) Household Type 6

(g) Household Type 7 (h) Household Type 8 (i) Household Type 9

Figure 3.18: Demand functions obtained for each household type for the 15-minute case study. The x-axis corresponds to the time period of the load duration curve while the y-axis represents the fuse limit. The grey tone indicates the valuation for an increment of fuse capacity, ranging from 0 to 500 €/MWh.

the 4-hour and 15-minute case studies.

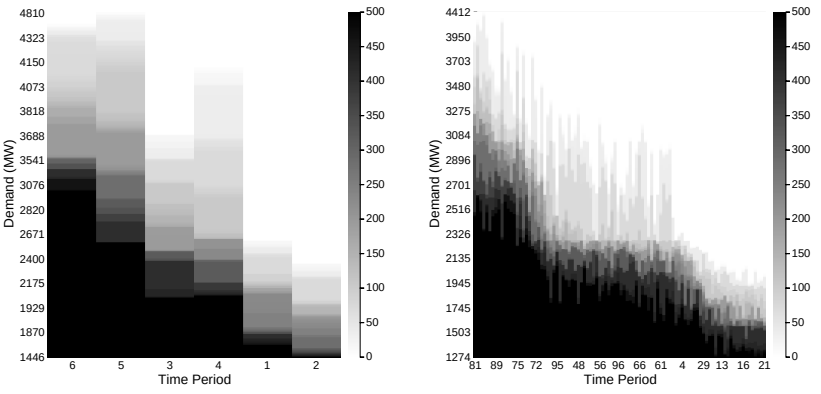

(a) 4-hour resolution (b) 15-minute resolution

Figure 3.19: Non-concave system-level demand functions.

4 Comparison of Priority Service with Multilevel Demand Subscription

4.1 Introduction

Whereas the previous chapter is focused on the design of service contracts for multilevel demand subscription and priority service, the focus of the present chapter is on the quantification of the trade-offs between the increased operational efficiency and complexity of multilevel demand subscription relative to priority service. The challenge in quantifying the benefits of multilevel demand subscription relate to the coexistence of local distributed renewable supply (rooftop solar) as well as local flexibility in the form of storage at the household level. This requires a careful modeling framework which is discussed in this chapter. This framework is then applied to a realistic model of the Belgian power market for two different time resolutions. By comparing these two time resolutions, this study also demonstrates the importance of using a more refined time scale in order to quantify the benefits of demand response more accurately in production simulation models. Finally, the performance of these two demand response schemes is also compared to the application of real-time pricing on the same system. Figure 4.1 presents the difference between the focus of the previous and the current chapter.

This chapter is organized as follows. First, section 4.2 presents the simulation framework that is used for quantifying the efficiency of multilevel demand subscription and priority service pricing. In section 4.3, the model used to analyze the difference between real-time pricing and the two targeted demand response schemes is described. Finally, section 4.4 analyzes the results that are obtained for a case study of the Belgian power system, while section 4.5 concludes the analysis. Furthermore, section 4.A in the appendix details all the mathematical notations used in this chapter.

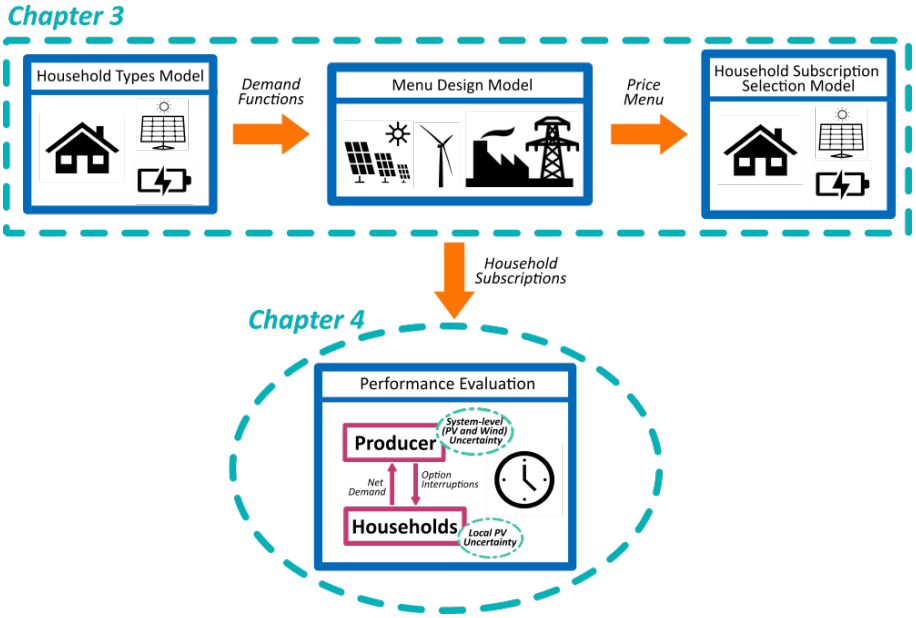

Figure 4.1: Chapter-by-chapter representation of the general framework applied for comparing Multilevel Demand Subscription with Priority Service.

4.2 Performance Evaluation Framework

In order to simulate the performances of different residential pricing methods, we need to account for the interplay between utility-scale and distributed rooftop solar uncertainty. Concretely, a realization of a sample path of uncertainty over the horizon of our analysis is a realization of $(\omega^U, \omega^H) \in \Omega^U \times \Omega^H$. Here, Ω^U is the set of sample paths of renewable supply from utility-scale renewable resources, whereas Ω^H is the set of sample paths of renewable supply from rooftop solar resources.

The interface between the utility and the household is the service contract. The service contract allows the utility and the household to decentralize their decision-making according to locally observable information related to uncertainty. This decentralization is represented in the left part of Figure 4.2. More specifically, from the point of view of the utility, the uncertainty in the system comprises utility-scale renewable supply and *net residential demand*. The net residential demand is driven by rooftop solar supply at the households, however the utility meters and reacts to net demand. Similarly, from the point of view of the household, a realization of uncertainty comprises of rooftop solar power supply as well as the *interruption of different service options*. The interruption patterns are of course driven by utility-scale renewable supply, however

the household does not observe or react to this information. Essentially, the residential service contracts can be viewed as a way of decentralizing a dynamic optimization problem under uncertainty (that of dispatching the *entire* system against *system-level* uncertainty) between the utility and the household.

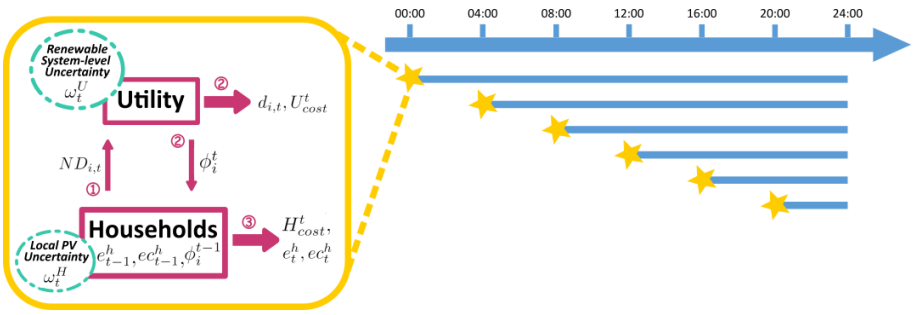

Figure 4.2: Illustration of the rolling optimization approach used to assess the performance of priority service and multilevel demand subscription for a model with 4-hour resolution. The stepsize is adjusted correspondingly for the model with 15-minute resolution.

In this section, we describe our proposal for simulating this decentralized decision-making process, so as to quantify the efficiency of priority service and multilevel demand subscription via a rolling horizon approach. This proposal bears similarities with the hierarchical coordination of transmission and distribution system operations proposed in [112, 137]. Our rolling optimization approach is described in Figure 4.2. At each period, there is an interaction between the utility and households after the local uncertainty of each sub-system (ω^U, ω^H) has been revealed.

First, in the spirit of a load following system, households (indexed by $h \in \mathcal{H}$) estimate their consumption for the present period by optimizing their behaviour until the end of the horizon. This is achieved by solving the household decision problem $(H_{h,t})$, given (i) the previous energy state of their residential storage (if any is available), indicated by e_{t-1}^h, (ii) the amount of energy left to consume based on their contract subscription, indicated by ec_{t-1}^h, and (iii) the interruption pattern of options faced at time period $t-1$, indicated by ϕ_i^{t-1}. This step results in the computation of a residential aggregated net demand $(ND_{i,t})$ for time period t, which is observed by the utility for each option $i \in \mathcal{I}$. Note that households use the information of the previous time period concerning the interruption of options because it corresponds to their best forecast of the interruption for the upcoming balancing interval.

Generators are then dispatched at system level in order to meet the net demand of all households in the population, while accounting for the uncertainty

of system-level renewable supply. This is achieved by solving the mathematical program (U_t). During this second step, the utility reacts to the net demand of households by only supplying a certain portion of that demand ($d_{i,t}$). This leads to a new interruption pattern of colors ϕ_i^t, and to a certain production cost U_{cost}^t for the current time period.

Finally, households adapt their originally planned behaviour in response to the actual supply that is provided by the system at the current time step (represented by the new interruption pattern of options ϕ_i^t). This third step leads to the computation of the shortage cost that the household actually experiences at the present time period (H_{cost}^t). We can further compute the new energy state of the battery, e_t^h, as well as the remaining energy credits left on the contract until the end of the horizon.

The overall procedure is described by Algorithm 1 and can also be summarized as follows:

1. Initialize the option interruption profile. All options are available, the energy stored in household batteries is equal to 0 kWh. The amount of energy credits available to each household are based on their contract subscription.

2. For every time step $t \in \mathcal{T}$ of the simulation horizon:

   (a) Sample a realization of household renewable supply $\omega_t^H \in \Omega^H$ and a realization of utility-scale renewable resources $\omega_t^U \in \Omega^U$ for that particular time stage.

   (b) Solve a household decision problem ($H_{h,t}$) for every type of household $h \in \mathcal{H}$ in order to obtain the requested demand by the households for that time stage.

   (c) Solve a utility decision problem (U_t) in order to determine the action of the utility in terms of supply decisions and interruption of options, based on the total demand requested by households at step (2b).

   (d) Update the household decisions ($H_{h,t}$) in order to account for the supply decisions of the utility, along with the actual interruption of options, in order to compute the shortage cost incurred by the household.

   (e) Increment t, update the state of the system, and return to step (2a).

In the remainder of this section, we describe the problems solved by the utility (U_t) and households ($H_{h,t}$). The utility model is discussed first, as it amounts to a simple economic dispatch model. We then define the multi-stage optimization that drives household consumption.

Algorithm 1 Performance evaluation framework using in the analysis of Chapter 4.

Require: Number of simulations n_{simu}

for $n \leftarrow 1$ to n_{simu} **do**
  $\phi_i^0 \leftarrow 1$
  $e_0^h \leftarrow 0$
  $ec_{i,0}^h \leftarrow \sum_{j \in \mathcal{J}} \Omega_{h,i,j}$
  for $t \leftarrow 1$ to $|\mathcal{T}|$ **do**
    $\omega_t^H \leftarrow \texttt{SampleH}(t)$
    $\omega_t^U \leftarrow \texttt{SampleU}(t)$
    $ND_{i,t} \leftarrow \texttt{H}(t, \phi_i^{t-1}, \omega_t^H, e_{t-1}^h, ec_{t-1}^h)$
    $\phi_i^t, d_{i,t}, U_{cost}^t \leftarrow \texttt{U}(t, ND_{i,t}, \omega_t^U)$
    $H_{cost}^t, e_t^h, ec_t^h \leftarrow \texttt{HCost}(t, \phi_i^t, \omega_t^H, d_{i,t}, e_{t-1}^h, ec_{t-1}^h)$
  end for
end for

4.2.1 Rolling Optimization for the Utility

The decisions of the utility are depicted by means of a single-period optimization problem. Inter-temporal unit commitment constraints (startup costs, min up/down time constraints, and ramp constraints), and pumped hydro constraints are ignored here since the focus of this study is on the benefits that can be achieved as a result of household flexibility. In future research, it could be interesting to extend this formulation in order to account for the intertemporal constraints of the utility.

Concretely, the utility solves the following problem[1]:

$$(U_t): \quad \max_{d_{i,t}, p_{g,t}} \ \sum_{i \in \mathcal{I}} \bar{V}_i \cdot d_{i,t} - \sum_{g \in \mathcal{G}} h_g(p_{g,t}) \tag{4.1}$$

$$s.t. \ f_g(p_{g,t}) \leq 0, \ g \in \mathcal{G} \tag{4.2}$$

$$d_{i,t} \leq ND_{i,t}, \ i \in \mathcal{I} \tag{4.3}$$

$$\sum_{i \in \mathcal{I}} d_{i,t} = \sum_{g \in \mathcal{G}} p_{g,t} + \omega_t^U \tag{4.4}$$

$$d_{i,t}, p_{g,t} \geq 0, \ i \in \mathcal{I}, g \in \mathcal{G} \tag{4.5}$$

The objective function of the utility is expressed in Eq. (4.1). Here, $h_g(p_{g,t})$ represents the cost incurred by the utility for producing $p_{g,t}$ from generator g. The valuation $\bar{V}_i$ corresponds to the estimate of the average valuation that the utility assigns to priority class i, based on how households decide to subscribe to the multilevel demand service. This estimation is given by the following

[1] We describe the problem for the case of multilevel demand subscription, of which priority service is a special instance.

expression:

$$\bar{V}_i = \frac{1}{|\mathcal{T}|} \sum_{t \in \mathcal{T}} \frac{\sum_{l \in \mathcal{L}: \sigma^*_{l,i,j(t)} = D_l} V_l(T_{j(t)}) \cdot D_l}{\sum_{l \in \mathcal{L}: \sigma^*_{l,i,j(t)} = D_l} D_l} \tag{4.6}$$

Here, $\sigma^*_{l,i,j}$ corresponds to the optimal subscription decision of consumer type l for option (i, j), and D_l corresponds to the demand requested by consumer type l given a certain valuation $V_l(T_j)$ for duration T_j. Note that $\sigma^*_{l,i,j}$ is the solution of problem (CP_l) of section 3.4.2 and $V_l(T_j)$ is given by the system load duration curve computed in section 3.3. Finally, $j(t)$ corresponds to the duration options that are served at a certain time period t. It has a similar interpretation to the binary parameter $N_{j,t}$ of model (MD) of section 3.4.3. In the presented formula, for each time period t, the fraction computes the weighted average of the valuation of consumers l that subscribe during the menu design process (see section 3.4) to options with reliability i and duration $T_{j(t)}$ that are served at time period t of actual operations. These obtained weighted averages are then averaged over the time horizon.

Regarding the remaining equations of the model, Constraint (4.2) expresses the production constraints of the utility. Constraint (4.3) implies that the utility may not offer more than the net demand that a certain priority class actually decides to consume at any given time period. The variable $d_{i,t}$ represents the demand served by the utility for reliability class i. Constraint (4.4) expresses the power balance constraint for the utility. The renewable supply ω^U_t in Constraint (4.4) is the utility-scale renewable production, which is sampled during the procedure described in Algorithm 1. The net demand $ND_{i,t}$ in Constraint (4.3) is obtained as the solution of the household rolling optimization which is presented in the following section.

4.2.2 Rolling Optimization for the Household

In contrast to the utility model, which has been simplified in order to relax inter-temporal dependencies, the household rolling optimization is represented as a dynamic optimization under uncertainty in this chapter, since our analysis is focused on the impact of residential sector flexibility to efficient system operations. The household faces uncertainty related to the supply of rooftop solar power (ω^H_t) at its premises and the interruption history of the service tiers (ϕ^t_i) in the home. This uncertainty is depicted in Figure 3.3 in the case of only two solar panel production possibilities per time period. The nodes of the scenario tree are named according to the realization of renewable supply (with 'L' indicating *low* solar supply, and 'H' indicating *high* solar supply) as well as the service interruption (with 'R' indicating that only the red color is served, 'RY' indicating that only the red and yellow color are served, and 'RYG' indicating that all colors are served).

In this rolling optimization, the household reacts to a history of realizations that have transpired up to stage t. For each stage t, given a stage uncertainty realization of solar production ω_t^H and interruption of services ϕ_i^t, we can describe the household model in terms of future stage costs. The future costs are captured by $\mathcal{H}_{h,t+1}(e_t, ec_{i,t}, \omega_t^H, \phi_i^t)$, namely the value function of the problem. The household model is therefore given by:

$$H_{h,t}(e_{t-1}, ec_{i,t-1}, \omega_t^H, \phi_i^t) =$$

$$\min_{\substack{bd_t, bc_t, e_t, ec_{i,t}, \\ nd_{i,t}, \widetilde{nd}_{i,t}}} V_{cut} \cdot ls_t + \mathcal{H}_{h,t+1}(e_t, ec_{i,t}, \omega_t^H, \phi_i^t) \tag{4.7}$$

$$s.t.\ 0 \leq bd_t \leq BD_h \tag{4.8}$$

$$0 \leq bc_t \leq BC_h \tag{4.9}$$

$$0 \leq e_t \leq E_h \tag{4.10}$$

$$e_t = e_{t-1} - \frac{bd_t \cdot \Delta t}{\eta_h^d} + bc_t \cdot \eta_h^c \cdot \Delta t \tag{4.11}$$

$$DP_{h,t} - ls_t - PV_h \cdot \omega_t^H + bc_t - bd_t = \sum_{i \in \mathcal{I}} nd_{i,t} \tag{4.12}$$

$$nd_{i,t} \leq \sum_{j \in \mathcal{J}} \Theta_{h,i,j} \cdot \phi_i^t,\ i \in \mathcal{I} \tag{4.13}$$

$$\widetilde{nd_{i,t}} \leq \sum_{j \in \mathcal{J}} \Theta_{h,i,j} \cdot \phi_i^t,\ i \in \mathcal{I} \tag{4.14}$$

$$nd_{i,t} \leq \widetilde{nd}_{i,t}\ i \in \mathcal{I} \tag{4.15}$$

$$ec_{i,t} = ec_{i,t-1} - \widetilde{nd}_{i,t},\ i \in \mathcal{I} \tag{4.16}$$

$$ls_t, \widetilde{nd}_{i,t}, ec_{i,t} \geq 0,\ i \in \mathcal{I} \tag{4.17}$$

Unserved load in the household is denoted as ls_t. Home battery charge and discharge are denoted as bc_t and bd_t respectively. The energy level of the home battery is denoted as e_t. The net demand of the household from the grid is denoted as $nd_{i,t}$, and is differentiated by reliability class $i \in \mathcal{I}$. Note that the net demand can be negative, in which case the household is injecting excess rooftop solar supply back to the grid but receives no payment or benefit from this action. The non-negative part of the net demand is indicated by the variable $\widetilde{nd}_{i,t}$. This variable is useful for computing the value of variable $ec_{i,t}$ which represents the amount of energy credits left to be used by the household at the end of time stage t. Note that the notation, variables and constraints are similar to the ones used for the model that quantifies the load duration curve of each household type (section 3.3) and for the household subscription decision model (section 3.5).

The objective function (4.7) describes the goal of the household, which is to minimize its expected cost of interruption. Note that the bill of the household

is already accounted for when the household chooses its subscription from the service menu (see section 3.5). The focus, here, is rather on optimally managing the consumption patterns within the household, *given* a certain choice of contract. The parameter V_{cut} quantifies the discomfort encountered by consumers when a portion of their load is not served. Constraints (4.8) and (4.9) represent the battery discharge and charge constraints respectively, with BD_h and BC_h corresponding to the battery discharge and charge limits of household $h \in \mathcal{H}$ respectively. Constraint (4.10) corresponds to the energy limit constraint of the battery, with E_h the energy storage limit of household h. Constraint (4.11) represents the charging dynamics of the home energy battery, where e_{t-1} is a parameter that has been determined in the previous step of the rolling optimization. The charge and discharge efficiency of the battery are denoted as η_h^c and η_h^d for household h, respectively. Note that household batteries are assumed to be empty at the beginning of the day, i.e. $e_0 = 0$. Constraint (4.12) expresses the power balance constraint of the household. The parameter $DP_{t,h}$ gives the inflexible demand of household h in stage t, while PV_h corresponds to the rooftop solar capacity installed in the household. The parameter $PV_h \cdot \omega_t^H$ indicates the rooftop solar supply sampled during the rolling procedure given in Figure 4.2. Constraints (4.13) and (4.14) express the upper limit on net demand that a household is entitled to based on its chosen contract. The parameter ϕ_i^t indicates whether a certain reliability level i is being served at a given stage of a sample path or not. This parameter is output by the utility model (U_t) which is developed in section 4.2.1. Constraint (4.16) expresses the energy limit of option $i \in \mathcal{I}$. The parameter $\Theta_{h,i,j}$ in the right-hand side represents the subscription that the household chooses for each reliability option i and each duration j.

The solution of $(H_{h,t})$ yields a net demand decision for each reliability option i for the current period, $nd_{i,t}^{\star}$, which we denote as $ND_{h,i,t}$ for every household $h \in \mathcal{H}$. The parameter $ND_{i,t}$ which is used in Constraint (4.4) is then the sum of this net demand over all household types:

$$ND_{i,t} = \sum_{h \in \mathcal{H}} N_h \cdot ND_{h,i,t}, \tag{4.18}$$

where N_h is the number of households of type $h \in \mathcal{H}$ in the population. Note that the implicit assumption in Eq. (4.18) is that the realization of uncertainty at every household of the same type is identical. Note that the two household decision steps at each time period of the presented three-step performance evaluation framework (see Algorithm 1) use the same optimization program, but with different interruption patterns. The first step uses the interruption pattern of the previous time step, ϕ_i^{t-1}, while the second uses its updated version, ϕ_i^t.

4.2.3 A Dynamic Programming Algorithm for Solving the Household Model

The current chapter focuses on quantifying the performance of multilevel demand subscription and priority service after designing the corresponding service menus. Therefore, the datasets presented in section 3.6 are used as the basis of our analysis, along with the menus and subscription results of the previous chapter (see section 3.7). Two case studies are therefore examined: a case study with a temporal resolution of 4 hours and a case study with a temporal resolution of 15 minutes. The number of possible outcomes per stage considered for renewable production increases from 4 in the 4-hour resolution case study to 100 for the 15-minute resolution (see section 3.6). Therefore, dynamic programming is required in order to compute the solution of the rolling optimization program for the household in a reasonable amount of time. The present section describes a customized solution strategy for the household model $(H_{h,t})$. As a reminder, this model is represented as a multistage stochastic program where uncertainty is represented by a set of finite outcomes and thus forms a scenario tree [14]. The value function of the household model is denoted as $H_{h,t}(e_{t-1}, ec_{i,t-1}, \omega_t^H, \phi_i^t)$, while the expectation of the value functions is denoted as:

$$\mathcal{H}_{h,t+1}(e_t, ec_{i,t}, \omega_t^H, \phi_i^t) = \mathbb{E}\Big[H_{h,t+1}(e_t, ec_{i,t}, \omega_{t+1}^H, \phi_i^{t+1})\Big|\omega_t^H, \phi_i^t\Big]$$

Note that, as expressed in Eq. (4.7), the value function is then simply the current period cost plus the expectation of the value functions of the next stage. The dynamic programming algorithm approximates $\mathcal{H}_{h,t+1}$ by supporting hyperplanes around the set of states, which are given by $e_t, ec_{i,t}$. Once a collection of supporting hyperplanes has been found, the expectation of the value function can be approximated as follows:

$$\mathcal{H}_{h,t+1}(e_t, ec_{i,t}, \omega_t^H, \phi_i^t) = \max_{k=1,\dots,K}\Big\{A_k + B_k \cdot e_t + \sum_{i\in\mathcal{I}} C_{k,i} \cdot ec_{i,t}\Big\}$$

Here, A_k is the intercept and $B_k, C_{k,i}$ are the supporting hyperplane coefficients. This parametrization allows us to approximate $(H_{h,t})$ by replacing $\mathcal{H}_{h,t+1}(e_t, ec_{i,t}, \omega_t^H, \phi_i^t)$ with an auxiliary variable θ along with the following constraints:

$$\theta \geq A_k + B_k \cdot e_t + \sum_{i\in\mathcal{I}} C_{k,i} \cdot ec_{i,t} \quad \forall k = 1, \dots, K \tag{4.19}$$

It now remains to find the coefficients of the supporting hyperplanes. The procedure used in this work for deriving their values is described as follows. First, let Γ_t denote a discretization of the state space at stage t.

For $t = T, \cdots, 2$:

1. For $\widehat{e}_{t-1}, \widehat{ec}_{i,t-1} \in \Gamma_{t-1}$:
   (a) For all $\xi_t = (\omega_t^H, \phi_i^t)$ at stage t: Solve the linear problem associated to $H_{h,t}(\widehat{e}_{t-1}, \widehat{ec}_{i,t-1}, \omega_t^H, \phi_i^t)$ and store the dual multiplier $\pi_{\xi_t,t}$.
   (b) Use the dual multipliers $\{\pi_{\xi_t,t}\}_{\xi_t \in \Omega_t}$ to build a supporting hyperplane that approximates $\mathcal{H}_{h,t}(e_{t-1}, ec_{i,t-1}, \omega_{t-1}^H, \phi_i^{t-1})$ around the trial state $\widehat{e}_{t-1}$, $\widehat{ec}_{i,t-1}$, for all uncertainty realizations ω_{t-1}^H, ϕ_i^{t-1}. Further details on how to build a supporting hyperplane can be found in [14].
2. In problem $H_{h,t-1}(e_{t-2}, ec_{i,t-2}, \omega_{t-1}^H, \phi_i^{t-1})$, replace the expected value functions $\mathcal{H}_{h,t}(e_{t-1}, ec_{i,t-1}, \omega_{t-1}^H, \phi_i^{t-1})$ by an auxiliary variable θ and add the supporting hyperplanes as expressed by Eq. (4.19).

As the algorithm evolves backwards in the number of stages, supporting hyperplanes are built around states in the set Γ_t to approximate the value functions of the preceding stages. This approach is in the spirit of other common algorithms such as stochastic dual dynamic programming (SDDP) [144]. Nevertheless, as opposed to the sampling-based scheme of SDDP, the dynamic programming scheme proposed here uses a discretization of the state space in order to ensure that the performance evaluation described in section 4.2 can characterize the optimal policy of the household at non-optimal parts of the state space, which may occur in the simulation.

4.3 Real-Time Pricing

Our focus in this section is in describing a model that represents the behaviour of the system under real-time pricing. We model real-time pricing by assuming perfect coordination between households and producers. The coordination assumption is equivalent to real-time pricing as established in [68, 146] for the case of multi-stage uncertainty.

Similarly to our proposed framework for modeling multilevel demand subscription, the model proposed in this section accounts for the realization of uncertainty at the household and the utility-scale level, represented by $\omega^H \in \Omega^H$ and $\omega^U \in \Omega^U$. We denote by $\omega_{[t]} = (\omega_{[t]}^H, \omega_{[t]}^U) \in \Omega_{[t]}^H \times \Omega_{[t]}^U = \Omega_{[t]}$ a realization of the stochastic process of household renewable production up to time stage t. The real-time pricing model is therefore described as follows:

$$(RTP): \min_{\substack{\mathbf{ls},\mathbf{nd},\mathbf{bd},\mathbf{bc},\\ \mathbf{e},\mathbf{ec},\mathbf{p},\mathbf{d},\\ \mathbf{e}^{PHS},\mathbf{p}^{pump},\\ \mathbf{p}^{prod}}} \sum_{t\in\mathcal{T}} \sum_{\omega_{[t]}\in\Omega_{[t]}} P_{t,\omega_{[t]}} \cdot \Big[\sum_{g\in\mathcal{G}} h_g(p_{g,t,\omega_{[t]}}) + \sum_{h\in\mathcal{H}} V_{cut} \cdot ls_{h,t,\omega_{[t]}} \Big] \tag{4.20}$$

$$\text{s.t. } 0 \leq bd_{h,t,\omega_{[t]}} \leq BD_h, \quad h \in \mathcal{H}, t \in \mathcal{T}, \omega_{[t]} \in \Omega_{[t]} \tag{4.21}$$

$$0 \leq bc_{h,t,\omega_{[t]}} \leq BC_h, \quad h \in \mathcal{H}, t \in \mathcal{T}, \omega_{[t]} \in \Omega_{[t]} \tag{4.22}$$

$$0 \leq e_{h,t,\omega_{[t]}} \leq E_h, \quad h \in \mathcal{H}, t \in \mathcal{T}, \omega_{[t]} \in \Omega_{[t]} \tag{4.23}$$

$$e_{h,t,\omega_{[t]}} = e_{h,t-1,\omega_{[t]}} - \frac{bd_{h,t,\omega_{[t]}} \cdot \Delta t}{\eta_h^d} + bc_{h,t,\omega_{[t]}} \cdot \eta_h^c \cdot \Delta t, \quad h \in \mathcal{H}, t \in \mathcal{T}, \omega_{[t]} \in \Omega_{[t]} \tag{4.24}$$

$$DP_{h,t} - ls_{h,t,\omega_{[t]}} + bc_{h,t,\omega_{[t]}} - PV_h \cdot \omega_t^H - bd_{h,t,\omega_{[t]}} = nd_{h,t,\omega_{[t]}}, \quad h \in \mathcal{H}, t \in \mathcal{T}, (\omega_{[t]}^H, \omega_{[t]}^U) \in \Omega_{[t]} \tag{4.25}$$

$$f_g(p_{g,t,\omega_{[t]}}) \leq 0, \quad g \in \mathcal{G}, t \in \mathcal{T}, \omega_{[t]} \in \Omega_{[t]} \tag{4.26}$$

$$d_{t,\omega_{[t]}} = \sum_{g \in \mathcal{G}} p_{g,t,\omega_{[t]}} + \omega_t^U - p_{t,\omega_{[t]}}^{pump} + p_{t,\omega_{[t]}}^{prod}, \quad t \in \mathcal{T}, (\omega_{[t]}^H, \omega_{[t]}^U) \in \Omega_{[t]} \tag{4.27}$$

$$0 \leq e_{t,\omega_{[t]}}^{PHS} \leq E^{PHS}, \quad t \in \mathcal{T}, \omega_{[t]} \in \Omega_{[t]}, \tag{4.28}$$

$$0 \leq p_{t,\omega_{[t]}}^{pump} \leq P^{pump}, \quad t \in \mathcal{T}, \omega_{[t]} \in \Omega_{[t]}, \tag{4.29}$$

$$0 \leq p_{t,\omega_{[t]}}^{prod} \leq P^{prod}, \quad t \in \mathcal{T}, \omega_{[t]} \in \Omega_{[t]}, \tag{4.30}$$

$$e_{t,\omega_{[t]}}^{PHS} = e_{t-1,\omega_{[t]}}^{PHS} + (p_{t,\omega_{[t]}}^{pump} \cdot \eta^{PHS} - p_{t,\omega_{[t]}}^{prod}) \cdot \Delta t, \quad t \in \mathcal{T}, \omega_{[t]} \in \Omega_{[t]}, \tag{4.31}$$

$$d_{t,\omega_{[t]}} = \sum_{h \in \mathcal{H}} N_h \cdot nd_{h,t,\omega_{[t]}}, \quad t \in \mathcal{T}, \omega_{[t]} \in \Omega_{[t]} \tag{4.32}$$

$$p_{g,t,\omega_{[t]}}, d_{t,\omega_{[t]}}, ls_{h,t,\omega_{[t]}} \geq 0, \quad g \in \mathcal{G}, t \in \mathcal{T}, \omega_{[t]} \in \Omega_{[t]} \tag{4.33}$$

The consumption of households is directly coordinated with the production of the system in this model. Thus, the objective is to minimize the expected total cost encountered by the system. This cost is given by the production cost of generators and the shortage costs of households. Here, $P_{t,\omega[t]}$ represents the probability of sample path $\omega_{[t]}$ occurring at time period t. Constraints (4.21) to (4.24) represent the dynamics of household batteries. The power balance constraint at the level of the household is given by Eq. (4.25). The generator restrictions in terms of production and their technical limitations are represented in Constraint (4.26). Constraint (4.27) represents the power balance constraint at the level of the system. Pump hydro system constraints are expressed by Eqs. (4.28) to (4.31) wit η^{PHS} being the efficiency of the pump hydro storage system. Variables $e_{t,\omega_{[t]}}^{PHS}$, $p_{t,\omega_{[t]}}^{pump}$ and $p_{t,\omega_{[t]}}^{prod}$ represent, respectively, the energy stored, the power pumped and the power produced by the pump hydro storage system at a certain time period t for a certain uncertainty path $\omega_{[t]}$.

Constraint (4.32) represents the link between the system and the households. The residential total demand is denoted by the variable $d_{t,\omega_{[t]}}$. This variable is computed as the sum of the demand from each household type mul-

tiplied by the number of households of that type present in the system. Note that we restrict this total demand variable to be non-negative. This implies that households can inject power back to the grid, but only for the purpose of serving other household loads, and not for enabling the system to also serve industrial load (which is represented as inelastic demand in our model).

To summarize, Constraints (4.21) to (4.25) characterize the behaviour of the households (similar to section 4.2.2), while Constraints (4.26) to (4.31) characterize the operation of the system (similar to section 4.2.1). Constraint (4.32) is then used to coordinate the action of both parts of the system.

In order to account for pump hydro storage in the utility model of the performance evaluation framework (see section 4.2.1) while isolating the effect of consumer-side inter-temporal flexibility in our analysis, pumped hydro resources are assumed to follow a fixed profile in the rolling utility model of section 4.2.1. This pump hydro storage profile is fixed using the solution of the real-time pricing model presented in this section. The same profile is used for priority service and multilevel demand subscription. Our goal in fixing the schedule of pumped hydro exogenously is to isolate the effect of residential storage on system operations, as opposed to obscuring this effect by other sources of flexibility (e.g. utility-scale storage). Another reason for fixing the pumped-hydro storage profile is to be able to decouple the utility problem from the household model. Indeed, it would have been computationally challenging to solve the utility program and the household program at once, while simultaneously accounting for future realizations of both pumped-hydro storage and household batteries.

4.4 Results

Using the simulation framework that is described in section 4.2, the data presented in section 3.6 and the menu design and menu subscription results that are derived in section 3.7 of the previous chapter, we are able to compare the performance of priority service (PSP), multilevel demand subscription (MDSP) and real-time pricing (RTP). The performance evaluation framework of section 4.2 along with the real-time pricing model of section 4.3 is solved for every day type, i.e. for weekends/weekdays of every season of the year (see the explanation of the long-term scenarios in section 3.6). Numerical experiments are performed using the **JuMP** package [36] in the **Julia** programming language [12]. The mathematical programs are solved using the **Gurobi** optimization solver [81] and run on the high performance computing Lemaitre3 cluster hosted at UCLouvain as part of the CECI facility. Concerning multilevel demand subscription and priority service, the simulation results are obtained using 1000 sample paths for each day type and each resolution. On the other hand, the real-time pricing model is solved using the stochastic dual dynamic

programming algorithm applied to the solar and wind uncertainty lattices directly.

A number of conclusions can be drawn from the simulations. This set of observations is covered in the present section. We divide the presentation into implications for the system in section 4.4.1 and observations related to households in section 4.4.2.

4.4.1 System-Wide Results

Table 4.1 presents key economic indicators for the case study with 4-hour resolution as they relate to system-level performance. The corresponding results for the case study with 15-minute resolution are presented in Table 4.2. The column 'RTP-NHS' corresponds to the results obtained using the real-time pricing model while considering that household local storage (batteries) are not used in a coordinated fashion by the system operator. This form of real-time pricing seems more realistic in terms of coordination assumptions than a perfect real-time pricing model, since the perfect coordination of storage assets in real time implicitly assumes a perfect ability of a massive number of households to anticipate real-time prices over the day. The residential shortage cost is calculated using the household rolling horizon model in the performance evaluation process that is described in section 4.2.2. The supplied energy and the production cost are computed using the producer model that is described in section 4.2.1. The total system cost is then given as the sum of residential shortage and production cost.

Table 4.1: Comparison of system-level performance for the case study with 4-hour resolution. Values are in [M€/month].

	RTP	RTP-NHS	PSP	MDSP
Total Production Cost [M€]	244.36	242.29	237.16	237.42
Estimated Industrial/Commercial Cost [M€]	157.78	157.78	157.78	157.78
Estimated Residential Cost [M€]	86.58	84.51	79.38	79.64
Shortage Cost Industrial Load [M€]	0	0	0	0
Total Residential Supply [TWh]	1.64	1.59	1.54	1.54
Total Residential Load Shortage Cost [M€]	123.34	139.72	166.55	165.27
Total Residential Payment [M€]	NA	NA	292.03	283.96
Total System Cost [M€]	367.7	382.01	403.7	402.69

Our first observation from the two previous tables is that multilevel demand subscription is able to supply slightly more energy to households, and thus reduces load shortage cost compared to priority service. Indeed, since multilevel demand subscription better discriminates consumers by means of the load duration curve, this paradigm is able to better infer the supply needed at certain time periods within the day. Consumers subscribe to less energy while adapting

Table 4.2: Comparison of system-level performance for the case study with 15-minute resolution. Values are in [M€/month].

	RTP	RTP-NHS	PSP	MDSP
Total Production Cost [M€]	243.67	240.34	237.44	239.01
Estimated Industrial/Commercial Cost [M€]	156.87	156.87	156.87	156.87
Estimated Residential Cost [M€]	86.8	83.47	80.57	82.14
Shortage Cost Industrial Load [M€]	0	0	0.7823	0.7823
Total Residential Supply [TWh]	1.6	1.55	1.48	1.51
Total Residential Shortage Cost [M€]	156.87	173.53	209.43	199.91
Total Residential Payment [M€]	NA	NA	285.36	272.53
Total System Cost [M€]	400.54	413.87	447.65	438.8

the timing of their consumption in order to better match the inflexible portion of their consumption profile with the availability of resources in the system.

We observe a reduction of 0.25% of the system cost compared to priority service. This amounts to about 1M€/month for the case study with 4-hour resolution. This value increases to 1.98% (i.e. about 10M€/month) when the resolution of the model is 15 minutes. Note that this gain underscores the importance of a more detailed model (finer resolution with a more detailed scenario tree) in accurately quantifying the efficiency of multilevel demand subscription.

Finally, we can observe that, although multilevel demand subscription shows improved performance compared to priority service in terms of overall system operational efficiency, both schemes are notably worse in terms of residential load shortage cost when compared to real-time pricing. Indeed, both schemes result in an increase of more than 9% of total system cost. This gaps reduces to approximately 5% if we consider real-time pricing without household storage (since perfect coordination of residential storage through real-time electricity markets is arguably a highly optimistic assumption in the first place). These results underscore the potential of real-time pricing as the golden standard of coordination for integrating residential demand response in power system operations.

4.4.2 Households

Insofar as households are concerned, we arrive to a number of conclusions from our simulations. These observations are performed across different household types and different demand response service offerings policies. These observations are highlighted and explained in the present section.

Household Cost Reduction

Figure 4.3 compares the total cost (subscription and interruption cost) between multilevel demand subscription and priority service for the case study with 4-hour resolution. The figure also details the portion of the cost that can be attributed to subscription costs. Figure 4.4 presents the same indicators for the case study with 15-minute resolution. Note that the household shortage cost of the present chapter is computed differently from the one given in Chapter 3. Indeed, the shortage cost of Chapter 3 is estimated by the household while subscribing to the demand response menu (see section 3.5). In the present chapter, it is now computed using the household model of the performance evaluation framework (see section 4.2.2) and therefore represents the shortage cost incurred by households during real-time operations of the system.

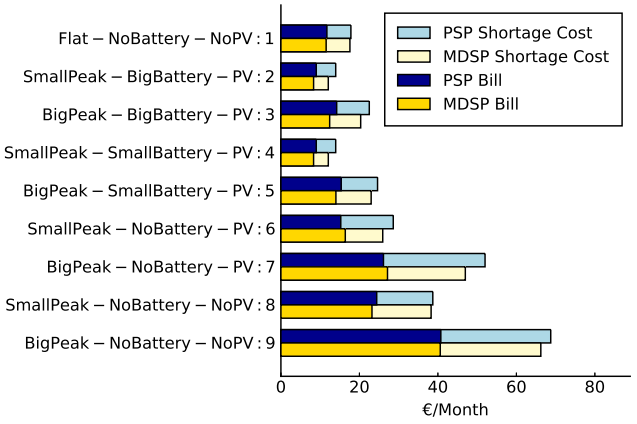

Figure 4.3: Comparison of the total cost and the subscription cost for different types of households under priority service and multilevel demand subscription (4-hour resolution).

We can observe from the case study with 15-minute resolution that all homes with multilevel demand subscription tend to face a lower total cost, a lower shortage cost and a lower subscription cost. However, this improvement is reduced with the introduction of batteries. This is due to the fact that batteries contribute to reducing the peak net demand of households, which implies that the benefits brought about by the options with shorter duration in multilevel demand subscription decrease for households with large consumption. Multilevel demand subscription is especially beneficial compared to priority service when a household owns rooftop solar panels but no battery. Indeed, options with shorter duration are especially helpful in this context because they enable households to use these options when rooftop solar panels are not producing. For these households, multilevel demand subscription reduces total cost by more than 20%, whereas this total cost reduction amounts to 10% when

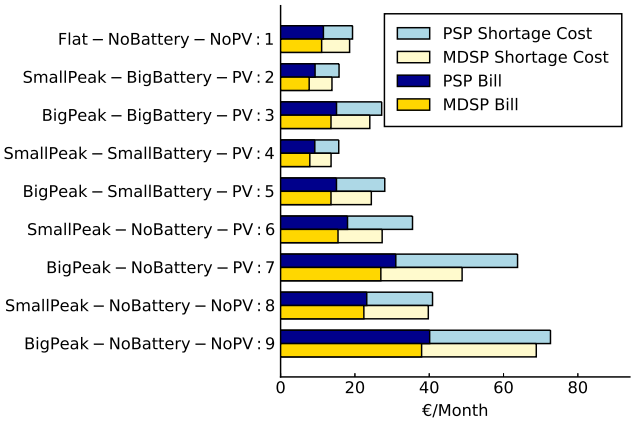

Figure 4.4: Comparison of the total cost and the subscription cost for different types of households under priority service and multilevel demand subscription (15-minute resolution).

a battery is added.

Instead, the total costs of households are very close under priority service and multilevel demand subscription for the case study with 4-hour resolution. The maximum reduction that is achieved by multilevel demand subscription in this case study is limited to 6.5%. These observations are consistent with the observations of section 3.7.3 in the sense that the total cost of households is reduced when faced with multilevel demand subscription. Moreover, we will not discussed the differences in electricity bill between the two schemes in this section since it is already detailed in the results of the previous chapter.

Finally, as we already observe in the discussion of the system-wide results of the previous section, the additional detail of the higher-resolution 15-minute model is justified. This is due to the fact that the higher temporal resolution allows for a more precise assessment of the impact of the two contracts on individual types of households since lower temporal resolution underestimates the economic benefit of subscribing to shorter duration options under multilevel demand subscription in terms of household cost reduction.

Service Comparison under Different Policies

As we observe in section 3.7.3, households tend to subscribe to a higher capacity under multilevel subscription than under priority service. On the other hand, the subscribed energy is less. This observation is driven by the offer of options with shorter duration in multilevel demand subscription. We are further interested in understanding the amount of procured energy that is actually used across different household types. For this purpose, we define a new metric

called the utilization rate computed as follows:

$$UR_h = \frac{\sum_{i \in \mathcal{I}} \sum_{t \in \mathcal{T}} \widetilde{nd}_{h,i,t} - e^h_{|\mathcal{T}|}}{\sum_{i \in \mathcal{I}} \sum_{j \in \mathcal{J}} \Theta_{h,i,j} \cdot T_j} \tag{4.34}$$

Here, $e^h_{|\mathcal{T}|}$ records the energy left in the battery at the end of the horizon during simulations. The utilization rate observed for priority service and multilevel demand subscription for the case study with 4-hour resolution is represented in Figure 4.5. For the case study with 15-minute resolution, the same quantity can be found in Figure 4.6.

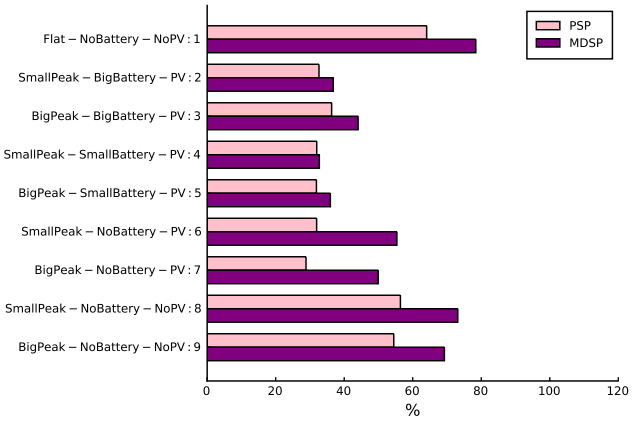

Figure 4.5: Service utilization percentage under priority service pricing and multilevel demand subscription for the case study with 4-hour resolution (left).

From these two figures, we can observe that multilevel demand subscription always exhibits a better utilization rate compared to priority service. Indeed, in the 4-hour test case, the lowest utilization ratio under multilevel demand subscription is given by 32.74%, while it amounts to 28.85% for priority service. This result is driven by the fact that households can choose options of shorter durations under multilevel demand subscription. Instead, in priority service, the capacity strip is procured for the entire horizon. Multilevel demand subscription therefore allows households to better exploit the subscribed energy. Consequently, multilevel demand subscription is not only advantageous to households by allowing higher peak capacity when needed, but also by more efficiently using their procured energy.

Note that households which own a battery tend to achieve a greater utilization of their purchased power, and are thus able to improve their utilization ratio for the 15-minute case study. However, this observation is not valid in

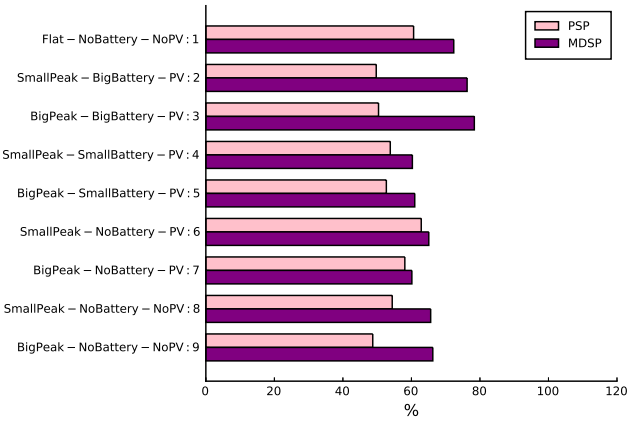

Figure 4.6: Service utilization percentage under priority service pricing and multilevel demand subscription for the case study with 15-minute resolution.

the 4-hour case study. This phenomenon can be explained by the short amount of time periods (only 6) present in the 4-hour case study. This rougher time resolution may prevent the local storage from fully exhibiting its full potential compared to the 96 time periods available in the 15-minute case study. Once again, we can find evidence of the value of a model with finer resolution for precisely identifying the effect of these two demand response schemes.

Cost-Benefit Analysis of Local Storage

Figures 4.3 and 4.4 indicate that local storage plays an important role in reducing the total cost faced by households under both priority service and multilevel demand subscription. Nevertheless, this reduction is less accentuated for the second scheme. This is due to the fact that multilevel demand subscription contains implicitly an energy cost in addition to the capacity cost, while the battery is mainly beneficial in terms of reducing capacity cost. Furthermore, the impact of storage on the utilization ratio of procured energy has already been commented above. Our analysis indicates that batteries improve the service utilization rate of households that own storage. Finally, Figures 4.7 and 4.8 describe the capacity subscription of each household type for each priority class for the case studies with 4-hour and 15-minute resolution under both demand response schemes. From these graphs we can observe that, as the size of the battery decreases, a household tends to subscribe to a larger total capacity, as well as a higher quantity under the "Red" option. Therefore, we can conclude that a battery is also beneficial for a household because it allows the household to reduce its electricity bill by shortening the needed total capacity subscription of that particular household while also allowing it to rely more on

less reliable options.

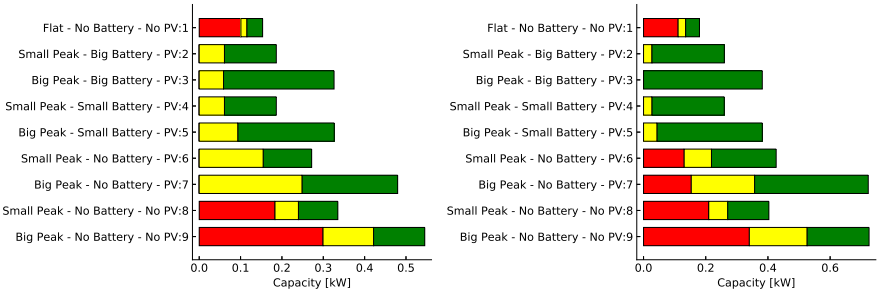

Figure 4.7: Capacity subscriptions of each household type to each option under priority service (left) and multilevel demand subscription (right) for the case study with 4-hour resolution.

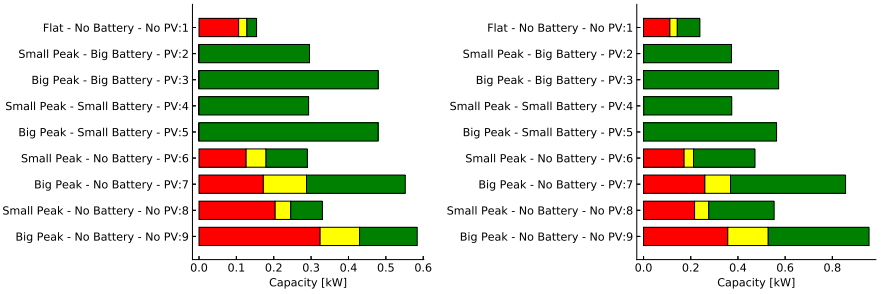

Figure 4.8: Capacity subscriptions of each household for each option under priority service (left) and multilevel demand subscription (right) for the case study with 15-minute resolution.

Having outlined the benefits of local storage, we are now interested in assessing whether the investment cost of a battery outweighs the benefits that we have quantified through our analysis. Table 4.3 presents the reduction in total cost for different household profiles when a small or large battery is added to the household for both simulation resolutions. Based on the assumption suggested by [117], the monthly cost of the large battery is estimated to be between 6.22 €/month and 36.48 €/month, while that of the small battery ranges from 2.86 €/month to 16.83 €/month. Therefore, by comparing the gains presented in Table 4.3 with the aforementioned investment costs, the investment cost of the large battery cannot be justified under either scheme for households with a small peak profile. Moreover, we observe that the benefits obtained with a small battery are almost equal to the ones achieved with a large battery for the household with a small peak profile. Therefore, it seems that the small battery is sufficient for this particular household type. However,

we note that the investment cost in a small battery for this profile is justifiable only in optimistic scenarios for multilevel demand subscription but seems worthwhile under priority service. Concerning households with a large peak, the small battery appears to always be a worthwhile investment, whereas the large battery is justified in optimistic scenarios, and only under priority service.

Table 4.3: Household total cost reduction in [€/month] for adding a small or a large battery for different household consumption profiles under both resolutions. The numbers reported in bold are cases for which the cost gains are superior to the respective battery investment cost.

Profiles	Battery Types	PSP		MDSP	
		4-hour	15-min	4-hour	15-min
Small Peak	Small	14.66	**19.85**	13.87	13.75
	Big	14.66	19.77	13.87	13.51
Big Peak	Small	**27.39**	**35.74**	**23.99**	**24.44**
	Big	29.5	**36.58**	26.66	24.84

Cost-Benefit Analysis of Local Rooftop Solar Panels

Figures 4.3 and 4.4 demonstrate that households with rooftop solar panels and without a battery experience the same level of shortage cost under priority service. Instead, multilevel demand subscription appears to be more valuable for households that only own rooftop solar panels. This phenomenon is already highlighted in an aforementioned discussion in the first paragraph of section 4.4.2. Therefore, investing in a battery when already owning rooftop solar panels may be favorable for certain household types, as we have discussed previously.

In order to verify that rooftop solar panels alone are not a viable investment for households, we compute the monthly investment cost of such an investment based on the assumptions of [117]. This cost is estimated by the following expression:

$$MC_{PV} = \frac{OC \cdot \frac{r}{12}}{1 - \frac{1}{(1+r)^T}}$$

Here, OC, r and T denote respectively the overnight investment cost, the annual discount rate and the lifespan of the PV installation. The Belgium mean PV installation cost amounts to 1.4€/W VAT excluded [103]. Based on estimates of BloombergNEF, a 34% reduction in PV installation cost by 2030 may be achievable [71]. Since we consider a forward-looking scenario towards 2050, we employ a total overnight cost of 2236.1€ and of 3577.7€ for the small peak and large peak households respectively. A lifetime of 25 to 30 years is assumed [10]. The annual discount rate is assumed to be the same as for the

battery (3 to 10%). Therefore, for households with a small peak, the monthly investment cost is estimated to amount between 9.51 and 20.53€/month, while it remains between 15.21 and 32.84€/month for households with large peaks. Table 4.4 presents the gain that is estimated for the two household profiles for both simulation resolutions under both demand response schemes. From the results depicted in this table, we can conclude that installing only rooftop solar panels is not worthwhile for any of the household types and under any of the demand response contracts. This conclusion can be affected by our decision not to pay consumers for exporting solar power to the grid. However, if it is decided to include a reward to consumers for providing electricity to the grid, one must handle the interplay that this decision has on the design of both priority service and multilevel demand subscription menus with care.

Table 4.4: Household total cost reduction in [€/month] when installing rooftop solar panels for different household consumption profiles under both resolutions.

Profiles	PSP		MDSP	
	4-hour	15-min	4-hour	15-min
Small Peak	10.08	5.39	12.33	12.42
Big Peak	16.74	8.86	19.24	19.96

Household Shortage Cost in Real-Time Operations

The analysis presented in the present chapter goes one step beyond the results of Chapter 3 by observing the impact of priority service and multilevel demand subscription on the system and different household types. Figure 4.9 compares the expected shortage cost experienced by households during the subscription phase to the shortage cost experienced according as we quantify it during real-time operation using the model of section 4.2.2. This can be interpreted as the difference between what shortage cost households *expect* to experience, versus the shortage cost that they *actually* experience. From this figure, we can observe that households actually face a larger shortage in real-time operations than what is expected in their subscription model. This is corroborated by the observed reliability of priority class in real-time conditions which is generally lower than the one predicted by the proposed menu. This phenomenon may be explained by the violation of the synchronization assumption in the original theory of priority service and multilevel demand subscription. Indeed, the synchronization between the consumption of households is not met in practice, whereas it is assumed in the original theory. Moreover, inter-temporal linking is also absent from [26]. This does not reflect the reality encountered by households and the utility.

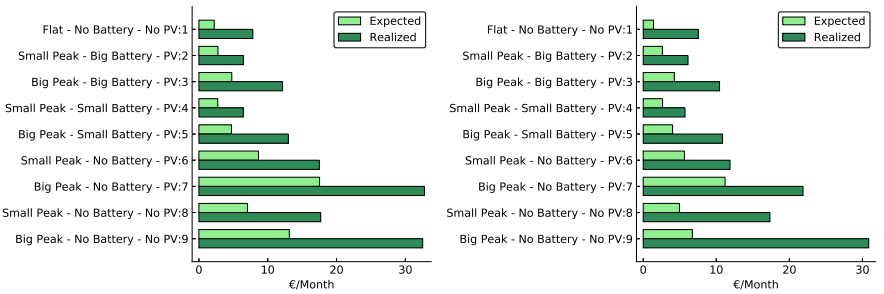

Figure 4.9: Comparison of the expected shortage cost from subscription with the realized shortage cost for different types of households under priority service (PSP) and multilevel demand subscription (MDSP).

Comparison with Real-Time Pricing

Real-time pricing has also been modeled in our analysis, alongside multilevel demand subscription and priority service, as already mentioned in section 4.3. Figure 4.10 presents the shortage cost experienced by each household type under every paradigm for both resolutions. Figure 4.11 compares the energy withdrawn from the grid by the household under real-time pricing, and compares it to the expected energy subscription of each household type.

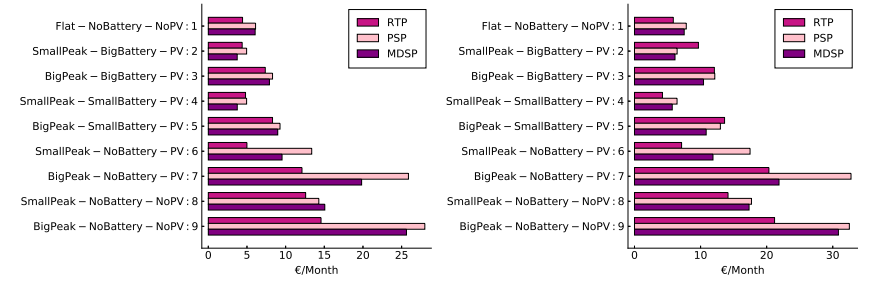

Figure 4.10: Comparison of the shortage cost for different types of households under priority service, multilevel demand subscription and real-time pricing for the 4-hour (left) and the 15-minute (right) resolution case studies.

In general, we observe that households incur greater shortage costs under priority service than under multilevel demand subscription. Moreover, real-time pricing is largely more beneficial for households than the two other schemes. A small exception to this rule can be detected for households with large batteries, for which multilevel demand subscription and sometimes even priority service may be more beneficial. This phenomenon can be explained by the information in Figure 4.11. Indeed, household types with large batteries withdraw more energy from the grid under real-time pricing than the amount

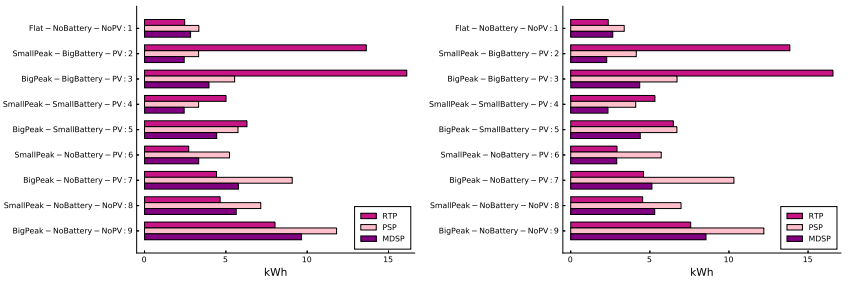

Figure 4.11: Comparison of the energy withdrawn from the grid under real-time pricing with the subscribed energy under priority service and multilevel demand subscription for the 4-hour (left) and the 15-minute (right) resolution case studies.

of energy that they subscribe to under priority service or multilevel demand subscription. This excess amount of energy is stored in the large battery under real-time pricing, in order to be used afterwards by the system for supplying other household types for time periods when less supply is available from the utility[2]. For other household types, we can observe that the energy withdrawn from the grid under real-time pricing is lower than the subscribed energy under priority service and multilevel demand subscription. Indeed, real-time pricing allows the user to access the exact amount of power it needs at a certain time period. Instead, the two other service contracts lead to power being bought but not used due to the duration of those options.

Finally, we can conduct a cost-benefit analysis for household batteries and solar panels under real-time pricing. In that case, the shortage cost gain is always smaller than 8€/month. Therefore, neither batteries or rooftop solar panels are worthy investments. Note that this conclusion may change if a service payment is considered in addition to the experienced household shortage cost.

4.5 Conclusion

In this chapter, we compare priority service and multilevel demand subscription as two alternative means of mobilizing demand response in the residential sector against the economic golden standard of real-time pricing. This analysis is motivated by our desire to investigate aggregator business models that achieve simplicity, privacy and control for residential consumers.

[2]Note however the difference in treatment between households under multilevel demand subscription or priority service who are not payed to provide electricity to the grid while it is the case under real-time pricing.

We first develop a framework for modeling the system-wide effects of residential flexibility under both schemes. Multilevel demand subscription is a generalized form of priority service. As such, it increases implementation complexity from the side of both the utility as well as the residential consumer. On the upside, it improves operational efficiency by allowing the utility to better discriminate flexible consumers. A model is also implemented for investigating the effect of real-time pricing under the same setting.

We examine this trade-off between simplicity and operational efficiency in a case study of the Belgian market. Many observations are highlighted from these experiments. First of all, the ability of multilevel demand subscription to better discriminate consumers results in a total cost reduction of about 2% relative to priority service, which represents about 10 M€/month for the experiment with 15-minute resolution. However, multilevel demand subscription and priority service appear to be significantly more costly for the system than real-time pricing. The consistency of these results is also observed in an experiment with a lower resolution, even though the improvement is smaller. Indeed, the lower resolution of the 4-hour model underestimates the system cost benefits of multilevel demand subscription along with household subscriptions to options with shorter durations. This underscores the value of an accurate model with finer time resolution at the level of 15 minutes for arriving at more reliable conclusions regarding the interplay of demand response and system operations.

Multilevel demand subscription is found to allow household to reduce their costs compared to priority service because capacity strips that are procured under priority service remain idle for a significant portion of the service horizon. This reduction amounts to 20% for households that only own solar panels and is limited to 10% when households also own a battery. Multilevel demand subscription also allows consumers to employ their subscribed energy more efficiently since households always exhibit an improved utilization rate than under priority service.

The benefits of solar panels and batteries in household is also quantified. Even though a battery allows households to reduce their total subscription and inconvenience cost, the investment cost of a battery may prohibit its acquisition, especially under multilevel demand subscription. Indeed, the benefit of batteries is reduced in this case because of the energy component already present in the multilevel demand subscription scheme with short duration. On the other hand, owing only solar panels without a battery seems to be unjustifiable in terms of household gains compared to investment cost.

Finally, the impact of real-time pricing is also analyzed for different household types. Real-time pricing always enables households to reduce their shortage cost compared to the two other schemes, except for households with large batteries that serve as a system reservoir for supporting other households dur-

ing periods of low renewable production.

On the basis of these observations, we conclude that it may become challenging to engage flexible households with installed renewable supply and storage using pure capacity tariffs. In future markets with distributed flexibility and storage, a mix of energy and capacity charges are likely to be necessary in order to improve the efficiency of operations and keep electricity service charges of households at acceptable levels.

4.A Notations

Notations used throughout this chapter are summarized in this section.

Sets

$\mathcal{G}, \lvert\mathcal{G}\rvert$	Set of generators and its cardinality
$\mathcal{L}, \lvert\mathcal{L}\rvert$	Set of consumer types and its cardinality
$\mathcal{H}, \lvert\mathcal{H}\rvert$	Set of households and its cardinality
$\mathcal{T}, \lvert\mathcal{T}\rvert$	Set of time periods and its cardinality
$\mathcal{I}, \lvert\mathcal{I}\rvert$	Set of reliability options and its cardinality
$\mathcal{J}, \lvert\mathcal{J}\rvert$	Set of duration options and its cardinality
Ω^U	Set of sample paths of renewable supply from utility-scale resources
Ω^H	Set of sample paths of renewable supply from rooftop solar resources

Parameters

n_{simu}	Number of simulations of the performance evaluation algorithm
ϕ_i^t	Indicator ranging from 0 to 1 included representing the interruption pattern of option i faced at time period t
$\bar{V}_i$	Estimate of average valuation that the utility assigns to priority class i based on how households decide to subscribe to the multilevel demand subscription service (or priority service)
$ND_{i,t}$	Residential aggregated net demand for priority class i at time stage t [MW]
$\sigma^*_{l,i,j}$	Optimal subscription quantity of consumer l under option (i,j) [MW]
$\Theta_{h,i,j}$	Optimal subscription quantity of household type h to option (i,j) [kW]
T_j	Duration of option j
$N_{j,t}$	Binary parameters that determines whether a certain duration option j is being served in time period t of actual operations or not
$V_l(T_j)$	Valuation of consumer type l when the duration is T_j [€/MWh]
D_l	Demand of consumer type l [MW]
V_{cut}	Penalty parameter if a shortage occurs for households, assumed to be 500 €/kWh
BD_h	Battery charge capacity in household of type h [kW]
BC_h	Battery discharge capacity in household pf type h [kW]

E_h Battery energy capacity in household of type h [kWh]

η_h^d Battery discharge efficiency for household type h

η_h^c Battery charge efficiency in household h

$DP_{h,t}$ Load (Demand Profile) of household h at stage t in scenario s [kW]

PV_h Solar panel capacity installed at household type h [kW]

Δt Number of time periods in an hour (e.g. 4 for the 4-hour case study and 0.25 for the 15-minute analysis)

N_h Number of households of type h

$P_{t,\omega_{[t]}}$ Probability of occurrence of uncertainty sequence $\omega_{[t]}$ up to stage t of the set of sample paths available

E^{PHS} Maximum energy that can be stored in the pump hydro storage system [MWh]

P^{pump} Maximum power that can be pumped by the pump hydro storage [MW]

P^{prod} Maximum power that can be produced by the pump hydro storage [MW]

η^{PHS} Efficiency of the pump hydro storage system [%]

OC Overnight investment cost [€]

r Annual discount rate [%]

T Installation lifetime [years]

MC_{PV} Monthly investment cost for rooftop solar panels [€/month]

UR_h Service utilization ratio for household type h [%]

$\overline{UR}_h$ Improved service utilization ratio for household type h [%]

$\bar{r}_i$ Realized reliability of priority class i under real-time system operating conditions [%]

Variables

e_t^h, e_t Energy stored in the battery at time period t for household type h [kWh]

$ec_{i,t}^h$, $ec_{i,t}$ Amount of energy left to consume for household type h at time period t based on its contract subscription for priority class i

$p_{g,t}$ Production of generator g at hour t [MW]

$d_{i,t}$ Supply to priority class i at hour t [MW]

$d_{t,\omega_{[t]}}$ Total supply at time stage t for the uncertainty sequence $\omega_{[t]}$ up to stage t [MW]

ls_t Load shedding at stage t [kW]

bd_t Discharge power of the battery at stage t [kW]

bc_t Charge power of the battery at stage t [kW]

$nd_{i,t}$ Net demand from the grid at stage t for priority class i [kW]

$\widetilde{nd}_{i,t}$ Positive version of variable $nd_{i,t}$ for priority class i [kW]

θ Auxiliary variable used for the approximation of the household rolling optimization program

$p_{t,\omega_{[t]}}^{pump}$ Power pumped by the pump hydro storage at time stage t for the uncertainty sequence $\omega_{[t]}^s$ up to stage t [MW]

$p^{prod}_{t,\omega_{[t]}}$ Power produced by the pump hydro storage at time stage t for the uncertainty sequence $\omega_{[t]}$ up to stage t [MW]

$e^{PHS}_{t,\omega_{[t]}}$ Energy stored in the pump hydro storage system at time stage t for the uncertainty sequence $\omega_{[t]}$ [MWh]

Functions

U^t_{cost} Utility cost encountered at time period t

H^t_{cost} Cost face by the total amount of households at time period t

h_g Cost function of generator g, including production costs

f_g Constraints of unit commitment problems, including production limits

$\mathbb{E}$ Expectancy operator

5 Hierarchical Coordination of Medium and Low Voltage Distribution Grids in the Presence of Demand Response

5.1 Introduction

The analysis presented in the previous chapters of this dissertation provide insights regarding the impact of priority service, and its generalization, on the system but also on the costs incurred by households. However, with the increased penetration of distribution-scale generation such as rooftop solar panels in households, but also flexible devices such as electric vehicles and heat pumps, demand response is bound to grow in use. The goal for power systems will be to manage to mobilize an increasing number of flexible resources from the residential and commercial sector so as to support power system operations such as real-time balancing and associated ancillary services. The present chapter therefore dives into the broad question of the efficient integration of demand response in electricity market operations by conducting a preliminary analysis of the topic. A hierarchical coordination of the different parts of the power system is already proposed in [112, 137], and is used as the underlying framework in this chapter. This hierarchical approach allows us to link several layers of power system operations by means of residual supply or demand functions that internalize the physics behind the corresponding layer. Since Papavasiliou *et al.* [137] focus on the coordination of European countries, while Mezghani [112] concentrates on the coordination of high-voltage and medium-voltage networks, we limit our focus on the coordination of medium-voltage with low-voltage transmission networks, i.e. distribution networks which typically connect the targeted residential flexible resources to the grid. Thus, the present chapter develops a methodology for aggregators who are responsible for groups of households to aggregate residential sector flexibility through priority service, while accounting for distribution network physics. The goal is to make this service available to system operators, while respecting the constraints of the electricity network. This hierarchical coordination, coupled with the demand response framework analyzed in this thesis, aims at enabling distributed resources of

distribution networks to be efficiently accounted for through residual demand functions in power system operations, while preventing the scale of power system operation decision models to grow in an intractable way. Even though we employ a hierarchical scheme in order to coordinate different portions of the electricity grid, there exist other coordination schemes, as highlighted for example in [82].

In the present chapter, low-voltage networks are accounted for using different models for representing distribution network physics. Typically, single-phase approximations are used for representing power flow constraints in power systems. However, these approximations rely on the assumption that power systems are operating in a balanced way. This assumption is typically inaccurate for low-voltage transmission networks which are often unbalanced. Therefore, in our analysis, we compare the effect that different formulations of power flow constraints have on the computed residual demand function of low-voltage networks for a simple one-line example.

This chapter is organized as follows. First, section 5.2 introduces the hierarchical framework that is used for computing residual demand functions for low-voltage networks in the presence of demand response. Then, section 5.3 presents the different formulations used for single-line approximations. In section 5.4, the three-phase unbalanced network models that are employed in our analysis are described. Finally, section 5.5 analyzes the results that are obtained for a small case study, while section 5.6 concludes the analysis. Furthermore, section 5.A in the appendix details the mathematical notations that are used in this chapter.

5.2 Hierarchical Coordination Framework

This section is dedicated to the exposition of the hierarchical coordination framework used in this chapter. Under this approach, power systems are divided in blocks that interact between each other by means of residual supply or demand functions. Figure 5.1 depicts this idea by considering the high-voltage transmission network, the medium-voltage distribution network and the low-voltage distribution network as the different layers of the total network[1]. This concept allows different actors, who are responsible for different parts of the network, to only exchange residual demand or supply functions, while maintaining privacy on networks characteristics. This principle is used in [137] for the coordination of several high-voltage transmission networks of different neighbouring European countries, and in [112] for coordinating high-voltage with medium-voltage transmission networks. As observed in Figure 5.1, the hierarchical approach proceeds as follows when considering priority service as

[1]Medium-voltage and low-voltage networks are represented in the Figure as radial networks, even though they may be meshed in practice.

the employed demand response paradigm. Firstly, at the low-voltage network, the aggregator passes on to the consumer the demand response menu[2]. From this menu, consumers subscribe to different options. The subscription quantity of each option for each location along with the subscribed valuation are transmitted by the aggregator to the low-voltage network operator (DSO). The DSO constructs the residual demand function by merging (according to the methodology presented in this chapter) the subscription information provided by the aggregator and the low-voltage power flow network constraints. This residual demand function is then transmitted to the medium-voltage network operator. The medium-voltage operator, based on the demand and production information at its level, along with network constraints, constructs a residual supply function that is passed on to the high-voltage network operator (TSO). The TSO then clears the market and determines a price for power while accounting for its network constraints and the residual supply functions provided by its connected medium-voltage networks. The power injected / withdrawn by the TSO at each interface with a medium-voltage network along with electricity price is passed down to the medium-voltage network operator that will decide on power supply at each part of its network. The supply decision at the interface with the lower-voltage network is then passed on to the DSO in order to enable it to reach its own dispatch decisions at its level. Every network operator is therefore responsible of their layer of the network. Regarding the low-voltage network, the operator can curtail consumers based on network constraints and electricity coming from the medium level using priority service. Indeed, the different options to which the consumer subscribes allow the operator to rank consumers and curtail them if needed based on the reliability ordering of the options, so as to balance the system while accounting for congestion in the low-voltage network.

As emphasized in the previous paragraph, residual demand or supply functions are computed by a particular block, in order to provide information on the amount of power that can be consumed or produced for a certain price. This curve can be computed for each network by only aggregating the supply or demand information of assets present in this network. However, as highlighted in [112, 137], it is important to account for network physics while aggregating such information, since network operating limits may prevent production assets from transporting their produced power to different parts of the network. In order to compute a residual demand function for a low-voltage network, the responsible network operator can therefore solve, during a certain time period, a set of optimization programs with a varying amount of power being withdrawn at the substation bus of the network. In the case where household flexibility is harnessed by means of priority service, the residual demand function model of

[2]In this thesis, the design of the priority service menu by the aggregator for the consumers does not account for network constraints and consumer location, which is a simplifying assumption.

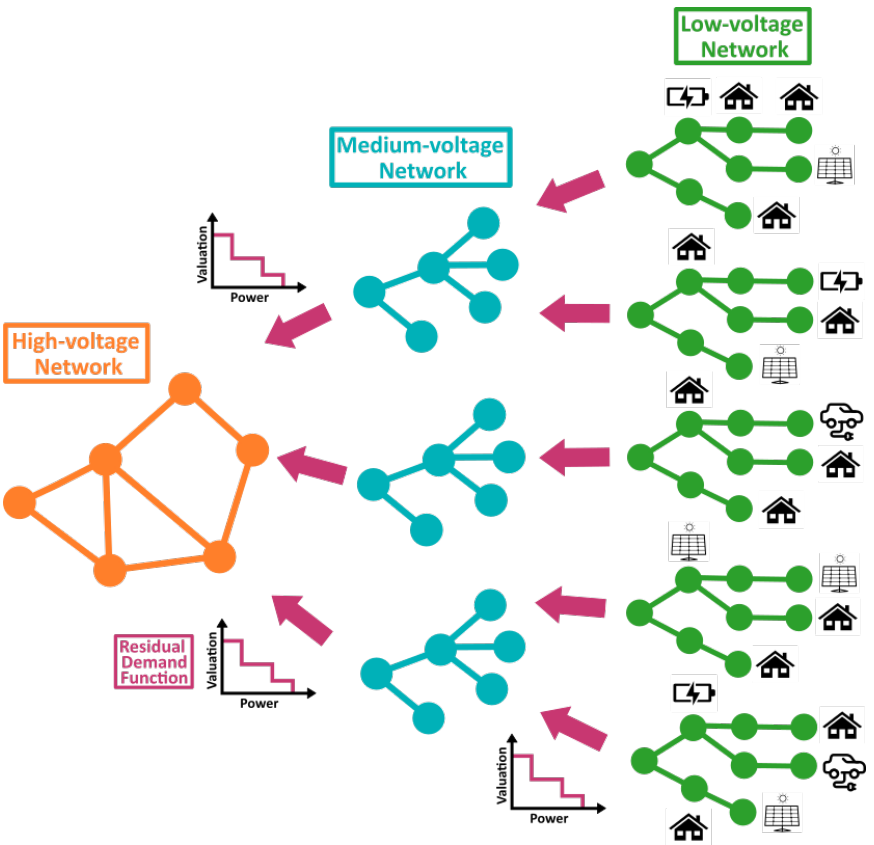

Figure 5.1: Representation of the hierarchical coordination principle considered in this dissertation.

the aggregator can be formulated as follows:

$$RDF(\bar{p}_0): \max_{\mathbf{nd},\mathbf{n},\mathbf{p_0}} \sum_{h\in\mathcal{H}}\sum_{i\in\mathcal{I}} MB_i \cdot nd_{i,h} \tag{5.1}$$

$$\text{s.t.} \quad 0 \leq nd_{i,h} \leq \Theta_{h,i}, \quad i \in \mathcal{I}, h \in \mathcal{H} \tag{5.2}$$

$$(\lambda): p_0 \leq \bar{p}_0, \tag{5.3}$$

$$(p_0, \mathbf{n}, \mathbf{nd}) \in \mathcal{N}et \tag{5.4}$$

The power consumed by household $h \in \mathcal{H}$ in a given priority class $i \in \mathcal{I}$ is represented by the variable $nd_{i,h}$. The goal of the aggregator is therefore to maximize the total benefit procured by serving households for which MB_i represents consumer marginal benefit for power of reliability class i. Constraint (5.2) outlines that household h can only consume power up to its subscription limit for a certain priority class i represented by parameter $\Theta_{h,i}$. Then, the amount of power that can be withdrawn by the network at the substation bus, indicated by p_0, to serve the demand is forced to be smaller than the fuse limit decided beforehand and denoted as $\bar{p}_0$. Finally, the set of variables representing household consumption, power withdrawal at the substation bus, and network state $\mathbf{n}$, are subject to the distribution network physics represented by the feasibility set $\mathcal{N}et$ in Eq. (5.4). The physics that govern distribution network flows can be represented via different formulations based on one- or three-phase equations which are respectively the focus of sections 5.3 and 5.4. By solving this optimization program for several values of P_0^{max}, the aggregator can construct its residual demand function using the dual λ of Constraint (5.3).

It is important to note that this hierarchical approach is exact if the lower-level problem is convex only when considering one time period and one connection point between two levels. Indeed, in the case of 2 connection points between the two levels, a multidimensional residual demand function must be created. To solve this issue, the multidimensional function can be approximated. It is observed in a stylized example in [137] that this issue does not affect results significantly, although, in realistic cases, it becomes more important [121]. Finally, note that this hierarchical approach has connections with bid filtering procedures considered by TSOs [121]. Accounting for network constraints implies that household bids are filtered with the aim of avoiding congestion during the dispatch phase. A study on the benefit of a hierarchical approach and a discussion on bid filtering in Norway is presented in [121].

5.3 Single-Phase Network Models

In order to compute a residual demand function that accounts for the characteristics of distribution networks, Constraint (5.4) of the aforementioned model is given by the *Power Flow* (PF) equations and the respective operating bounds

of each network variable. The PF equations define a nonlinear mapping between power injections at each bus and power flows on lines. There exist two different ways to model these constraints: the *Bus Injection model* (BIM) and the *Branch Flow model* (BFM) [165]. These two models are equivalent and their use depends on the variables and data chosen by the user.

In this section, we focus on the derivation of the power flow equations by assuming balanced system operation, so that the equations can be derived using only a single phase. This formulation will be extended to unbalanced three-phase operation cases in section 5.4. The optimal power flow model will be described along with some of its relaxations and approximations for the bus injection and branch flow formulations respectively. The following references [60, 104, 165] provide a detailed explanation of the different formulations.

5.3.1 Bus Injection Model

Without loss of generality, power networks can be modeled by an undirected graph with a set of nodes $\mathcal{N}$ and a set of edges $\mathcal{E}$. Let V_j be the complex voltage at bus $j \in \mathcal{N}$, where $s_j^g = p_j^g + \mathbf{i}q_j^g$ and $s_j^d = p_j^d + \mathbf{i}q_j^d$ correspond respectively to the complex apparent power generated or consumed at node j of the power system. We denote $s_j = s_j^g - s_j^d$ in order to simplify the exposition. We denote as $z_{jk} = r_{jk} + \mathbf{i}x_{jk}$ the impedance of line (j,k). Its inverse, the admittance of the line, is expressed as $y_{jk} = z_{jk}^{-1} = g_{jk} + \mathbf{i}b_{jk}$. Finally, the variable $S_{jk} = P_{jk} + \mathbf{i}Q_{jk}$ represents the apparent departing power flow from node j to node k, while I_{jk} corresponds to the current along the same line. To complete the exposition, these notations are depicted in Figure 5.2.

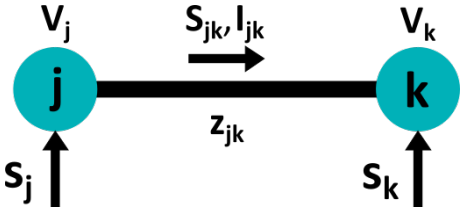

Figure 5.2: Illustration of notation that is used for deriving the power flow equations.

The bus injection model is defined by the following three power flow equations, which are derived from Kirchhoff's laws:

$$P_{jk} + \mathbf{i}Q_{jk} = V_j(V_j^* - V_k^*)y_{jk}^*, \quad (j,k) \in \mathcal{E} \tag{5.5}$$

$$\sum_{(j,k)\in\mathcal{E}} P_{jk} = p_j, \quad j \in \mathcal{N} \tag{5.6}$$

$$\sum_{(j,k)\in\mathcal{E}} Q_{jk} = q_j, \quad j \in \mathcal{N} \tag{5.7}$$

Eqs. (5.6) and (5.7) provide the active and reactive power balance at each bus while accounting for power losses along lines. Note that the $(*)$ sign represents the mathematical operation that computes the complex conjugate of a complex number.

A number of constraints can be added to the previous set of equations in order to express the supplementary characteristics of distribution networks. Among these, we note that voltage magnitude must usually satisfy certain stability limits. A deviation of more than 5% from of its nominal value is typically not allowed[3]. Moreover, the amplitude of the apparent power flowing through a line may be bounded by a line capacity limit. Finally, the power generation or demand at a certain node is limited. All of the aforementioned constraints are described by the four following inequalities:

$$\underline{V}_j \leq |V_j| \leq \bar{V}_j, \quad j \in \mathcal{N} \tag{5.8}$$

$$P_{jk}^2 + Q_{jk}^2 = |S_{jk}| \leq \bar{S}_{jk}, \quad (j,k) \in \mathcal{E} \tag{5.9}$$

$$\underline{p}_j \leq p_j \leq \bar{p}_j, \quad j \in \mathcal{N} \tag{5.10}$$

$$\underline{q}_j \leq q_j \leq \bar{q}_j, \quad j \in \mathcal{N} \tag{5.11}$$

By observing the set formed by Constraints (5.5) to (5.11), we note that these equations form a nonconvex feasibility set, due for example to the quadratic equality of Constraint (5.5). Several relaxations or approximations of this formulation can be derived in order to obtain convex and even linear formulations. First of all, before presenting these simpler formulations, we replace the complex voltage of this set by its polar definition ($V_j = |V_j|e^{\theta_j}$). Eq. (5.5) becomes:

$$P_{jk} = g_{jk}|V_j|^2 - |V_j||V_k|(g_{jk}\cos(\theta_j - \theta_k) + b_{jk}\sin(\theta_j - \theta_k)), \ (j,k) \in \mathcal{E} \tag{5.12}$$

$$Q_{jk} = -b_{jk}|V_j|^2 - |V_j||V_k|(g_{jk}\sin(\theta_j - \theta_k) - b_{ij}\cos(\theta_j - \theta_k)), (j,k) \in \mathcal{E} \tag{5.13}$$

Two linear approximations can be derived based on these two equations, and are detailed in the following paragraphs.

Direct Current Power Flow Approximation (BIM-DCOPF) This new linear formulation is obtained by applying the following assumptions:

1. Voltage magnitudes are assumed to equal to 1pu ($|V_j| = 1$);

2. Conductance is ignored since it is assumed to be negligible compared to the susceptance of the line ($g_{jk} << b_{jk}$ so $g_{jk} = 0$);

[3]The European norm (EN50160) being applied for distribution networks allows statistical variations of +/-10% during 95% of the time on a daily basis. Network operators are legally required to comply and therefore usually adopt stricter standards internally, such as allowed deviations of 5 to 6%.

3. Voltage differences between nodes are assumed to be small, which allows us to replace the sine function directly by the difference between the two angles;

4. Reactive power flows are assumed to be negligible, and are therefore removed.

Based on these assumptions, the complete version of the BIM-DCOPF linear program is given by the following set of equations:

$$P_{jk} = b_{jk}(\theta_k - \theta_j), \quad (j,k) \in \mathcal{E} \tag{5.14}$$

$$\sum_{(j,k)\in\mathcal{E}} P_{jk} = p_j, \quad j \in \mathcal{N} \tag{5.15}$$

$$\underline{p}_j \leq p_j \leq \bar{p}_j, \quad j \in \mathcal{N} \tag{5.16}$$

$$P_{jk} \leq \bar{S}_{jk}, \quad (j,k) \in \mathcal{E} \tag{5.17}$$

This formulation is mostly used for modeling high-voltage transmission networks [112].

Decoupled Linear Power Flow Approximation (BIM-DecoupledOPF) To improve the above linear formulation by considering reactive power flows and voltage, the Decoupled Linear Power Flow formulation is proposed based on the original set of equations. All the above assumptions except the one related to reactive power are used in this formulation. Moreover, regarding reactive power, a linearization is obtained by only assigning the voltage magnitude of a single bus to 1pu. The following formulation is obtained:

$$P_{jk} = b_{jk}(\theta_k - \theta_j), \quad (j,k) \in \mathcal{E} \tag{5.18}$$

$$\sum_{(j,k)\in\mathcal{E}} P_{jk} = p_j, \quad j \in \mathcal{N} \tag{5.19}$$

$$\underline{p}_j \leq p_j \leq \bar{p}_j, \quad j \in \mathcal{N} \tag{5.20}$$

$$P_{jk} \leq \bar{S}_{jk}, \quad (j,k) \in \mathcal{E} \tag{5.21}$$

$$Q_{jk} = b_{jk}(|V_k| - |V_j|), \quad (j,k) \in \mathcal{E} \tag{5.22}$$

$$\sum_{(j,k)\in\mathcal{E}} Q_{jk} = q_j, \quad j \in \mathcal{N} \tag{5.23}$$

$$\underline{q}_j \leq q_j \leq \bar{q}_j, \quad j \in \mathcal{N} \tag{5.24}$$

$$\underline{V}_j \leq |V_j| \leq \bar{V}_j, \quad j \in \mathcal{N} \tag{5.25}$$

This formulation is less employed in practice [165]. The two linear formulations presented above neglect losses and the coupling between real and reactive power flows, compared to the original formulation.

5.3.2 Branch flow Model

Now that the Bus Injection formulation is presented, in this section we focus on the Branch Flow formulation of Kirchhoff's laws, that is also used for obtaining useful power flow models. The Branch Flow formulation is given by the following set of constraints [104]:

$$\sum_{(k,m)\in\mathcal{E}} S_{km} = \sum_{(j,k)\in\mathcal{E}} (S_{jk} - z_{jk}|I_{jk}|^2) + s_k, \quad k \in \mathcal{N} \tag{5.26}$$

$$I_{jk} = y_{jk}(V_j - V_k), \quad (j,k) \in \mathcal{E} \tag{5.27}$$

$$S_{jk} = V_j I_{jk}^*, \quad (j,k) \in \mathcal{E} \tag{5.28}$$

Eq. (5.26) represents the apparent power balance at each bus. Constraint (5.27) is Ohm's law, while Eq. (5.28) defines the power flowing through a line. These three equations replace Constraints (5.5) to (5.7) of the Bus Injection model. Therefore, Constraints (5.8) to (5.11), which represent supplementary characteristics of the system, can be added to complete the Branch Flow model. The interest in using the Branch Flow model is in the fact that the Bus Injection model is prone to numerical errors relative to this formulation due to the voltage difference of Eq. (5.5) [104]. Therefore, it is interesting to provide convex relaxations or approximations of this problem. Some of them are presented in the remaining paragraphs of this section. The present formulation includes line losses.

Quadratic Relaxation (BFM-QRACOPF) A quadratic relaxation of Eqs. (5.26)-(5.28) can be obtained by combining the two last constraints and taking the squared magnitude of the equality. Two new variables are defined which represent respectively the squared magnitude of the voltage $v_j = |V_j|^2$ and the current $l_{jk} = |I_{jk}|^2$. The quadratic relaxation formulation is given by:

$$\sum_{(k,m)\in\mathcal{E}} S_{km} = \sum_{(j,k)\in\mathcal{E}} (S_{jk} - z_{jk} l_{jk}) + s_k, \quad k \in \mathcal{N} \tag{5.29}$$

$$v_j - v_k = 2 \cdot \mathrm{Re}\{z_{jk}^* S_{jk}\} - |z_{jk}| l_{jk}, \quad (j,k) \in \mathcal{E} \tag{5.30}$$

$$|S_{jk}|^2 = v_j l_{jk}, \quad (j,k) \in \mathcal{E} \tag{5.31}$$

Note that this formulation is still non-convex because of the quadratic equality. However, this relaxation is exact for radial networks which is a reasonable starting point of an approximation for distribution networks [104]. This formulation accounts for power losses through lines by means of the term $-z_{jk} l_{jk}$ in Eq. 5.29.

Second Order Cone Relaxation (BFM-SOCPOPF) From the previous quadratic relaxation, a second order cone relaxation can easily be obtained by relaxing the quadratic equality into an inequality:

$$|S_{jk}|^2 \leq v_j l_{jk}, \quad (j,k) \in \mathcal{E} \tag{5.32}$$

Note that this new formulation forms a convex set.

Branch Flow Linear Approximation (BFM-LinDistFlow) A linear approximation of the nonconvex formulation can be obtained by ignoring the line losses. It allows us to remove the current variable from the formulation which leads to the following new system:

$$\sum_{(k,m)\in\mathcal{E}} S_{km} = \sum_{(j,k)\in\mathcal{E}} S_{jk} + s_k, \quad k \in \mathcal{N} \tag{5.33}$$

$$v_j - v_k = 2 \cdot \mathrm{Re}\{z_{jk}^* S_{jk}\}, \quad (j,k) \in \mathcal{E} \tag{5.34}$$

Since this linear approximation neglects line losses, it tends to underestimate the required power for supplying loads. However, compared to the two linear approximations presented for the Bus Injection model, this formulation does not fix voltage magnitude, nor does it neglect reactive power [104].

5.4 Unbalanced Three-Phase Network Models

Since distribution networks are typically not loaded in a balanced fashion, the single-phase approximation employed in the previous section may be inaccurate. We therefore decided to include in our analysis three-phase power flow formulations, in order to more accurately account for the behavior of the distribution network. This section presents the two three-phase formulations that are used in this chapter. Regarding notations, three phases per node must now be considered. They are denoted by a, b and c. The complex voltage and apparent power injection at each bus are now vectors for which each entry corresponds to a different phase. They are respectively denoted by $V_j = (V_j^\phi, \phi \in \{a,b,c\})$ and $s_j = (s_j^\phi, \phi \in \{a,b,c\})$ for each bus $j \in \mathcal{N}$ of the power network. For each line connecting bus j to k, the impedance is now expressed as a 3 by 3 complex matrix $z_{jk} = (z_{jk}^{\phi_j\phi_k}, (\phi_j, \phi_k) \in \{a,b,c\} \times \{a,b,c\})$. The current on the line is given by $I_{jk} = (I_{jk}^\phi, \phi \in \{a,b,c\})$. The power flow on the line is represented by $S_{jk} = V_j I_{jk}^H \in \mathbb{C}^{3\times 3}$, where the $()^H$ operator provides the hermitian transpose of a vector or matrix. Finally, we also define these two new notations: $v_j = V_j V_j^H \in \mathbb{C}^{3\times 3}$ and $l_{jk} = I_{jk} I_{jk}^H \in \mathbb{C}^{3\times 3}$. Note that the diagonal of the two aforementioned matrices is real, because it respectively represents the squared magnitude of the voltage and the current on each phase.

Even though the literature on optimal power flow and its convex relaxations for single-phase approximations is well developed [104], the literature on three-phase unbalanced optimal power flow problems with convex relaxations is currently expanding [72,142,152] along with practical implementations [70,170]. The proposed formulations in this section are only derived based on the Branch Flow model. For details, we invite the reader to refer to [72, 152].

The three-phase Branch Flow formulation is given by the following three power flow equations:

$$\text{diag}\left(\sum_{(k,m)\in\mathcal{E}} S_{km}\right) = \text{diag}\left(\sum_{(j,k)\in\mathcal{E}} (S_{jk} - z_{jk} l_{jk})\right) + s_k, \quad k \in \mathcal{N} \tag{5.35}$$

$$V_j - V_k = z_{jk} I_{jk}, \quad (j,k) \in \mathcal{E} \tag{5.36}$$

$$l_{jk} = I_{jk} I_{jk}^H \text{ and } S_{jk} = V_j I_{jk}^H, \quad (j,k) \in \mathcal{E} \tag{5.37}$$

Eq. (5.35) represents the power balance at each bus of the power system. Ohm's law is expressed by means of Eq. (5.36), while the power flow on a line and the squared current are defined in Eq. (5.37). The Branch Flow formulation is equivalent to the Bus Injection model in terms of optimal solution, even though it enhances numerical stability as for the single-phase approximation [72]. From this formulation, one relaxation and one approximation can be obtained as detailed in the following paragraphs.

Three-phase Semidefinite Power Flow Relaxation (BFM-SDPOPF3) The above set of three equations can be reformulated as follows:

$$\text{diag}\left(\sum_{(k,m)\in\mathcal{E}} S_{km}\right) = \text{diag}\left(\sum_{(j,k)\in\mathcal{E}} (S_{jk} - z_{jk} l_{jk})\right) + s_k, \quad k \in \mathcal{N} \tag{5.38}$$

$$v_j - v_k = z_{jk} S_{jk}^H + S_{jk} z_{jk}^H - z_{jk} l_{jk} z_{jk}^H, \quad (j,k) \in \mathcal{E} \tag{5.39}$$

$$\begin{pmatrix} v_j & S_{jk} \\ S_{jk}^H & l_{jk} \end{pmatrix} \in \mathbb{S}^+, \quad (j,k) \in \mathcal{E} \tag{5.40}$$

$$\text{rank}\begin{pmatrix} v_j & S_{jk} \\ S_{jk}^H & l_{jk} \end{pmatrix} = 1, \quad (j,k) \in \mathcal{E} \tag{5.41}$$

where $\mathbb{S}^+$ stands for the set of hermitian positive semidefinite matrices. The presented set of three equations provide the same solution as the full unbalanced three-phase power flow model for radial networks [72]. The semidefinite power flow relaxation is therefore obtained by removing Eq. (5.41). A distributed resolution of this model is presented in [142].

Three-phase Linear Power Flow Approximation (BFM-LinDist3Flow) A linear approximation of this three-phase unbalanced power flow model is proposed in [6,72,152]. This approximation is based on the following assumptions:

1. Line losses are small ($z_{jk} l_{jk} << S_{jk}, \ (j,k) \in \mathcal{E}$) and therefore are ignored;

2. Voltages are nearly balanced: $\frac{V_j^a}{V_j^b} \approx \frac{V_j^b}{V_j^c} \approx \frac{V_j^c}{V_j^a} \approx e^{\mathbf{i}\frac{2\pi}{3}}$.

The following set of equations therefore provides the aforementioned linear approximation:

$$\sum_{(k,m)\in\mathcal{E}} \text{diag}(S_{km}) = \sum_{(j,k)\in\mathcal{E}} \text{diag}(S_{jk}) + s_k, \quad k \in \mathcal{N} \tag{5.42}$$

$$v_j - v_k = \gamma^P_{jk} \cdot \text{diag}(P_{jk}) + \gamma^Q_{jk} \cdot \text{diag}(Q_{jk}), \quad (j,k) \in \mathcal{E} \tag{5.43}$$

$$\gamma^P_{jk} = \begin{pmatrix} -2r^{aa}_{jk} & r^{ab}_{jk} - \sqrt{3}x^{ab}_{jk} & r^{ac}_{jk} + \sqrt{3}x^{ac}_{jk} \\ r^{ba}_{jk} + \sqrt{3}x^{ba}_{jk} & -2r^{bb}_{jk} & r^{bc}_{jk} - \sqrt{3}x^{bc}_{jk} \\ r^{ca}_{jk} - \sqrt{3}x^{ca}_{jk} & r^{cb}_{jk} + \sqrt{3}x^{cb}_{jk} & -2r^{cc}_{jk} \end{pmatrix}, \quad (j,k) \in \mathcal{E} \tag{5.44}$$

$$\gamma^Q_{jk} = \begin{pmatrix} -2x^{aa}_{jk} & x^{ab}_{jk} + \sqrt{3}r^{ab}_{jk} & x^{ac}_{jk} - \sqrt{3}r^{ac}_{jk} \\ x^{ba}_{jk} - \sqrt{3}r^{ba}_{jk} & -2x^{bb}_{jk} & x^{bc}_{jk} + \sqrt{3}r^{bc}_{jk} \\ x^{ca}_{jk} + \sqrt{3}r^{ca}_{jk} & x^{cb}_{jk} - \sqrt{3}r^{cb}_{jk} & -2x^{cc}_{jk} \end{pmatrix}, \quad (j,k) \in \mathcal{E} \tag{5.45}$$

Regarding other constraints representing supplementary characteristics of the network (see Eqs. (5.8) to (5.11)), their formulation can be extended to the three-phase case in the following way:

$$\underline{V}_j \leq \text{diag}(v_j) \leq \bar{V}_j, \quad j \in \mathcal{N} \tag{5.46}$$

$$\underline{s}_j \leq |s_j| \leq \bar{s}_j, \quad j \in \mathcal{N} \tag{5.47}$$

$$|\text{diag}(S_{jk})| \leq \bar{S}_{jk}, \quad (j,k) \in \mathcal{E} \tag{5.48}$$

5.5 Case Study and Results

The models presented in the previous sections (5.3 and 5.4) are applied on a one-line example, in order to illustrate the impact that each formulation has on the resulting demand function. The settings used for this example are presented in Figure 5.3. The chosen base apparent power is 1kVA, so as to be consistent with household power consumption and the chosen base voltage is 416V, which is the same as the IEEE European Low Voltage Test Feeder [91].

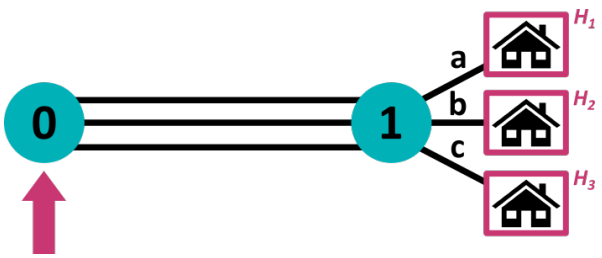

Figure 5.3: Distribution network setting used for the case study.

We consider a distribution network composed of a unique three-phase (denoted a, b and c) line. The resistance and reactance matrix of the line are

given by the following quantities [91, 98]:

$$r = \begin{pmatrix} 2.821 & 1.128 & 1.007 \\ 1.128 & 2.788 & 1.128 \\ 1.007 & 1.128 & 2.821 \end{pmatrix} \cdot 10^{-3}\ [pu],$$
$$x = \begin{pmatrix} 29.013 & 2.135 & -0.927 \\ 2.135 & 26.274 & 2.135 \\ -0.927 & 2.135 & 29.013 \end{pmatrix} \cdot 10^{-3}\ [pu]$$

When a single-line approximation is used, the 3 by 3 matrices are replaced by the mean of their diagonal elements. Bus 0 represents the substation bus of the distribution network. The reactive power that can be sent into the distribution network is limited to 10kVAr, while the active power is limited to 12kW. The voltage at bus 0 is assumed to be equal to $1\angle 0°$, $1\angle -240°$ and $1\angle 240°$ per unit respectively for phase a, b and c. At bus 1 of the distribution network, three households are connected, each one to a different phase. These three households subscribe to a common aggregator using priority service pricing. Their respective demand functions for active power are given in Figure 5.4 where the marginal benefit for each priority class is respectively in decreasing order 5, 3.5 and 1 €/kW. Regarding reactive power consumption, households are assumed to have a power factor of 0.95 [91], therefore the reactive power consumed by the household is given by 0.3287 times its active power consumption. Finally, the voltage magnitude at bus 1 is assumed to be able to deviate from its nominal value by 5% (between 0.95 and 1.05 per unit) as emphasized in the previous section.

The considered case study takes into account only a subset of the formulations presented previously: BIM-DCOPF, BIM-DecoupledOPF, BFM-QRACOPF, BFM-SOCPOPF, BFM-LinDistFlow, BFM-LinDist3Flow and BFM-SDPOPF3. Figure 5.5 presents the evolution of the total benefit obtained with each of the aforementioned formulations by varying the maximum allowed withdrawal of active power at the substation node from 0 to 12kW. The residual demand function is therefore given by the successive dual values of the constraint limiting the entry of generated power at the substation node, as explained in section 5.2. The resulting curve is presented in Figure 5.6 for different optimal power flow models. Regarding solving time, a significant difference between the computational time of the models is not observed for such an illustrative example. However, as emphasized in [70], the authors observe that expanding the scale of the used distribution network for three-phase models rapidly increases the required solving time. Moreover, this computational time is also dependent on the chosen three-phase problem formulation.

From the two presented figures, several conclusions can be drawn regarding the effect of network power formulations on the obtained residual demand function. Regarding the single phase approximation, we observe that both

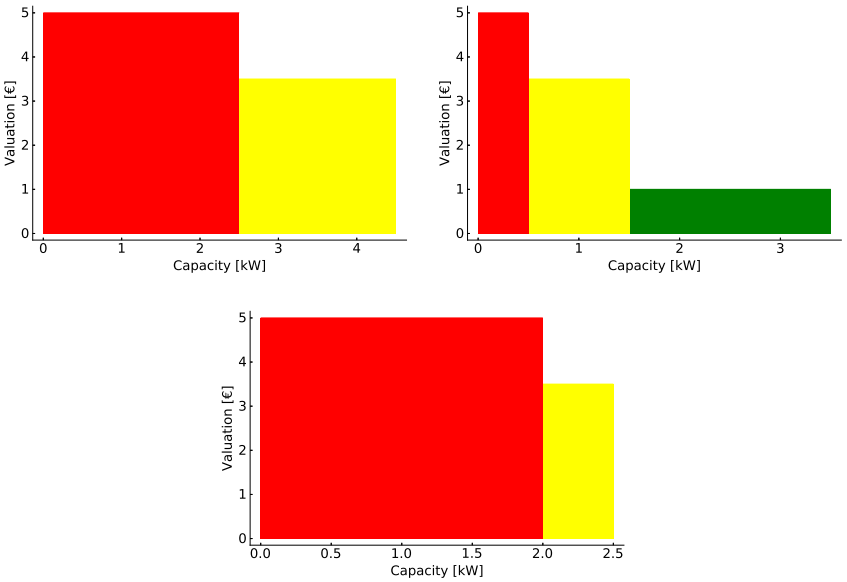

Figure 5.4: Household capacity subscription under priority service pricing used for the case study. Subscription of household 1 is given on the upper left, household 2 on the upper right and household 3 at the bottom respectively.

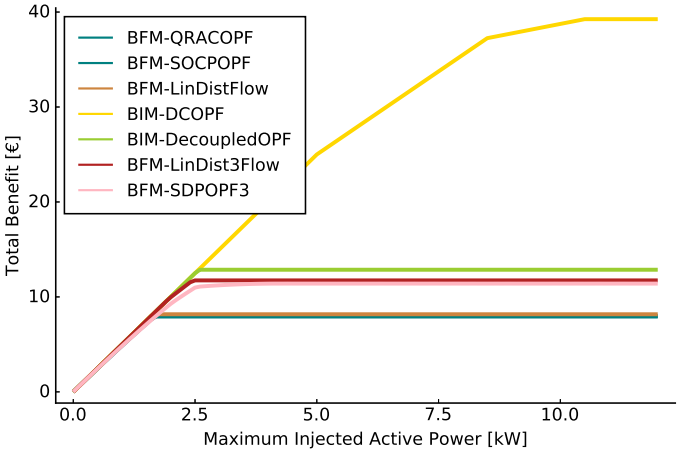

Figure 5.5: Evolution of the total benefit obtained for different optimal power flow formulations by varying the maximum allowed active power withdrawal at the substation node.

BFM-QRACOPF and BFM-SOCPOPF provide the same results, which shows that the second-order cone formulation is exact for this example. These two formulations, compared to the linear approximations, reach a peak in total benefit

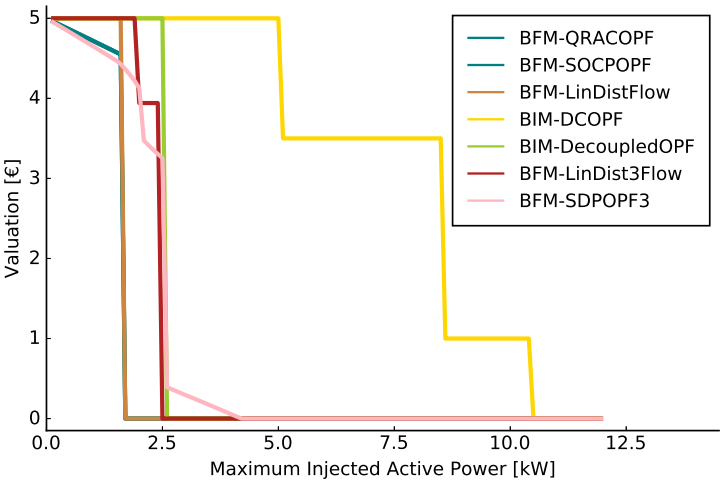

Figure 5.6: Residual demand function of the distribution network obtained for several optimal power flow formulations.

at approximately 2kW. This is due to the lower bound on voltage magnitude. The corresponding constraint does not permit more power to be consumed by the distribution network, since this would result in a violation of voltage limits. We detect the same saturation effect for the BFM-LinDistFlow formulation at a slightly higher level of injected active power. This is due to the same effect, even though it occurs at a higher injected active power, since this formulation neglects the effect of power losses along the lines, which also impacts the voltage at the household nodes. The BIM-DecoupledOPF saturation is even higher because, even though the model accounts for reactive and active power flow, this formulation does not take into consideration the interplay between these two quantities which lead to larger possibilities before violating the lower voltage bound constraint. In order to highlight the effect of the lower voltage magnitude limit on the resulting residual demand function, Figure 5.7 presents the total benefit obtained when removing the lower voltage magnitude limit from the different formulations. We therefore observe that, without this bound, all the linear formulations exhibit a similar behaviour as the BIM-DCOPF formulation, which does not account for reactive power flow and therefore voltage limits. Note that the BFM-QRACOPF and BFM-SOCPOPF formulations do not exhibit a saturation anymore but are still below the linear formulations because they both account for power losses along lines.

Regarding the three-phase models, we observe that they are also affected by the lower voltage bound, even though their saturation level seems to be superior to the one-phase nonlinear formulations. Finally, we can observe that the residual demand function for the three formulations BFM-QRACOPF, BFM-

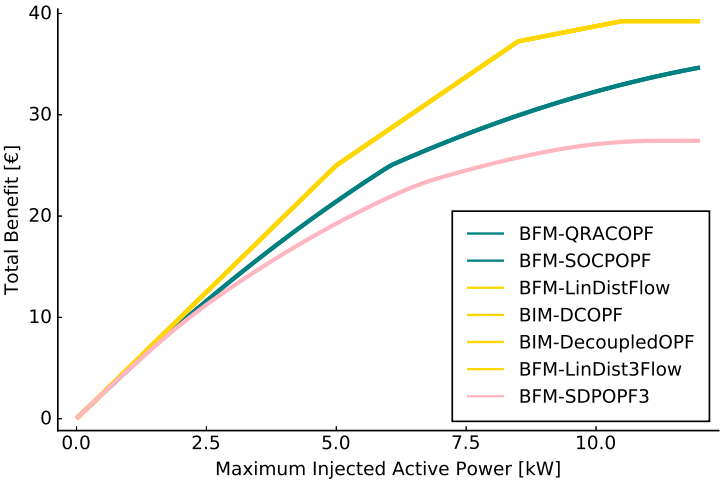

Figure 5.7: Evolution of the total benefit obtained for different optimal power flow formulations without voltage magnitude lower bound by varying the maximum allowed active power withdrawal at the substation node.

SOCPOPF and BFM-SDPOPF3 decreases gradually between 0 and 2kW compared to their corresponding linear approximations. Power losses are the cause of this decrease. Indeed, the linear approximations do not account for power losses, while these three formulations do. Therefore, if the substation node procures 2kW for the distribution network, only a smaller portion of these 2kW will be consumed at the households, because of the power lost during distribution.

5.6 Conclusion

In this chapter, we propose a framework for aggregators to coordinate with DSO in order to participate efficiently in electricity market operations in the presence of priority service. This is achieved by computing residual demand functions, while accounting for power flow constraints. Even though the importance of taking into account network physics in these residual demand functions is already highlighted in [112, 137], we show by employing several power flow formulations that they produce different residual demand functions for a simple one-line example. The importance of the formulation choice is therefore also essential for creating accurate residual demand functions. Indeed, due to certain modeling choices, the aggregator may be prompted to absorb more power than what the distribution network can physically manage. The inverse effect may also appear with an aggregator not seeing the benefit of increasing its power withdrawal from the substation node.

5.A Notations

All the notations used throughout this chapter are summarized in the different parts of this section.

Sets

$\mathcal{H}, \lvert\mathcal{H}\rvert$	Set of households and its cardinality
$\mathcal{I}, \lvert\mathcal{I}\rvert$	Set of reliability options and its cardinality
$\mathcal{N}et$	Feasibility set representing the physics behind distribution network
$\mathcal{N}$	Set of buses present in the distribution network
$\mathcal{E}$	Set of lines connecting two bus of the distribution network
$\{a, b, c\}$	Set of phases of a three-phase power networks
$\mathbb{S}^+$	Set of hermitian positive semidefinite matrix

Parameters

$\bar{p}_0$	Maximum amount of injected power at the root node of the distribution network [kW]
MB_i	Consumer marginal benefit for power of priority class i [€/kW]
$\Theta_{h,i}$	Subscribed quantity by household h for the reliability option i [kW]
z_{jk}	Impedance of line connecting bus j to bus k of the distribution network [Ω]
r_{jk}	Resistance of line connecting bus j to bus k of the distribution network [Ω]
x_{jk}	Reactance of line connecting bus j to bus k of the distribution network [Ω]
y_{jk}	Admittance of line connecting bus j to bus k of the distribution network [S]
g_{jk}	Conductance of line connecting bus j to bus k of the distribution network [S]
b_{jk}	Susceptance of line connecting bus j to bus k of the distribution network [S]
$\underline{V}_j$	Voltage magnitude lower limit at bus j of the distribution network [V]
$\bar{V}_j$	Voltage magnitude upper limit at bus j of the distribution network [V]
$\bar{S}_{jk}$	Apparent power magnitude flowing from bus j to bus k upper limit [kVA]
$\underline{p}_j$	Active power injected at bus j lower limit [kW]
$\underline{q}_j$	Reactive power injected at bus j lower limit [kVAr]
$\bar{p}_j$	Active power injected at bus j upper limit [kW]
$\bar{q}_j$	Reactive power injected at bus j upper limit [kVAr]

Variables

$nd_{i,h}$	Power consumption of household h from priority class i [kW]
λ	Dual variable of the fuse limit constraint in the residual demand function creation program
p_0	Active power injected at the substation node of the distribution network [kW]

$\mathbf{n}$	Variable representing all variables needed to represent the distribution network physics
V_j	Complex voltage at bus j of the distribution network [V]
θ_j	Complex voltage phase angle at bus j of the distribution network
s_j	Apparent power injected at bus j of the distribution network ($s_j = s_j^g - s_j^d$) [kVA]
p_j	Active power injected at bus j of the distribution network ($p_j = p_j^g - p_j^d$) [kW]
q_j	Reactive power injected at bus j of the distribution network ($q_j = q_j^g - q_j^d$) [kVAr]
s_j^g	Apparent power generated at bus j of the distribution network [kVA]
p_j^g	Active power generated at bus j of the distribution network [kW]
q_j^g	Reactive power generated at bus j of the distribution network [kVAr]
s_j^d	Apparent power consumed at bus j of the distribution network [kVA]
p_j^d	Active power consumed at bus j of the distribution network [kW]
q_j^d	Reactive power consumed at bus j of the distribution network [kVAr]
S_{jk}	Apparent power flowing from bus j to bus k of the distribution network [kVA]
P_{jk}	Active power flowing from bus j to bus k of the distribution network [kW]
Q_{jk}	Reactive power flowing from bus j to bus k of the distribution network [kVAr]
I_{jk}	Current flowing from bus j to bus k of the distribution network [A]

Functions

$RDF(\bar{p}_0)$	Function providing the residual demand function valuation for a maximum injected power at the substation node $\bar{p}_0$
$\lvert\cdot\rvert$	Magnitude of a complex number
$(\cdot)^*$	Complex conjugate of a complex number
$(\cdot)^H$	Hermitian operation on a complex matrix
$\mathbf{Re}\{\cdot\}$	Real part of a complex number
$\mathbf{diag}(\cdot)$	Return a vector formed by the diagonal elements of a matrix
$\mathbf{rank}(\cdot)$	Return the rank of a matrix

6 Conclusions and Future Perspectives

As emphasized in the introduction of this dissertation, residential demand response has recently gained increasing attention in the scientific literature as well as in practical applications since it is perceived as a valuable option for enabling the deeper penetration of renewable energies. The different contributions of this work therefore focus on the application of a residential electricity tariff, referred to as priority service, and its generalized form, namely multilevel demand subscription. Both service definitions are predicated on considering electricity as a service with different degree of quality.

First, in Chapter 2, a consumer-centric methodology is proposed for investigating the impact of priority service on consumer comfort and bills. In order to compare priority service to real-time pricing on a fair basis, a priority service menu is designed which is based on real-time prices. The original priority service theory is also extended in order to include a general form of service charges. Two simulations are conducted, which consider a Texas and a Belgian household. The case study allows us to quantify the essential role played by introducing energy service charges in alleviating the cost of priority service, relative to real-time pricing.

Subsequently, multilevel demand subscription, the extension of priority service, is considered in Chapters 3 and 4. The former chapter focuses on the design of priority service and multilevel demand subscription as two demand response options for the system to mobilize residential flexible demand. In order to achieve this objective, a method is proposed for the utility to approximate the system load duration curve, which is an essential input for the design of a demand response menu. Then, a mixed integer linear program is proposed to compute both menus while relaxing restrictive assumptions of the original theory. Finally, an optimization program is constructed for enabling households to select efficiently capacity strips from the proposed utility menu. Chapter 4 develops a framework for modeling the system-wide effects of residential flexibility under both priority service and multilevel demand subscription relative

to the economic golden standard of real-time pricing. In both chapters, a realistic case study of the Belgian market is performed. The case study allows us to examine the trade-off between simplicity and operational efficiency for each of these three proposed demand response schemes.

Finally, Chapter 5 presents preliminary results of a methodology for aggregating residential sector flexibility through priority service, while accounting for power flow constraints in the low-voltage network. This framework enables distributed resources of distribution networks to be efficiently accounted for through residual demand functions, while maintaining scalability in power system operations. Low-voltage network constraints are taken into account in this chapter through different formulations, approximations, and relaxations, based on either three phases or a single-phase approximation of power flow. The impact of these different formulations on the obtained residual demand function is analyzed on a simple one-line distribution network example.

In the remainder of the present chapter, a summary of the important conclusions obtained for each analysis undertaken in this dissertation is performed in section 6.1, while section 6.2 is dedicated to the exposition of future interesting directions that have been inspired by the analysis conducted in the present thesis.

6.1 Summary of the Key Messages

The common main theme of this dissertation is the importance of adding an energy component to capacity-based tariffs. Indeed, whether this energy component is represented by adding energy service charges to the original priority service pricing theory in the first study or with an added differentiation with respect to duration in the second investigation, it enables to reduce the cost faced by households while allowing increased operational efficiency for the system. Therefore, in future electricity markets with distributed flexibility and storage, a mix of energy and capacity charges is likely to be necessary for increasing the efficiency of operations while keeping electricity service charges of households at acceptable levels. The use of these two components in tandem is also advocated in [61]. The other significant outcomes resulting from the present work are summarized in the following sections.

6.1.1 Consumer-centric Comparison of Priority Service with and without Service Charges to Real-Time Pricing

- **Importance of service charges:** Our work shows that adding energy service charges is essential for a viable implementation of priority service pricing in a practical setting. It allows households to decrease "wasted

expenditures" by shifting charges from the capacity to the energy component of the service.

- **Priority service expenditures:** Priority service pricing is significantly more expensive for households than real-time pricing. Indeed, under real-time pricing, consumers only pay for the electricity they actually use, while under priority service, consumers pay for reserving capacity that may not be entirely employed at any given time interval. The results that pertain to real-time pricing in this work are idealized, since we consider consumers as rational agents that react instantaneously to prices. In practice, this assumption may not hold. This will lead to a degradation of the observed performance of real-time pricing.

- **Effect of batteries:** The benefit for households in investing in batteries is studied for real-time pricing and priority service. In the real-time pricing setting, even though a battery allows a reduction in the electricity bill by 25 %, the consumer fails to recover the cost of investing in home energy storage. However, if consumers are constrained to choose among priority service contracts, the gain provided by batteries is sufficient to cover battery investment costs.

- **Subscription duration:** A significant benefit is observed in consumer costs when using weekly priority service contracts instead of yearly ones. Indeed, renewing subscription on a weekly basis allows consumers to better adapt their contract to the weekly fluctuations of their load, thereby reducing their incurred cost. There is therefore a significant added value for consumers to change their subscription relatively frequently, however this undermines the claimed advantage of simplicity in priority service.

6.1.2 Comparison of Priority Service and Multilevel Demand Subscription to Real-Time Pricing in terms of System Operation

- **Operational efficiency:** Even though multilevel demand subscription increases the implementation complexity from both the aggregator and the household sides, it improves operational efficiency by allowing the utility to better discriminate flexible consumers. This results in a total cost reduction of about 2% relative to priority service, which amounts to 10M€/month for the 15-minute case study for Belgium. However, multilevel demand subscription and priority service appear to be significantly more costly for the system than real-time pricing. As detailed previously, the performance of real-time pricing in this work is an ideal benchmark compared to a real-world setting.

- **Comparison of household energy/capacity subscription for different pricing policies:** Households can better match their actual con-

sumption with multilevel demand subscription compared to priority service. Indeed, they subscribe to less energy, and more capacity, than under priority service. Households are also shown to employ their subscription more efficiently under multilevel demand subscription because of a higher utilization rate than under priority service pricing.

- **Households expenditures under different pricing policies:** Households experience a lower bill and a lower total cost under multilevel demand subscription than under priority service. This is due to capacity strips procured under priority service that remain idle for a significant portion of the service horizon. This reduction amounts to 20% for households that only own solar panels and is limited to 10% when households also own a battery.

- **Cost-benefit analysis of local storage:** Even though a battery allows households to reduce their total subscription and inconvenience cost, the investment cost of a battery may prohibit its acquisition, especially under multilevel demand subscription. Indeed, the benefit of batteries is reduced in this case because of the energy component already present in the multilevel demand subscription scheme by means of short durations.

- **Cost-benefit analysis of local rooftop solar panels:** Owning only solar panels without a battery seems to be unjustifiable in terms of household gains compared to investment cost. Note, however, that this type of households are the ones that are most rewarded by changing from priority service to multilevel demand subscription in terms of total cost reduction.

- **Effect of real-time pricing on households:** Real-time pricing always enables households to reduce their shortage cost compared to the two other schemes, except for households with large batteries that serve as a system reservoir for supporting other households during periods of low renewable production[1].

- **Influence of the model resolution:** The consistency of all previous conclusions is observed for two different resolutions. We note that the lower resolution underestimates the benefits of multilevel demand subscription compared to priority service for both the system and households. This observation stresses the value of an accurate model with finer time resolution at the level of 15 minutes for arriving at more reliable conclusions regarding the interplay between demand response and system operations.

[1]Note however the difference in treatment between households under multilevel demand subscription or priority service who are not payed to provide electricity to the grid while it is the case under real-time pricing.

6.1.3 Combination of Distribution Network Physics with Priority Service

- **Importance of the employed network model:** Our analysis underscores the importance of carefully choosing the network model that is employed for computing the residual demand function. Indeed, due to certain modeling choices, an aggregator may be prompted to absorb more power than what the distribution network can physically manage.

6.2 Future Perspectives

Since the interest in demand response for future power systems continues to grow, in this last section we detail possibilities for future research on the subject that are triggered by the present work.

Chapter 5 proposes a preliminary investigation on the interaction between DSO and priority service. Several improvements or research directions can be considered:

- **Larger distribution networks with more components:** It would be interesting to deepen the analysis of Chapter 5 by applying the proposed methodology on larger distribution networks, such as the European network from the proposed IEEE unbalanced distribution networks test cases [91,153] to see if the conclusions from this chapter maintain with increasing scale. Roland in [151] describes typical characteristics of low- and medium-voltage networks which can also be helpful for creating larger-scale examples. Moreover, components of distribution networks such as transformers, shunts or switches are not considered in the proposed formulations. It would be interesting to observe the impact that they may have on the creation of the residual demand function.

- **Network charges:** Although we investigate the issue of coordinating aggregators with DSO in Chapter 5, it would be worthwhile to study the impact of network charges on the design of the priority service and multilevel demand subscription menus.

- **Subsidies for batteries and rooftop solar panels:** It would be valuable to study the impact of batteries and solar panels on the distribution network in terms of network investment for the DSO. In the case in which demand response indeed reduces required investments in networks, it may create another stream of revenue for batteries or rooftop solar panels that can be provided by the DSO to the consumer so as to actually enable households to cover battery investment costs.

- **Capacity expansion planning:** It would be relevant to analyze the impact that demand response in the form of priority service or multilevel demand subscription can have on capacity expansion decisions of power networks in terms, for example, of the amount of renewable resources that can be absorbed by power networks.

The approach presented in this manuscript focuses on the consumer and the impact of different demand response schemes on its electricity bill but also comfort. An extension of this work can also be created for which the main focus is on the aggregator that designs such demand response contracts. Indeed, how the aggregator owning no specific assets but only interacting with the wholesale electricity market can buy enough power to satisfy its consumers while respecting the proposed reliability is an interesting direction for future research. Moreover, studying the influence of the incorporation of several demand response aggregators that bid into the market on the wholesale electricity price is a further direction of research. Such variations can be inspired by the research of [20].

Finally, home energy management system is a field of research in its own right. The study provided in this dissertation uses it as a tool to measure the impact of priority service or multilevel demand subscription on residential consumers. However, it would be valuable to develop home energy management systems that can manage the daily consumption of consumers. Indeed, such a home energy router can gain knowledge, through repeated experience, about the consumption patterns of households, the interruption patterns of different colors, as well as the discomfort of consumers from different interruption events. It is particularly relevant since the interruption patterns of colors and the arrival patterns of appliances are random. This allows the home energy router to continuously improve by gradually learning how to best serve the needs of the household. This creates a scope for the application of learning, such as reinforcement learning algorithms, in home energy scheduling, for which an increasing body of literature is currently being developed [140, 180].

Bibliography

[1] O. Abrishambaf, F. Lezama, P. Faria, and Z. Vale. Towards transactive energy systems: An analysis on current trends. *Energy Strategy Reviews*, 26:100418, 2019.

[2] P. J. Agrell. Incentive regulation of networks. *Reflets et perspectives de la vie économique*, 54(1):103–132, 2015.

[3] M. H. Albadi and E. F. El-Saadany. A summary of demand response in electricity markets. *Electric power systems research*, 78(11):1989–1996, 2008.

[4] APERe. Observatoire belge des énergies renouvelables. `http://www.apere.org/fr/observatoire-energies-renouvelables`.

[5] I. Aravena, A. Papavasiliou, and A. Papalexopoulos. A Distributed Computing Architecture for the Large-Scale Integration of Renewable Energy and Distributed Resources in Smart Grids. In W.-J. Hwang, editor, *Recent Progress in Parallel and Distributed Computing*. InTech, July 2017.

[6] D. B. Arnold, M. Sankur, R. Dobbe, K. Brady, D. S. Callaway, and A. Von Meier. Optimal dispatch of reactive power for voltage regulation and balancing in unbalanced distribution systems. In *2016 IEEE Power and Energy Society General Meeting (PESGM)*, pages 1–5, 2016.

[7] ARPA-E. PERFORM - Performance-based Energy Resource Feedback, Optimization, and Risk Management: Project Descriptions. `https://arpa-e.energy.gov/sites/default/files/documents/files/PERFORM_Project_Descriptions.18.20.pdf`. Accessed on: 07-10-2020.

[8] S. L. Arun and M. P. Selvan. Intelligent residential energy management system for dynamic demand response in smart buildings. *IEEE Systems Journal*, 12(2):1329–1340, 2018.

[9] M. Beaudin and H. Zareipour. Home energy management systems: A review of modelling and complexity. *Renewable and Sustainable Energy Reviews*, 45:318–335, May 2015.

[10] N. Berg. What will happen to solar panels after their useful lives are over? https://www.greenbiz.com/article/what-will-happen-solar-panels-after-their-useful-lives-are-over#:~:text=But%20the%20solar%20panels%20generating,t%20long%20from%20being%20retired., may 2018.

[11] P. Bertoldi, P. Zancanella, B. Boza-Kiss, et al. Demand response status in eu member states. *EUR 27998 EN*, pages 1–140, 2016.

[12] J. Bezanson, A. Edelman, S. Karpinski, and V. B. Shah. Julia: A fresh approach to numerical computing. *SIAM review*, 59(1):65–98, 2017.

[13] P. C. Bhagwat and L. Meeus. Reliability options: Can they deliver on their promises? *The Electricity Journal*, 32(10):106667, 2019.

[14] J. R. Birge and F. Louveaux. *Introduction to stochastic programming*. Springer Science & Business Media, 2011.

[15] E. Bitar and S. Low. Deadline differentiated pricing of deferrable electric power service. In *2012 IEEE 51st IEEE Conference on Decision and Control (CDC)*, pages 4991–4997, 2012.

[16] E. Bitar and Y. Xu. Deadline differentiated pricing of deferrable electric loads. *IEEE Transactions on Smart Grid*, 8(1):13–25, 2017.

[17] S. Borenstein, M. Jaske, and A. Rosenfeld. Dynamic pricing, advanced metering and demand response in electricity markets. Technical Report 105, University of California Energy Institute, October 2002.

[18] D. S. Callaway. Tapping the energy storage potential in electric loads to deliver load following and regulation, with application to wind energy. *Energy Conversion and Management*, 50(5):1389–1400, 2009.

[19] D. S. Callaway and I. A. Hiskens. Achieving controllability of electric loads. *Proceedings of the IEEE*, 99(1):184–199, 2011.

[20] C. Campaigne and S. Oren. Firming renewable power with demand response: an end-to-end aggregator business model. *Journal of Regulatory Economics*, 50(1):1–37, Aug. 2016.

[21] W. Cardinaels and I. Borremans. Linear: Demand response for families. Technical report, Linear consortium, 2014.

[22] CEZ Electro Bulgaria. Supply prices confirmed by CWER. https://www.cez.bg/en/prices/electricity-prices/for-supply.html.

[23] H.-P. Chao. Competitive electricity markets with consumer subscription service in a smart grid. *Journal of Regulatory Economics*, 41(1):155–180, Feb. 2012.

[24] H.-P. Chao and S. S. Oren. Robert b. wilson - Beyond the 2020 Nobel prize for economic sciences. *Energy Economics*, 95, 2021.

[25] H.-P. Chao, S. S. Oren, S. A. Smith, and R. B. Wilson. Multilevel demand subscription pricing for electric power. *Energy economics*, 8(4):199–217, 1986.

[26] H.-P. Chao and R. Wilson. Priority Service: Pricing, Investment, and Market Organization. *The American Economic Review*, 77(5):899–916, 1987.

[27] S. Chen and C.-C. Liu. From demand response to transactive energy: state of the art. *Journal of Modern Power Systems and Clean Energy*, 5(1):10–19, Jan. 2017.

[28] W. Chen, L. Qiu, and P. Varaiya. Duration-deadline jointly differentiated energy services. In *IEEE 54th Annual Conference on Decision and Control (CDC)*, 2015.

[29] Z. Chen, L. Wu, and Y. Fu. Real-time price-based demand response management for residential appliances via stochastic optimization and robust optimization. *IEEE Transactions on Smart Grid*, 3(4):1822–1831, 2012.

[30] S. G. C. Collaborative. 2011 state of the consumer report, 2011.

[31] F. E. R. Commission. Demand response compensation in organized wholesale energy markets - Final Report Rule. Technical report, march 2011.

[32] Commission de Régulation de l'Électricité et du Gaz (CREG). Les contrats à prix dynamique : des contrats d'électricité pour des consommateurs dynamiques. `https://www.creg.be/fr/news/les-contrats-a-prix-dynamique-des-contrats-delectricite-pour-des-consommateurs-dynamiques`, May 2021.

[33] P. Cramton. Lessons from the 2021 Texas electricity crisis. Working paper, Mar. 2021.

[34] R. D'hulst, W. Labeeuw, B. Beusen, S. Claessens, G. Deconinck, and K. Vanthournout. Demand response flexibility and flexibility potential of residential smart appliances: Experiences from large pilot test in Belgium. *Applied Energy*, 155:79–90, Oct. 2015.

[35] P. Du and N. Lu. Appliance commitment for household load scheduling. *IEEE Transactions on Smart Grid*, 2(2):411–419, 2011.

[36] I. Dunning, J. Huchette, and M. Lubin. Jump: A modeling language for mathematical optimization. *SIAM Review*, 59(2):295–320, 2017.

[37] Eesti Energia. Electricity contract and packages - eesti energia. https://www.energia.ee/en/era/elekter/elektrileping-ja-paketid?customers=home-customer&packages=spot.

[38] Electrica Furnizare S.A. Oferte energie electrică în piaţa concurenţială. https://www.electricafurnizare.ro/preturi-si-tarife/.

[39] Electricity Authority of Cyprus. Domestic use tariffs. https://www.eac.com.cy/EN/RegulatedActivities/Supply/tariffs/Documents/Domestic%20Use%20Tariffs%20-%202021.pdf.

[40] Elektro Energija. Dokumenti in ceniki. https://www.elektro-energija.si/za-dom/dokumenti-in-ceniki.

[41] Elia. Grid data. https://www.elia.be/en/grid-data, Nov. 2019.

[42] ELMUEMASZ. Villamos energia tarifák. https://elmuemasz.hu/egyetemes-szolgaltatas/szolgaltatasok/villamos-energia/villamos-energia-tarifak.

[43] Endesa. Pvpc: What is the regulated rate? https://www.endesa.com/en/discover-energy/energy-and-more/vpsc-voluntary-price-small-consumer.

[44] Enea. Offer for home. https://www.enea.pl/en/offer-for-home.

[45] Eneco. Électricité verte: comparez nos tarifs - Eneco Belgique. https://eneco.be/fr/electricite-gaz.

[46] Enefit Latvia. Elektrîba mãjai. https://www.enefit.lv/en/majai/elektriba.

[47] Enemalta. Tariffs, billing and payments. https://www.enemalta.com.mt/services/tariffs-billing-and-payments/.

[48] Energia. All energy plans. https://www.energia.ie/plans-and-switching-info/all-energy-plans.

[49] ENGIE. Conditions de prix énergie - ENGIE. https://www.engie.be/fr/energie/electricite-gaz/prix-conditions.

[50] Enovos. Green electricity for your home. https://www.enovos.lu/en/individuals/electricity.

[51] ERCOT. Electricity Reliability Council of Texas (ERCOT). http://www.ercot.com.

[52] O. Erdinc, N. G. Paterakis, T. D. P. Mendes, A. G. Bakirtzis, and J. P. S. Catalao. Smart Household Operation Considering Bi-Directional EV and ESS Utilization by Real-Time Pricing-Based DR. *IEEE Transactions on Smart Grid*, 6(3):1281–1291, May 2015.

[53] ESO. Distribution service rates - Tariff plans, prices, payment methods and debts. https://www.eso.lt/en/home/electricity/tariff-plans-prices-settlement-and-debts/distribution-service-rates_524.html.

[54] EURELECTRIC. Dynamic pricing in electricity supply: A EURELECTRIC position paper. http://www.eemg-mediators.eu/downloads/dynamic_pricing_in_electricity_supply-2017-2520-0003-01-e.pdf, feb 2017.

[55] European Commission. EU reference scenario 2016. https://ec.europa.eu/energy/en/data-analysis/energy-modelling, October 2017.

[56] European Commission. Report from the commission to the european parliament, the council, the european economic and social comittee and the committee of the regions: Energy prices and costs in europe - part iv: Impact of price regulation. https://ec.europa.eu/transparency/regdoc/rep/10102/2019/EN/SWD-2019-1-F1-EN-MAIN-PART-5.PDF, Jan. 2019.

[57] European Commission. Report from the commission to the european parliament, the council, the european economic and social comittee and the committee of the regions: Renewable energy progress report. https://ec.europa.eu/energy/sites/ener/files/renewable_energy_progress_report_com_2020_952.pdf, Oct. 2020.

[58] European Network of Transmission System Operators for Electricity (ENTSO-E). ENTSO-E Vision on Market Design and System Operation towards 2030. Technical report, ENTSO-E.

[59] EVN. Strom von evn - mit stromtarifen energiekosten sparen. https://www.evn.at/Privatkunden/Strom/EVN-Strom-Haushalt-Standard.aspx.

[60] M. Farivar and S. H. Low. Branch flow model: Relaxations and convexification - part i. *IEEE Transactions on Power Systems*, 28(3):2554–2564, 2013.

[61] A. Faruqui and C. Bourbonnais. The tariffs of tomorrow: Innovations in rate designs. *IEEE Power and Energy Magazine*, 18(3):18–25, 2020.

[62] A. Faruqui and S. George. The value of dynamic pricing in mass markets. *The Electricity Journal*, 15(6):45–55, 2002.

[63] A. Faruqui and S. George. Quantifying customer response to dynamic pricing. *The Electricity Journal*, 18(4):53–63, 2005.

[64] A. Faruqui, D. Harris, and R. Hledik. Unlocking the 53 billion savings from smart meters in the EU: How increasing the adoption of dynamic tariffs could make or break the EU's smart grid investment. *Energy Policy*, 38(10):6222–6231, 2010.

[65] A. Faruqui, R. Hledik, S. Newell, and H. Pfeifenberger. The Power of 5 Percent. *The Electricity Journal*, 20(8):68–77, Oct. 2007.

[66] A. Faruqui and S. Sergici. Household response to dynamic pricing of electricity: a survey of 15 experiments. *Journal of regulatory Economics*, 38(2):193–225, 2010.

[67] A. Faruqui, S. Sergici, and C. Warner. Arcturus 2.0: A meta-analysis of time-varying rates for electricity. *The Electricity Journal*, 30(10):64–72, 2017.

[68] M. Ferris and A. Philpott. Dynamic risked equilibrium. *Operations Research Submitted*, 2018.

[69] Fluvius. Profils de consommation réelle des clients résidentiels pour l'électricité (résolution 15minutes). `https://www.fluvius.be/nl/thema/nutsvoorzieningen/open-data`.

[70] D. M. Fobes, S. Claeys, F. Geth, and C. Coffrin. Powermodelsdistribution. jl: An open-source framework for exploring distribution power flow formulations. *Electric Power Systems Research*, 189:106664, 2020.

[71] S. Gambone. Will solar panels be cheaper in the future? `https://www.paradisesolarenergy.com/blog/will-solar-panels-be-cheaper-in-the-future#:~:text=Bloomberg%20and%20their%2065%20market,moving%20in%20a%20downward%20direction.`, 2019.

[72] L. Gan and S. H. Low. Convex relaxations and linear approximation for optimal power flow in multiphase radial networks. In *2014 Power Systems Computation Conference*, pages 1–9, 2014.

[73] K. Garifi, K. Baker, D. Christensen, and B. Touri. Stochastic Home Energy Management Systems with Varying Controllable Resources. In *2019 IEEE Power Energy Society General Meeting (PESGM)*, page 5, Aug. 2019.

[74] J. Gärttner. *Group formation in smart grids: Designing demand response portfolios*. PhD thesis, Karlsruher Institut für Technologie (KIT), 2016.

[75] A. Gautier, J. Jacqmin, and J.-C. Poudou. The prosumers and the grid. *Journal of Regulatory Economics*, 53(1):100–126, 2018.

[76] A. S. Gazafroudi, M. Shafie-khah, E. Heydarian-Forushani, A. Hajizadeh, A. Heidari, J. M. Corchado, and J. P. S. CatalÃ£o. Two-stage stochastic model for the price-based domestic energy management problem. *International Journal of Electrical Power & Energy Systems*, 112:404–416, Nov. 2019.

[77] C. Gérard and A. Papavasiliou. A comparison of priority service versus real-time pricing for enabling residential demand response. In *2019 IEEE Power Energy Society General Meeting (PESGM)*, pages 1–5, 2019.

[78] H. C. Gils. Assessment of the theoretical demand response potential in europe. *Energy*, 67:1–18, 2014.

[79] N. Good, E. Karangelos, A. Navarro-Espinosa, and P. Mancarella. Optimization Under Uncertainty of Thermal Storage-Based Flexible Demand Response With Quantification of Residential Users' Discomfort. *IEEE Transactions on Smart Grid*, 6(5):2333–2342, Sept. 2015.

[80] Gudbrandsdal Energi. All power agreements. `https://www.ge.no/stromavtale/all`.

[81] Gurobi Optimization, LLC. Gurobi optimizer reference manual. `http://www.gurobi.com`, 2020.

[82] S. Y. Hadush and L. Meeus. DSO-TSO cooperation issues and solutions for distribution grid congestion management. *Energy Policy*, 120:610–621, 2018.

[83] T. M. Hansen, E. K. P. Chong, S. Suryanarayanan, A. A. Maciejewski, and H. J. Siegel. A Partially Observable Markov Decision Process Approach to Residential Home Energy Management. *IEEE Transactions on Smart Grid*, 9(2):1271 – 1281, Mar. 2018.

[84] G. W. Hart. Nonintrusive appliance load monitoring. *Proceedings of the IEEE*, 80(12):1870–1891, 1992.

[85] M. Hayn, A. Zander, W. Fichtner, S. Nickel, and V. Bertsch. The impact of electricity tariffs on residential demand side flexibility: results of bottom-up load profile modeling. *Energy Systems*, 9(3):759–792, Aug. 2018.

[86] X. He, N. Keyaerts, I. Azevedo, L. Meeus, L. Hancher, and J.-M. Glachant. How to engage consumers in demand response: A contract perspective. *Utilities Policy*, 27:108–122, 2013.

[87] HELEN. Electricity products and prices - helen. `https://www.helen.fi/en/electricity/electricity-products-and-prices`.

[88] HEP Operator Distribucijskog Sustava. Tarifni modeli. `https://www.hep.hr/ods/korisnici/kucanstvo/tarifni-modeli/34`.

[89] T. Hubert and S. Grijalva. Modeling for residential electricity optimization in dynamic pricing environments. *IEEE Transactions on Smart Grid*, 3(4):2224–2231, 2012.

[90] IEA, IRENA, UNSD, World Bank, and WHO. Tracking sdg7: The energy progress 2020. `https://trackingsdg7.esmap.org/data/files/download-documents/01-sdg7-executivesummary_0.pdf`, 2020.

[91] IEEE PES AMPS DSAS Test Feeder Working Group. IEEE PES Distribution Systems Analysis Subcommittee Radial Test Feeders. `https://site.ieee.org/pes-testfeeders/resources/`.

[92] K. Jespers, Y. Dams, K. Aernouts, P. Simus, F. Jacquemin, and L. Delaite. Energy consumption survey for belgian households. Technical report, FPS Economy, SMEs, Self-employed and Energy- STATISTICS BELGIUM, 2012.

[93] X. Jin, K. Baker, D. Christensen, and S. Isley. Foresee: A user-centric home energy management system for energy efficiency and demand response. *Applied Energy*, 205:1583–1595, Nov. 2017.

[94] A. R. Jordehi. Optimisation of demand response in electric power systems, a review. *Renewable and sustainable energy reviews*, 103:308–319, 2019.

[95] P. L. Joskow. Incentive regulation and its application to electricity networks. *Review of Network Economics*, 7(4), 2008.

[96] T. Kaneda. PVScenarioGenerator. `https://github.com/TakuKaneda/PVScenarioGenerator`, 2019.

[97] KELWATT by Selectra. Prix du kwh électricité: les tarifs en France. `https://www.kelwatt.fr/guide/prix-electricite-france`.

[98] W. Kersting. Radial distribution test feeders. *IEEE Transactions on Power Systems*, 6(3):975–985, 1991.

[99] B. J. Kirby. *Spinning reserve from responsive loads*. Citeseer, 2003.

[100] S. Koch, J. L. Mathieu, and D. S. Callaway. Modeling and control of aggregated heterogeneous thermostatically controlled loads for ancillary services. In *Proc. PSCC*, pages 1–7. Citeseer, 2011.

[101] P. Kohlhepp, H. Harb, H. Wolisz, S. Waczowicz, D. Müller, and V. Hagenmeyer. Large-scale grid integration of residential thermal energy storages as demand-side flexibility resource: A review of international field studies. *Renewable and Sustainable Energy Reviews*, 101:527–547, 2019.

[102] Kotimaan Energia. Löydä edullinen sähkösopimus ja säästä - kotimaan energia. `http://www.kotimaanenergia.fi/sahkoa-kotiin`.

[103] R. Livios. Combien de panneaux solaires devez-vous installer et quel en est le coût ? https://www.livios.be/fr/info-construction/techniques/energie/energies-renouvelables/combien-de-panneaux-solaires-devez-vous-installer-et-quel-en-est-le-cout/?authId=f97b3410-2789-41ea-9eb4-770c3d190b4b&referrer=https%3A%2F%2Fsearch.lilo.org%2Fresults.php%3Fq%3Dlivios%2Bprix%2Bpanneaux%2Bphotovoltaiques&referer=https%3A%2F%2Fsearch.lilo.org%2Fresults.php%3Fq%3Dlivios%2Bprix%2Bpanneaux%2Bphotovoltaiques, may 2020.

[104] S. H. Low. Convex relaxation of optimal power flow - part i: Formulations and equivalence. *IEEE Transactions on Control of Network Systems*, 1(1):15–27, 2014.

[105] K. Ma, T. Yao, J. Yang, and X. Guan. Residential power scheduling for demand response in smart grid. *International Journal of Electrical Power & Energy Systems*, 78:320–325, 2016.

[106] S. H. Madaeni and R. Sioshansi. The impacts of stochastic programming and demand response on wind integration. *Energy Systems*, 4(2):109–124, 2013.

[107] MälarEnergi. Fast eller rörligt elpris - vilket passar mig bäst? https://www.malarenergi.se/el/elavtal/vara-avtal/.

[108] K. Margellos and S. Oren. Capacity Controlled Demand Side Management: A Stochastic Pricing Analysis. *IEEE Transactions on Power Systems*, 31(1):706–717, 2016.

[109] J. L. Mathieu, S. Koch, and D. S. Callaway. State estimation and control of electric loads to manage real-time energy imbalance. *IEEE Transactions on Power Systems*, 28(1):430–440, 2013.

[110] Mega. Prix du gaz et de l'électricité en Belgique - Mega. https://www.mega.be/fr/electricite-et-gaz/tarif-gaz-electricite?gclid=EAIaIQobChMI3ubb-N_47wIVjdayCh1clADsEAAYBCAAEgJWf_D_BwE.

[111] M. Metz and C. Doetsch. Electric vehicles as flexible loads - A simulation approach using empirical mobility data. *Energy*, 48(1):369 – 374, 2012. 6th Dubrovnik Conference on Sustainable Development of Energy Water and Environmental Systems, SDEWES 2011.

[112] I. Mezghani. *Coordination of Transmission and Distribution System Operations in ELectricity Markets*. PhD thesis, UCLouvain, 2021.

[113] Moixa. Moixa smart battery user manual. https://www.moixa.com/wp-content/uploads/2019/02/V4_Moixa_User_Manual_online_UM004.pdf, February 2020.

[114] T. Morstyn and M. D. McCulloch. Multiclass energy management for peer-to-peer energy trading driven by prosumer preferences. *IEEE Transactions on Power Systems*, 34(5):4005–4014, 2019.

[115] T. Morstyn, A. Teytelboym, C. Hepburn, and M. D. McCulloch. Integrating p2p energy trading with probabilistic distribution locational marginal pricing. *IEEE Transactions on Smart Grid*, 11(4):3095–3106, 2020.

[116] T. Morstyn, A. Teytelboym, and M. D. Mcculloch. Bilateral Contract Networks for Peer-to-Peer Energy Trading. *IEEE Transactions on Smart Grid*, 10(2):2026–2035, Mar. 2019.

[117] Y. Mou. *Nonlinear Pricing Schemes for Mobilizing Residential Flexibility in Power Systems*. PhD thesis, UCLouvain, 2020.

[118] Y. Mou, A. Papavasiliou, and P. Chevalier. Application of priority service pricing for mobilizing residential demand response in belgium. In *European Energy Market (EEM), 2017 14th International Conference on the*, pages 1–5. IEEE, 2017.

[119] Y. Mou, A. Papavasiliou, and P. Chevalier. A bi-level optimization formulation of priority service pricing. *IEEE Transactions on Power Systems*, 35(4):2493–2505, 2020.

[120] MVV Energie AG. Stromprodukte. `https://www.mvv.de/de/energie/strom/stromprodukte`.

[121] N-SIDE. Study - System balancing solutions with detailed grid data. Technical report, april 2020.

[122] S. Nan, M. Zhou, and G. Li. Optimal residential community demand response scheduling in smart grid. *Applied Energy*, 210:1280–1289, 2018.

[123] M. Navarro, L. Giupponi, C. Ibars, D. Gregoratti, and J. Matamoros. Distributed algorithms for demand management and grid stability in smart grids. In *Communication and Networking in Smart Grids*, pages 35–72. CRC Press, 2012.

[124] A. Nayyar, M. Negrete-Pincetic, K. Poolla, and P. Varaiya. Duration-differentiated energy services with a continuum of loads. *IEEE Transactions on Control of Network Systems*, 3(2):182–191, 2016.

[125] B. Neenan, J. C. Kinnell, M. Bingham, and S. Hickman. Consumer preferences for electric service alternatives. *The Electricity Journal*, 29(5):62–71, 2016.

[126] M. Negrete-Pincetic, A. Nayyar, K. Poolla, F. Salah, and P. Varaiya. Rate-constrained energy services in electricity. *IEEE Transactions on Smart Grid*, 9(4):2894–2907, 2016.

[127] A. Nilsson, D. Lazarevic, N. Brandt, and O. Kordas. Household responsiveness to residential demand response strategies: Results and policy implications from a swedish field study. *Energy policy*, 122:273–286, 2018.

[128] N. O'Connell, P. Pinson, H. Madsen, and M. O'Malley. Benefits and challenges of electrical demand response: A critical review. *Renewable and Sustainable Energy Reviews*, 39:686–699, 2014.

[129] Octopus Energy. Octopus energy: Switch to afford renewable energy online. `https://octopus.energy/`.

[130] D. O'Neill, M. Levorato, A. Goldsmith, and U. Mitra. Residential Demand Response Using Reinforcement Learning. In *2010 First IEEE International Conference on Smart Grid Communications (SmartGridComm)*, pages 409–414, 2010.

[131] S. Oren. A Historical Perspective and Business Model for Load Response Aggregation Based on Priority Service. In *2013 46th Hawaii International Conference on System Sciences*, pages 2206–2214, Wailea, HI, USA, Jan. 2013. IEEE.

[132] S. S. Oren. Product differentiation and product line pricing in service industries. Technical report, EPRI, 1987.

[133] S. S. Oren. Distributed resource integration in the US: A markets perspective. In *CITIES 4th General Consortium Meeting*, 2017.

[134] A.-G. Paetz, E. Dütschke, and W. Fichtner. Smart homes as a means to sustainable energy consumption: A study of consumer perceptions. *Journal of consumer policy*, 35(1):23–41, 2012.

[135] D. Papadaskalopoulos, G. Strbac, P. Mancarella, M. Aunedi, and V. Stanojevic. Decentralized participation of flexible demand in electricity markets - Part II: Application with electric vehicles and heat pump systems. *IEEE Transactions on Power Systems*, 28(4):3667–3674, 2013.

[136] A. Papalexopoulos, J. Beal, and S. Florek. Precise mass-market energy demand management through stochastic distributed computing. *IEEE Transactions on Smart Grid*, 4(4):2017–2027, 2013.

[137] A. Papavasiliou, M. Bjørndal, G. Doorman, and N. Stevens. Hierarchical balancing in zonal markets. In *2020 17th International Conference on the European Energy Market (EEM)*, pages 1–6. IEEE, 2020.

[138] A. Papavasiliou and Y. Smeers. Remuneration of flexibility using operating reserve demand curves: A case study of Belgium. *The Energy Journal*, pages 105–135, 2017.

[139] A. Papavasiliou, Y. Smeers, and G. de Maere d'Aertrycke. Study on the general design of a mechanism for the remuneration of reserves in scarcity situations. Technical report, Université Catholique de Louvain and Tractebel, 2019.

[140] K. Paridari, D. Azuatalam, A. C. Chapman, G. Verbič, and L. Nordström. A plug-and-play home energy management algorithm using optimization and machine learning techniques. In *2018 IEEE International Conference on Communications, Control, and Computing Technologies for Smart Grids (SmartGridComm)*, pages 1–6. IEEE, 2018.

[141] Pecan Street Inc. Dataport. `https://www.pecanstreet.org/dataport/`.

[142] Q. Peng and S. H. Low. Distributed algorithm for optimal power flow on an unbalanced radial network. In *2015 54th IEEE Conference on Decision and Control (CDC)*, pages 6915–6920, 2015.

[143] PER. Electricity. `https://www.pre.cz/en/households/electricity/`.

[144] M. V. Pereira and L. M. Pinto. Multi-stage stochastic optimization applied to energy planning. *Mathematical programming*, 52(1):359–375, 1991.

[145] I. Pérez-Arriaga and C. Knittel. Utility of the future. Technical report, MIT Energy Initiative, December 2016.

[146] A. Philpott, M. Ferris, and R. Wets. Equilibrium, uncertainty and risk in hydro-thermal electricity systems. *Mathematical Programming*, 157(2):483–513, 2016.

[147] Prix-Elec by Selectra. Tarif Tempo EDF : Grille tarifaire en 2021 et CGV. `https://prix-elec.com/tarifs/fournisseurs/edf/tempo`.

[148] Public Power Corporation SA.-Hellas. Residential tariffs. `https://www.dei.gr/en/oikiakoi-pelates/timologia`.

[149] Z. Ren, W. Yan, X. Zhao, W. Li, and J. Yu. Chronological probability model of photovoltaic generation. *IEEE Transactions on Power Systems*, 29(3):1077–1088, 2014.

[150] I. Richardson, M. Thomson, D. Infield, and C. Clifford. Domestic electricity use: A high-resolution energy demand model. *Energy and Buildings*, 42(10):1878–1887, Oct. 2010.

[151] J.-M. Roland. Analyzing retail pricing options in distribution systems. Master's thesis, EPL, UCLouvain, 2019.

[152] M. D. Sankur, R. Dobbe, E. Stewart, D. S. Callaway, and D. B. Arnold. A linearized power flow model for optimization in unbalanced distribution systems. *arXiv preprint arXiv:1606.04492*, 2016.

[153] K. P. Schneider, B. A. Mather, B. C. Pal, C.-W. Ten, G. J. Shirek, H. Zhu, J. C. Fuller, J. L. R. Pereira, L. F. Ochoa, L. R. de Araujo, R. C. Dugan, S. Matthias, S. Paudyal, T. E. McDermott, and W. Kersting. Analytic considerations and design basis for the ieee distribution test feeders. *IEEE Transactions on Power Systems*, 33(3):3181–3188, 2018.

[154] J. Schwartz. Energy worldviews: Engaging consumers by aligning rate design strategies with personal choice. *The Electricity Journal*, 31(9):34–37, 2018.

[155] F. C. Schweppe, M. C. Caramanis, R. D. Tabors, and R. E. Bohn. *Spot Pricing of Electricity*. Springer Science & Business Media, 2013.

[156] SEAS-NVE. Alle elprodukter. `https://seas-nve.dk/sel/alle-produkter/`.

[157] Servizio Elettrico Nazionale. Usi domestici. `https://www.servizioelettriconazionale.it/it-IT/tariffe/uso-domestico`.

[158] A. Shapiro. Analysis of stochastic dual dynamic programming method. *European Journal of Operational Research*, 209(1):63–72, 2011.

[159] SSE. Ceny elektriny pre domàcnosti. `https://www.sse.sk/domacnosti/elektrina/sadzby?page_id=5521`.

[160] N. W. Stauffer. Tomorrow's power grid: Adjusting demand to meet supply. `https://energy.mit.edu/news/tomorrows-power-grid/`, August 2012.

[161] G. Strbac. Demand side management: Benefits and challenges. *Energy policy*, 36(12):4419–4426, 2008.

[162] SU ELETRICIDADE. Tarifas baixa tensão normal. `https://sueletricidade.pt/pt-pt/page/601/tarifas-baixa-tensao-normal`.

[163] T. Sweetnam, M. Fell, E. Oikonomou, and T. Oreszczyn. Domestic demand-side response with heat pumps: controls and tariffs. *Building Research & Information*, 47(4):344–361, 2019.

[164] Synergrid. Synthetic load profiles (SLP). `http://www.synergrid.be/index.cfm?PageID=16896`, Oct. 2017.

[165] J. A. Taylor. *Convex optimization of power systems*. Cambridge University Press, 2015.

[166] Tesla. Tesla Powerwall. `https://www.tesla.com/powerwall`.

[167] J. Torriti, M. G. Hassan, and M. Leach. Demand response experience in europe: Policies, programmes and implementation. *Energy*, 35(4):1575–1583, 2010.

[168] K. M. Tsui and S. C. Chan. Demand response optimization for smart home scheduling under real-time pricing. *IEEE Transactions on Smart Grid*, 3(4):1812–1821, 2012.

[169] W. Tushar, C. Yuen, T. K. Saha, T. Morstyn, A. C. Chapman, M. J. E. Alam, S. Hanif, and H. V. Poor. Peer-to-peer energy systems for connected communities: A review of recent advances and emerging challenges. *Applied Energy*, 282:116131, 2021.

[170] M. Vanin, H. Ergun, R. D'hulst, and D. Van Hertem. Comparison of linear and conic power flow formulations for unbalanced low voltage network optimization. *Electric Power Systems Research*, 189:106699, 2020.

[171] Vatenfall. Enkel-, dal- en normaaltarief uitgelegd. `https://www.vattenfall.nl/producten/energie/prijzen/enkeltarief-daltarief-normaaltarief/`.

[172] Verbund. Wechseln sie jetzt zu verbund-strom aus 100% wasserkraft! `https://www.verbund.com/de-at/privatkunden/strom`.

[173] M. Vesterberg and C. K. B. Krishnamurthy. Residential end-use electricity demand: Implications for real time pricing in sweden. *The Energy Journal*, 37(4), 2016.

[174] Viteos. Tarifs électriques. `https://viteos.ch/infos-pratiques/tarifs-electriques/`.

[175] M. L. Weitzman. Prices vs. quantities. *The review of economic studies*, 41(4):477–491, 1974.

[176] Z. Wen, D. O'Neill, and H. Maei. Optimal Demand Response Using Device-Based Reinforcement Learning. *IEEE Transactions on Smart Grid*, 6(5):2312–2324, 2015.

[177] B. Wilkin. National Survey Report of PV Power Applications in Belgium 2018. Technical report, International Energy Agency, 2019.

[178] B. Wilkin, S. Delhaye, and J. D'Hernoncourt. 21% de renouvelables dans l'électricité consommée en Belgique en 2019. `http://renouvelle.be/fr/statistiques/21-de-renouvelables-dans-lelectricite-consommee-en-belgique-en-2019`.

[179] X. Yan, Y. Ozturk, Z. Hu, and Y. Song. A review on price-driven residential demand response. *Renewable and Sustainable Energy Reviews*, 96:411–419, 2018.

[180] D. Zhang, S. Li, M. Sun, and Z. O'Neill. An optimal and learning-based demand response and home energy management system. *IEEE Transactions on Smart Grid*, 7(4):1790–1801, 2016.

[181] B. Zhou, W. Li, K. W. Chan, Y. Cao, Y. Kuang, X. Liu, and X. Wang. Smart home energy management systems: Concept, configurations, and scheduling strategies. *Renewable and Sustainable Energy Reviews*, 61:30–40, Aug. 2016.

[182] ZOME. ZOME Energy Networks. `https://enterprise.zomepower.com/`.